SKI Report 95:42

SITE-94

The Central Scenario for SITE-94: A Climate Change Scenario

Louisa M. King-Clayton
Neil A. Chapman
Fritz Kautsky
Nils-Olof Svensson
Ghislain de Marsily
Emmanuel Ledoux

December 1995

ISSN 1104-1374
ISRN SKI-R--95/42--SE

SKI
STATENS KÄRNKRAFTINSPEKTION
Swedish Nuclear Power Inspectorate

SKI Report 95:42

SITE-94

The Central Scenario for SITE-94: A Climate Change Scenario

Louisa M. King-Clayton [1]
Neil A. Chapman [1]
Fritz Kautsky [2]
Nils-Olof Svensson [3]
Ghislain de Marsily [4]
Emmanuel Ledoux [5]

[1] QuantiSci Ltd, Melton Mowbray, UK
[2] Swedish Nuclear Power Inspectorate, Stockholm, Sweden
[3] Department of Quaternary Geology, Lund, Sweden
[4] Université VI Paris, Paris, France
[5] Ecole des Mines de Paris, Fontainebleau, France

December 1995

NORSTEDTS TRYCKERI AB
Stockholm 1997

PREFACE

This report concerns a study which is part of the SKI performance assessment project SITE-94. SITE-94 is a performance assessment of a hypothetical repository at a real site. The main objective of the project is to determine how site specific data should be assimilated into the performance assessment process and to evaluate how uncertainties inherent in site characterization will influence performance assessment results. Other important elements of SITE-94 are the development of a practical and defensible methodology for defining, constructing and analysing scenarios, the development of approaches for treatment of uncertainties and evaluation of canister integrity. Further, crucial components of an Quality Assurance program for Performance Assessments were developed and applied, including a technique for clear documentation of the Process System, the data and the models employed in the analyses, and of the flow of information between different analyses and models.

Björn Dverstorp
Project Manager

Executive Summary

Part of the SITE-94 Project involves the construction of scenarios to assist in the evaluation of the future behaviour of a deep repository for spent fuel. The project uses data from the Äspö site and assumes that a repository is constructed (reduced in size to approximately 10%) at about 500 m depth in granitic bedrock in this coastal area of SE Sweden. The scenario construction process involves the definition of all the features, events and processes (FEPs) which affect the behaviour of a repository system. A Central Scenario, involving prediction of the climate and consequent surface and subsurface environments at the site for the next c.120 000 years, lies at the heart of the scenario definition work. It is stressed that as predictions of future climate are ultimately uncertain, it is the intention of the Central Scenario to provide an *illustration* of the potential degree of variability and significance of future climate changes on the evolution of a deep repository site. Performance Assessment calculations also require that it must ultimately provide a *single*, albeit non-unique, temporal sequence, with associated impacts, onto which other scenarios can be superimposed (Chapman et al., 1995). However, it is also necessary to identify as many of the potential variables involved in the future glacial evolution of the site as possible, in addition to defining a single scenario sequence. This allows at least a qualitative understanding of the assumptions and uncertainties involved in defining a single Central Scenario and may allow alternative scenarios to be erected if necessary.

The Central Scenario thus includes the following main components: a deterministic description of the most probable climate state for Sweden, with special reference to the Äspö area; a description of the likely nature of the surface and geological environment in the site area at each stage of the climate sequence selected; and quantitative information on how these changes might affect the disposal system.

The Central Climate Change Scenario is based on the climate models ACLIN (Astronomical climate index), the model by Imbrie & Imbrie (1980) and the PCM model by Berger et al. (1990). These models suggest glacial maxima at c.5000, 20 000, 60 000 and 100 000 years from now. The Äspö region is predicted to be significantly affected by the latter three glacial episodes, with the ice sheet reaching and covering the area during the latter two episodes (by up to c.2200 m and 1200 m thickness of ice, respectively). Only periglacial conditions are predicted to affect the area during the glacial episode at c.20 000 years from now and no glacial effects are predicted at c.5000 years. Permafrost thicknesses over the next 120 000 years have been calculated. Assumptions, estimates and alternatives to the prescribed climate evolution are discussed.

Following definition of a realistic, albeit non-unique, climate sequence, the objective of scenario development is to provide an indicator of the physical, chemical and hydrogeological conditions at the front of and beneath the

advancing and retreating ice sheets, with the aim of identifying critical aspects for Performance Assessment modelling. The effect of various factors, such as ice loading, the development of permafrost, temperature changes and sea level changes, are considered in terms of their impact on hydrogeology, groundwater chemistry, rock stress and surface environments.

The groundwater flow beneath Äspö is likely to be modified significantly at all stages of a glacial cycle. Local groundwater flow patterns will be re-organised on a continental scale, a probable function of the ice sheet thickness distribution. Groundwater flow is restricted during the periglacial and early ice advance stages and then undergoes large-scale enhancement and modification during the main duration of the ice sheet. A net downward and outward flow vector beneath the ice sheet and a strong upward flow beyond it is expected owing to basal meltwater overpressuring and ice loading effects. The main periods of groundwater discharge, which are of considerable significance to the Performance Assessment of a potential repository, are considered to occur during the early advance and late retreat phases of a glacial cycle. The latter discharge phase is considered to be more significant than the former phase which is inhibited by the development of permafrost in the proglacial zone. During ice sheet retreat, permafrost is unlikely to exist in the proglacial zone and, hence, groundwater discharge ahead of the ice sheet will be uninhibited and high. However, both phases are likely to be of moderately short duration (tens to thousands of years), depending on the advance/retreat rates of the ice sheet. During initial ice advance, Äspö will lie under the outer cold-based zone of the ice sheet which is underlain by permafrost, such that sub-glacial discharge is inhibited. In the proglacial region, permafrost may seal off potential sub-glacial aquifers or fault zones which would otherwise allow groundwater discharge. Excess pore pressures are likely to exist which may tend to cause hydrofracturing in the permafrost and pressure release. The Äspö area is not predicted to underlie the central, cold-based zone of the ice sheet at any stage of a glacial cycle, where the groundwater will be essentially stagnant. Rather, Äspö is considered to be situated beneath the zone of melting for the majority of the time of ice coverage (except during initial ice advance), where groundwater flow will occur, with head gradients increasing towards the ice sheet margins. Sub-glacial meltwater tunnels are expected to form under these conditions, particularly where bedrock transmissivity is low and is therefore unable to accommodate all the glacial meltwater as groundwater flow. The presence of tunnels may complicate the local groundwater flow patterns.

The chemistry of the groundwater beneath Äspö appears to be influenced markedly throughout a glacial cycle. It tends to become more saline as it is trapped beneath the permafrost in the periglacial and early glacial advance phases. Radionuclides may also concentrate during these phases if they have been released from the potential repository. As the base of the ice sheet and the permafrost melt, the groundwaters become increasingly dilute as glacial meltwater is forced downwards into the bedrock. Oxygenated waters may be forced deeper, particularly via more transmissive fracture zones, by a

combination of head increases and permafrost sealing. Maximum depths of penetration may be reached during the glacial maximum and it is possible that oxidising conditions may reach repository depths, a scenario of great significance for the stability and release from the near-field of the repository. Flushing by dilute meltwaters continues until the ice sheet retreats away from the Äspö region and marine water begins to infiltrate the bedrock. Subsequent damming of the Baltic may temporarily induce minor infiltration of dilute or brackish waters until the sea is re-established. As the land surface continues to rebound and the sea level returns to present-day levels, continued extension of the bedrock will cause near-surface, meteoric waters to be flushed down to greater depths.

During loading by the ice sheet, the bedrock is expected to undergo bulk compression, whereas subsequent glacial unloading causes expansion of the rock volume, which may in turn affect the hydraulic properties of the rock. A significant period in terms of rock mechanics at Äspö appears to occur during the final retreat of the ice sheet as the rock mass begins to unload and undergo uplift. During this period, fault reactivation and associated seismic activity may occur. Stresses in the bedrock, on the other hand, will be at a maximum when the maximum ice sheet thickness overlies the potential repository site. At this point, the bedrock will be under maximum compression and fracture apertures will be reduced, particularly those with horizontal or subhorizontal orientations. However, the complexity of the fracture system will result in a differential stress distribution in the rock mass and sub-glacial porewater pressures will further complicate the reaction of the bedrock to glacial loading, tending to open fractures rather than to close them. The relationship between glacial loading, rock mechanics and hydraulic properties of the rock is complex and requires more work in the future.

The numerous estimates and assumptions made during the development of the Central Scenario are outlined, in addition to the description of alternative climate and hydrogeological scenarios.

Wherever possible, direct observations and measurements of features have been sought to provide information. However, it has been found that there appears to be a general lack of observational data on the direct effects of an ice sheet on the hydrogeology, hydrogeochemistry and rock mechanics of the underlying bedrock. Although this is understandable on practical grounds, it means that there is a dependence on the modelling of the processes which may occur below an ice sheet. In particular, the response of fractured crystalline bedrock to glacial conditions may be significantly different to that of interbedded aquifers and aquitards.

In order to address many of the uncertainties, it is clear that the following are necessary: improved models of climate (including anthropogenic effects) and of the thermo-chemical-hydrological-mechanical coupled behaviour of the rock-water-ice system; more focussed data collection and interpretation in

several areas, such as present-day sub-glacial hydrogeological environments, palæo-chemical indicators (chemical and isotopic studies of fracture coatings and their hydrochemical zonation) and palæo-seismic indicators. Palaeohydrogeological data may hold the key to answering many of the uncertainties regarding the impact of past glaciations on groundwater flow, chemistry and rock mechanical behaviour. For example, analysis of fracture infilling minerals, such as calcite, may provide valuable evidence on the depth to which glacial meltwaters have penetrated in the past and the mechanical history of the fractures.

Contents

List of Figures

1 Introduction

1.1 Background to the SITE-94 Programme

Part of the SITE-94 Project involves the construction of scenarios to assist in the evaluation of the future behaviour of a deep repository for spent fuel. The project uses data from the Äspö site (Figure 1.1) and assumes that a repository is constructed in this coastal area of Sweden. The scenario construction process first involves the definition of all the features, events and processes (FEPs) which affect the behaviour of a repository system.

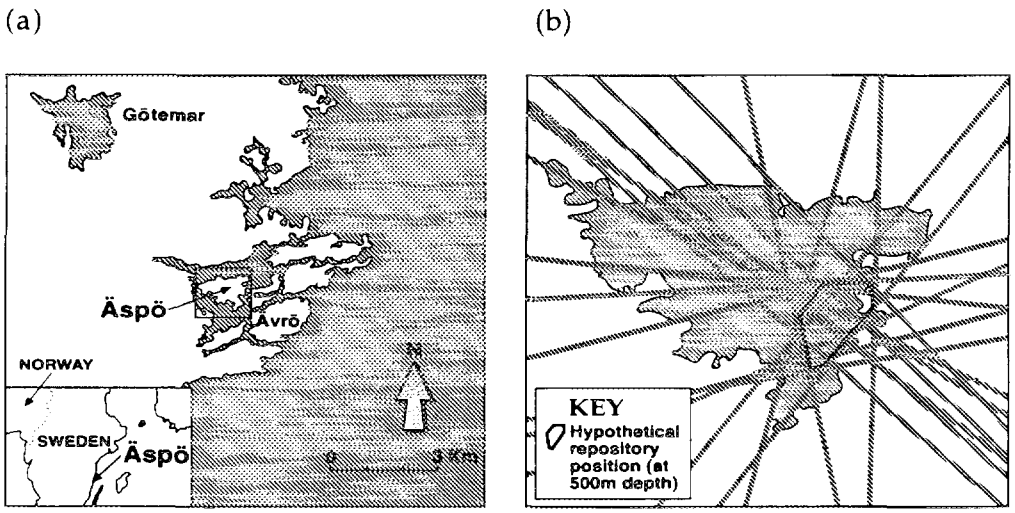

Figure 1.1. **(a)** The location of Äspö in SE Sweden. **(b)** The hypothetical location of the repository at 500 m depth between various fracture zones (inset box in Figure 1.1a).

The majority of the FEPs identified have been incorporated into a Reference Case 'Process System', which is an organised assembly of all the FEPs required for the description of barrier performance and radionuclide behaviour in a repository and its surrounding environment, and which can be predicted with at least some degree of determinism from a given set of external conditions (Andersson, 1989). This Process System has been developed into a complex Reference Case Process Influence Diagram (PID) which connects all FEPs that impact on each other in a logical fashion via influence lines (Chapman et al., 1995).

The external conditions which determine the behaviour of the Process System are caused by the FEPs which remain outside the Process System: the External FEPs or EFEPs. Scenarios are constructed by imposing EFEPs, individually or in combinations, onto the PID and determining which

influences are modified, either quantitatively or in terms of the nature of the impact. In this way, sets of consequence calculations specific to each scenario can be developed.

A large group of the EFEPs identified in SITE-94 (and many earlier scenario development exercises) relates to climate change and its effects on the surface environment. It was decided that, for the SITE-94 analysis, a full account must be taken of predicted changes in the climate of Sweden, and that a deterministic description of the most likely sequence of climatic events should lie at the core of all the safety assessment analyses carried out.

For this reason, it was decided to develop a 'Central Scenario' (CS) which incorporates climate change and then to construct an appropriate version of the PID which takes account of a prescribed climate and surface environment model. A key function of the CS is to provide a temporal framework for the evolution of the site on which to superimpose other EFEPs. One of the problems with generic scenario production is the difficulty involved in selecting times of impact or the time-sequencing of scenarios. A reference timeframe helps to make justifiable choices which provide more useful illustrations. This Central Scenario PID would then form the basis from which all other scenarios would be developed. In other words, if a scenario to evaluate, say, the impact of mining, needed to be developed, then its timing and impacts should be superimposed on the central, climate change scenario.

The Central Scenario thus requires the following main components:

- a deterministic description of the most probable climate state for Sweden, with special reference to the Äspö area;
- a description of the likely nature of the surface environment in the site area at each stage of the climate sequence selected;
- quantitative information on how these changes might affect the disposal system, such that impact points on the PID could be identified and impacts tracked quantitatively through the influence diagram.

It was decided that the timescale of the Central Scenario should be about 100 000 years, as a justifiable description of climate sequence beyond this would become more difficult. Also, this order of magnitude of time falls in well with the principal period of concern in a repository safety assessment. In the event, as the climate sequence model was developed, the actual timescale of the Central Scenario was most conveniently fixed at 120 000 years into the future, with a description which also extended some 10 000 years into the past (see Section 2).

1.1.1 Repository state

In the Reference Case on which the Central Scenario is based, it is assumed that a number of containers of waste are failed at the time of repository closure. There are pin-holes in the outer copper container, but these do not penetrate the inner steel containers. Voids in the containers are filled with sand. Consequently, any changes in future climate could potentially affect radionuclide releases relatively rapidly, and certainly within the 125 000 year period of the Central Scenario.

Other aspects of the Reference Case (which are thus included in the Central Scenario) are that the buffer is emplaced in a 'wet mode' (i.e. no account is taken of buffer resaturation time) and that the repository is completed, backfilled and sealed according to specification. The effects of rock volume resaturation after closure are to be considered in the analysis.

1.2 Objectives and Structure

The central theme of the climate change scenario developed below is that of cyclical glacial conditions affecting the site. A fundamental aspect of the Central Scenario is, thus, the provision of an indicator of the physical and hydrological conditions prevailing during the advance and retreat of an ice sheet, with the aim of identifying critical aspects for modelling impacts of the glaciation EFEP on the far-field groundwater flow component of the PID. This work looks specifically for information on the existence of free water under ice sheets, hydraulic connection between free water in, on and under the ice with groundwater in the underlying rock, the rate of ice build-up and decay at a site-scale and evidence for the geometry of the ice front.

The effect of these and other related features, such as the development of permafrost and sea level changes, are considered in terms of their impact on the following regions of the PID:

- rock stress
- hydrogeology
- groundwater chemistry
- surface conditions

This report, thus, contains:

- an initial description of the climate model developed for the Äspö area with an accompanying broad-scale outline of the predicted surface conditions (Section 2);

- a general review on glacial and ice sheet behaviour and a discussion of the impacts of glaciations on far-field bedrock (Sections 3 & 4);

- a more detailed illustration of the potential surface conditions at the site at each stage of a single glacial cycle, with particular emphasis on the passage of ice (especially the ice-front) across the site (Section 5);

- an illustration of the potential surface conditions at the site at each stage of the 120 000 year climate sequence at the site (Section 6);

- indications of the magnitude of changes in key physical and chemical parameters in the bedrock at each stage of the CS (Section 7);

- a discussion of alternative scenarios to the main CS (Sections 2 & 5);

- final conclusions (Section 9).

Together, this information forms the Central Scenario description for SITE-94. It is stressed that, as predictions of future climate are ultimately uncertain (Section 2), it is the intention of the Central Scenario to provide an *illustration* of the *potential* degree of variability and significance of future climatic changes on the evolution of a deep repository site. However, Performance Assessment calculations also require that it must ultimately provide a *single,* albeit non-unique, evolutionary sequence, with associated impacts, onto which other scenarios can be superimposed. However, it is also necessary to identify as many of the potential variables involved in the future glacial evolution of the site as possible, in addition to defining a single scenario sequence. This allowed at least a qualitative understanding of the assumptions and uncertainties involved in defining a single Central Scenario, and may allow alternative scenarios to be erected if necessary.

2 On the Relation Between Past and future Climates

2.1 Introduction

Attempting to predict future climate changes is a difficult task, requiring knowledge and understanding of the earth's past climate changes as well as a model for predicting the future. Soon after it was recognised that vast areas of Europe and North America have been glaciated, the amount of evidence for more than one glaciation increased. It is now known that a period of glaciations, especially in the Northern Hemisphere, started some 2.3 million years ago and, since then, during the Quaternary period, a considerable number of glaciations, interrupted by warmer interglacials, have been documented (Figure 2.1). The periodicity of the glacial/interglacial sequence approaches a 100 000 year cycle during the middle and late Pleistocene (Figure 2.1). This knowledge of Quaternary glaciations allows a preliminary prognosis of future glaciations. The last interglacial, the Eemian (c.115 000-130 000 years BP), was c.10 000 - 15 000 years long. As the present warm period, the Holocene, has lasted about this long and as the Holocene climatic optimum passed several thousand years ago, it is probable that the cooling of the next glaciation has already begun. The great uncertainty in this simple prediction is that it does not consider the causes of the glacial/interglacial cycles. A more elaborate prognosis of future climate would need a climate model based on the variables which regulate the glacial/interglacial cycles. This report aims to present a probable scenario of future climate and glaciations based on a number of published climate models. It is important to note that, as a scenario and not a prognosis, it describes a plausible sequence of events, not accounting for alternative paths and parameters.

Many theories on the origin of the glacial cycles have been presented, but it was not until the 1970's that a theory, the Milankovitch theory, was commonly accepted. The general acceptance of the Milankovitch forcing of climate, and its confirmation through oxygen isotope stratigraphy in deep-sea sediments, makes it, at present, the best tool for climate predictions within the time-span relevant for deposition of spent nuclear fuel. In this scenario description, Milankovitch forcing on climate and its likely implications for future glacial-interglacial cycles, sea level changes, and crustal movements of glaciated regions are, thus, presented and discussed.

The scenario is described in general for the whole of Scandinavia and more specifically for the Stockholm and Äspö regions. The basis for the development of the SITE-94 climate change scenario are the Climate model by Imbrie & Imbrie (1980), the ACLIN (Astronomical climate index) model, and the PCM model by Berger et al. (1990). All of these models consider the Milankovitch orbital parameters as the main factor for large-scale climate forcing. In applying the results of these models, it is important to note that they are not appropriate for frequencies more rapid than c.20 000 years.

In the scenario of future climate changes, the possible effects of human activities (e.g. greenhouse warming) have not been considered, as they are difficult to assess quantitatively in detail. Human effects could prolong the present state of climate or result in global warming, but this effect is not considered to hinder the next cold phase, merely delay it in the perspective of the next 120 000 years. It must also be remembered that the current, ongoing rise in atmospheric CO_2 content owing to the use of fossil fuels will only give a short lived climatic effect. This as the fossil fuel resources will be extinguished in a rather short time. The anthropogenic CO_2 effect on the climate could, thus, be expected to cease within, perhaps, 1000 years. More long-lived effects on the global climate could be expected only if warming during this short period were to trigger some major climate regulator with long periodicity (such as the melting of large ice sheets).

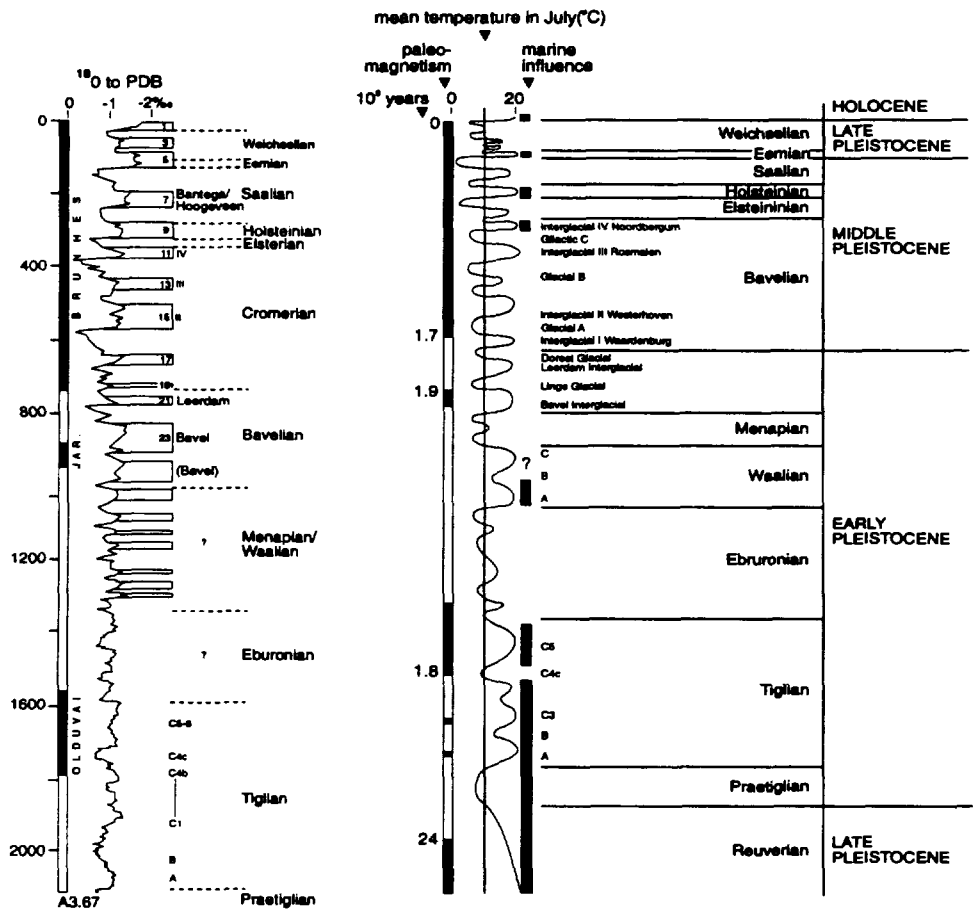

Figure 2.1. Quaternary climate stratigraphy for the Netherlands compared to a marine ∂ ^{18}O record (core V 28-239 from Shackleton & Opdyke, 1973). From Zagwijn (1989).

2.2 Climate Variations and Milankovitch Forcing

The variation of incoming solar radiation due to Earth-orbital changes was proposed by the astronomer Milankovitch (1941), who suggested that the glacial-interglacial cycles were controlled by seasonal, especially summer, insolation variations around the latitude of 65°N. These insolation anomalies were caused by cyclic changes in the three Earth orbital parameters: eccentricity (cycles of ~100 000 and 413 000 years), obliquity (with a 41 000 year cycle) and precession, with a cycle around 22 000 years (Figures 2.2 and 2.3). At middle and low latitudes, the precessional parameters are strongest, while the 41 000-year tilt period is strongest at winter high latitudes. The eccentricity variations cause only minor shifts in the average annual amount of insolation received (Berger, 1984); however, eccentricity is the primary control on the amplitude of the precessional signal, which in turn controls the seasonal distribution of insolation received (Ruddiman & Wright, 1987). From astronomical calculations (e.g. Berger, 1978, 1995), the form of these orbital changes is known for the past and for the future (Figure 2.2). Hays et al. (1976) were the first to demonstrate detailed evidence that these orbital cycles dominate the ^{18}O signal in the deep sea sediments which reflect the global ice volume. Later, Imbrie et al. (1984) refined the methodology and analysed the last 700 000 years, further confirming the theory. In Imbrie et al. (1992), the responses to Milankovitch forcing are discussed and combined into a dynamic system model.

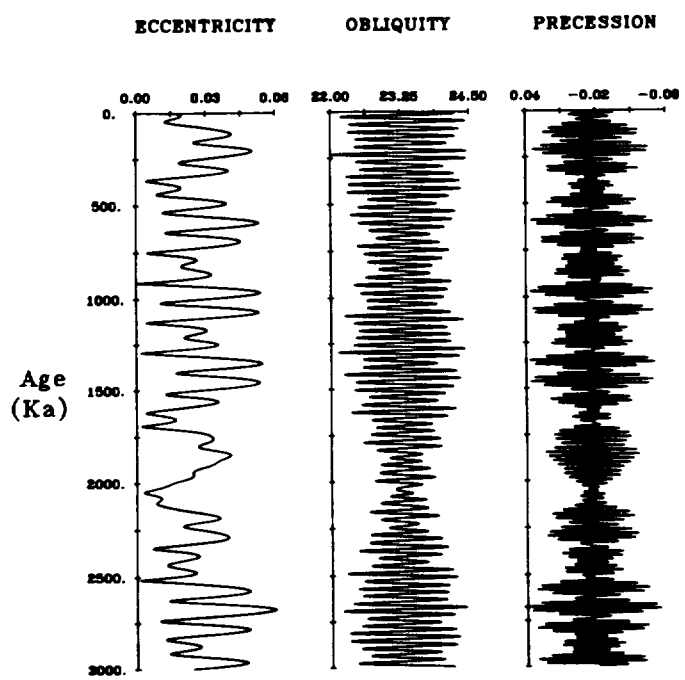

Figure 2.2. Variations over the last 3 000 000 years of the three major components of the earth's orbit around the sun: eccentricity, obliquity, and precession. Precession is shown as the precessional index (e sin w), which incorporates the modulating effect of eccentricity. From Ruddiman & Wright (1987).

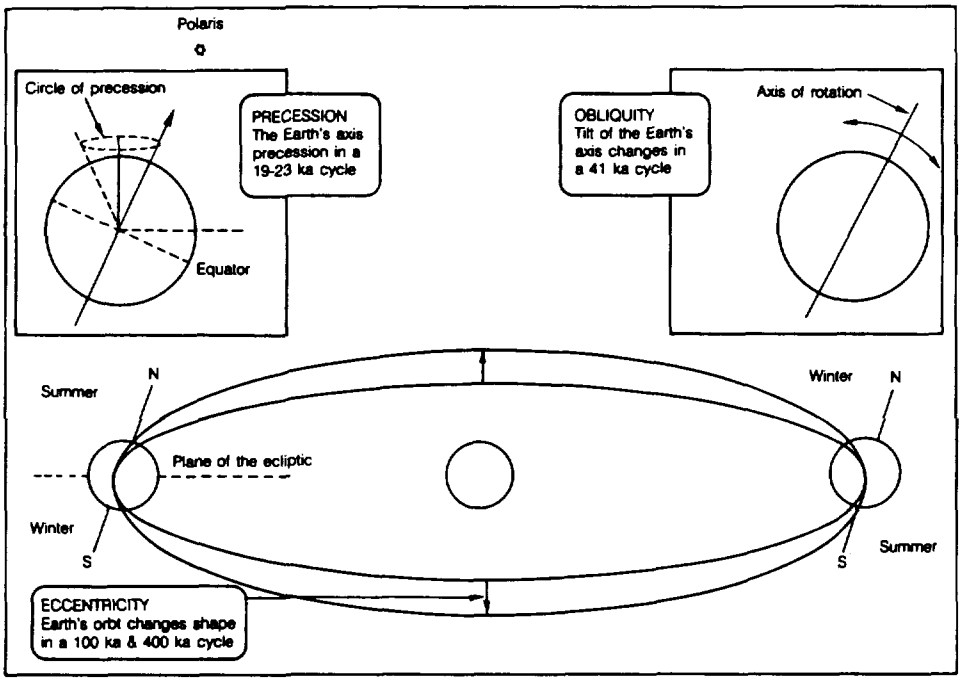

Figure 2.3. Principles of Earth's orbital elements. From Ruddiman & Wright (1987).

One weak point in the theory of Milankovitch forcing of the glacial cycles is that the 100 000-year cycle of glaciations is so prominent during the late Pleistocene. The orbital variations show a parameter with this periodicity, the eccentricity, but its impact on insolation is very weak (Hays et al., 1976, Imbrie et al., 1993). To explain the dominance of these 100 000-year cycles, other factors, such as the regulating effect of large ice sheets or changes in deep ocean circulation or ocean-ice interactions, often have to be included in the models. The model by Imbrie & Imbrie (1980) incorporates a non-linear component, designating that the impact of insolation on ice volume is delayed and deglaciation is four times as rapid as the building up of glaciers. However, the model still does not give enough power to the 100 000-year cycle. Imbrie et al. (1993) gives a thorough discussion of the 100 000-year cycle and explains it with the self-regulating effect of northern hemisphere ice sheets—after they reach a critical size, they cease to respond as Milankovitch slaves. Peltier (1987) discusses and models the importance of glacial isostatic adjustment in the mechanism of long-term climatic change. In the model by Peltier, glaciations are forced by insolation changes and a 100 000-year cycle for glaciations is reached by applying a reasonable viscosity of the mantle. In a model by Saltzman & Verbitsky (1992), intermittent episodes with either 40 000-year or 100 000-year periodicity are obtained in a dynamic system forced by Milankovitch and regulated by CO_2 effects and glacio-isostatic downwarping of bedrock. Liu (1992) proposes that variations in the frequency of the obliquity cycle can give rise to strong 100 000-year forcing of climate which, primarily, will give rapid glacier melting.

In the search for the 100 000-year climate cycle, a previously unknown 100 000-year cycle of orbital inclination has been identified, which might interact with climate through regulating accretion of interplanetary dust (Muller & MacDonald, 1995; Brownlee, 1995; Farley & Paterson, 1995).

Other factors which may regulate the ice sheets are basal sliding and the feedback between sea level and ice sheet extent, as discussed by Denton & Hughes (1983). In conclusion, it seems probable that Milankovitch forcing has triggered the periodicity of past glaciations and will in the future. However, other variables have influenced the dynamics and enhanced the 100 000-year periodicity. Among these, the self regulating effect of large ice sheets, induced changes in the CO_2 content of atmosphere and the glacio-isostatic depression of glaciated areas seem to be the most important.

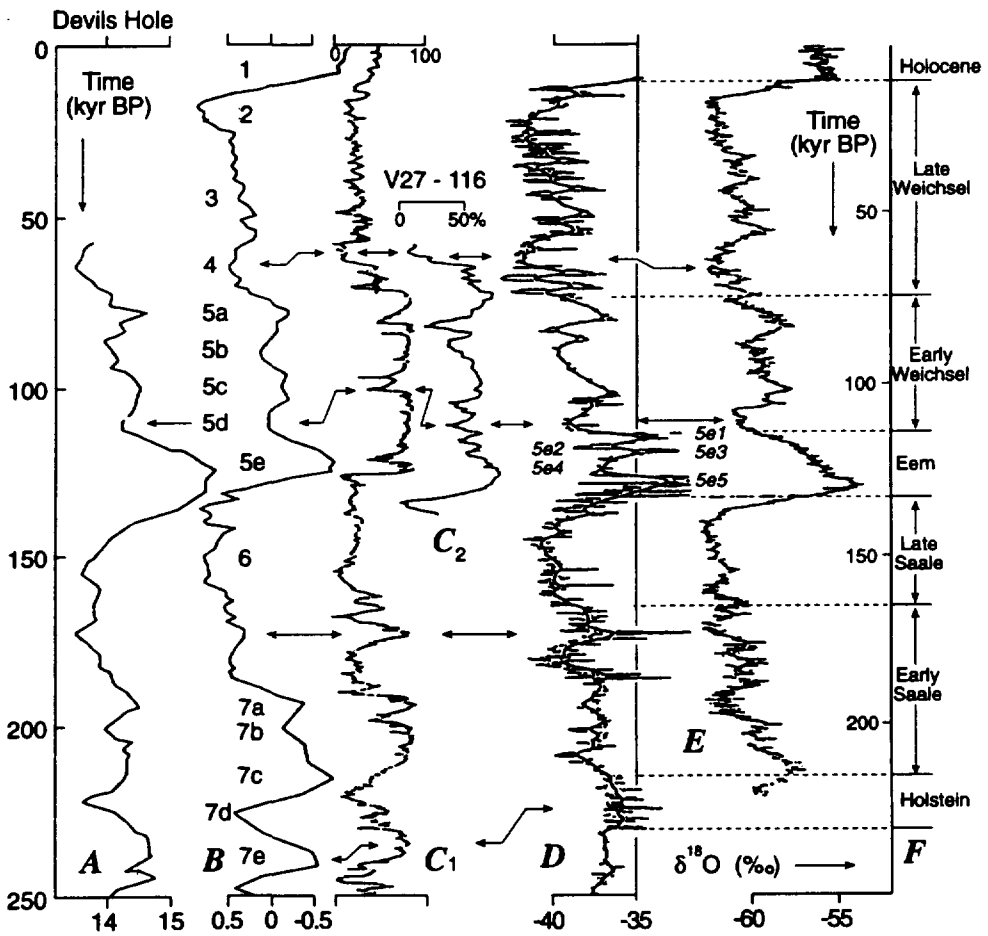

Figure 2.4. Different climate records for the last glacial cycles. **(A)** ∂ ^{18}O variations in calcite from Devils Hole. **(B)** SPECMAP standard marine isotope curve. **(C_1)** grey scale measurements on marine core DSDP site 609. **(C_2)** Calcium carbonate content in marine core V27-116. **(D)** ∂ ^{18}O record of the GRIP summit ice core from Central Greenland. **(E)** ∂ ^{18}O record from Vostok ice core from East Antarctica. From Dansgaard et al. (1993).

Recent results from central Greenland ice cores have been presented by Dansgaard et al. (1993; Figure 2.4). Detailed ^{18}O measurements show that the climate during the last 230 000 years has been very unstable, with abrupt climate changes during the last two glacial-interglacial cycles. Development during the Holocene has differed in that the ^{18}O record shows a gradual, more stable development. These findings further emphasise that Milankovitch forcing gives only part of the background for climatic changes and that the North Atlantic region at least has been affected by 'flip-flop' variation of climate which is not fully understood at present and is, thus, hard to predict.

2.3 The Relation Between Climate and Global Sea Level

The growth and decay of large ice sheets influences global sea level in several ways. The most important contribution is glacio-eustasy, which is directly related to the amount of water frozen into glaciers. At present, a considerable amount of water is frozen into glaciers. Estimations of eustatic sea level potential shows that the melting of the Antarctic ice sheet could produce a 65 m sea level rise, the melting of the Greenland ice 7 m and the melting of small ice caps only a few tenths of a metre. An extreme in the sea level scenario would result from a climate warm enough to melt these glaciers. The resulting eustatic sea level rise would, however, be moderated and unevenly distributed owing to the isostatic effects of disappearing ice and increased loading on the ocean floors. In addition, a sea level rise in the order of 1 to 2 m could occur owing to the thermal expansion of oceans (Manabe & Stouffer, 1995).

The other extreme in sea level would occur during culmination of a glacial period, with large amounts of water frozen into continental ice sheets. During the last glacial maximum, glacio-eustasy resulted in a sea level c.120 m lower than today (Fairbanks, 1989) and similar values are given for the second to last glacial (Chappell and Shackleton, 1986). The large ice sheets also influence sea level by their gravitational force, the glacio-geoidal eustasy. This causes a redistribution of water, sea level rise near the ice and fall further away (Fjeldskaar & Kanestrom, 1980). The glacier-induced redistribution of water between oceans and land affects sea level through a global hydro-isostatic effect; the sea-floor of the oceans is depressed by the load of water released from the melting glaciers, and vice versa during glacier build-up. The mass in the mantle transported away from below the oceans during a sea level rise will be transferred to the continental areas and cause a land uplift there (Clark et al., 1978). As a consequence of the hydro-isostatic effect, the global sea level rise will only be registered in its full extent in oceanic areas; at a continental margin the registered sea level rise will be lower. In the case of a rapid sea level rise, isostatic equilibrium will be delayed, thereby both deflecting the geoid and modifying the rate of sea level change. As a result, this effect will, thus, considerably disturb the shape of a reconstructed shore displacement curve. To estimate the extent of hydro-isostatic deflection at a continental margin, such as Sweden, where it causes shoreline tilting and

uplift, is difficult. For example, the model by Clark et al. (1978) was not refined enough to resolve this. The response of the Baltic Sea to hydro-isostasy during a glacial cycle is not possible to predict without geophysical modelling and is, thus, not accounted for in the scenario described below. A rough estimate of the effect would be that the glacio-eustatic sea level lowering during a major glacial build-up and maximum would be several tens of metres less here than at an oceanic island, if glacio-isostasy were not taken into account.

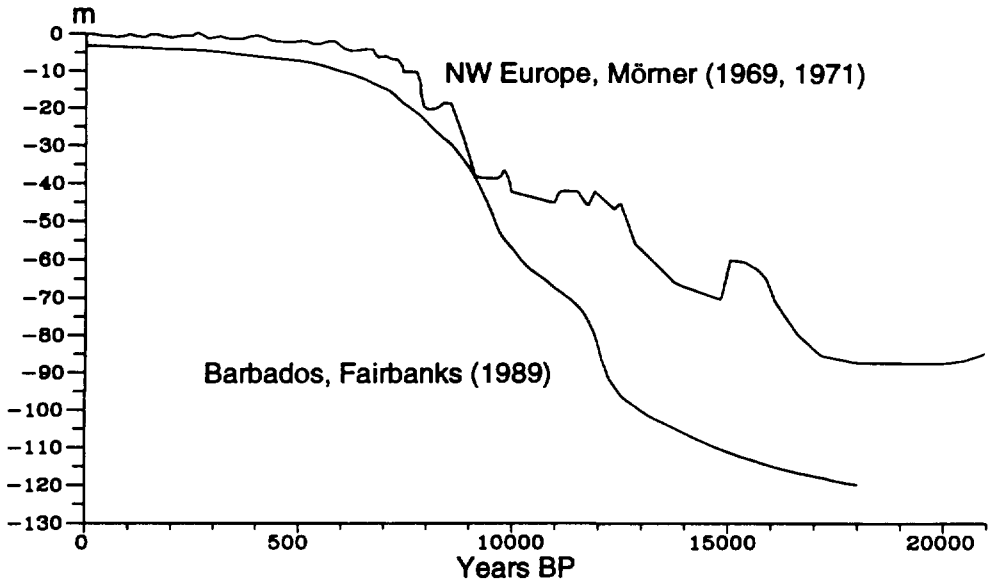

Figure 2.5. Eustatic sea level curves from Barbados (Fairbanks, 1989) and for NW Europe (Mörner, 1969; 1971).

Records of past sea level fluctuations for the time period before the mid Holocene outside the area of glacio-isostatic uplift are quite scarce. The most detailed record is a sea level curve reconstructed from corals at Barbados (Fairbanks, 1989; Figure 2.5). In this study, offshore coral reefs were investigated by drillholes down to a depth of 140 metres. A coral species, *Acropora palmata*, which is known to live at water depths less than 5 metres, was sampled and dated using ^{14}C to establish the sea level rise. The curve (Figure 2.5) shows a sea level rise from -120 m at 18 000 years BP, at a time close to the last glacial maximum. The highest rate of sea level rise was recorded in the early Holocene, owing to the large amounts of meltwater reaching the oceans at that time. Mörner (1969, 1971) has constructed a eustatic sea level curve for NW Europe (Figure 2.5) using shoreline data from a glacio-isostatically affected area. He based his eustatic curve on isostatic land upheaval, deduced from changes in shoreline gradients, and combined it through iterative testing with detailed shore displacement curves and previously published approximate eustatic curves. The curve by Mörner

(1969, 1971) shows a somewhat smaller total eustatic sea level rise than registered at Barbados by Fairbanks (1989). These differences between NW Europe and Barbados in the total sea level rise could be because of the difference in hydro-isostasy between oceanic and continental areas discussed above. Sea level records predating the last glacial maximum are also scarce. Uplifted shore terraces at New Guinea (Chappell and Shackleton, 1986) give a reasonably continuous record for the last glacial period (Figure 2.6). In constructing the scenario, the sea level records from New Guinea and Barbados are very important as they are the main source of knowledge on global sea level changes during a full glacial cycle.

Another method of estimating past sea levels in detail is through interpretation of oxygen isotope ratios of foraminifera from deep sea sediments. Ideally, the oxygen isotope composition of marine sediments should closely reflect the global ice volume and the glacio-eustatic component of sea level change, as heavier isotopes are enriched in seawater during glacier build-up. A major problem with this method, as shown by Shackleton (1987) and Fairbanks (1989), is that a significant part of the observed isotope variation is not ascribed to glacial volume and sea level, but is due to temperature changes of seawater. Shackleton (1987) attempted to derive the sea level induced part of oxygen isotope variations to obtain detailed reconstructions of past sea level (Figure 2.6). This attempt is based on a combination of ^{18}O data from both planktonic and benthonic foraminifera and is, thus, intended to minimise the effect of temperature variations.

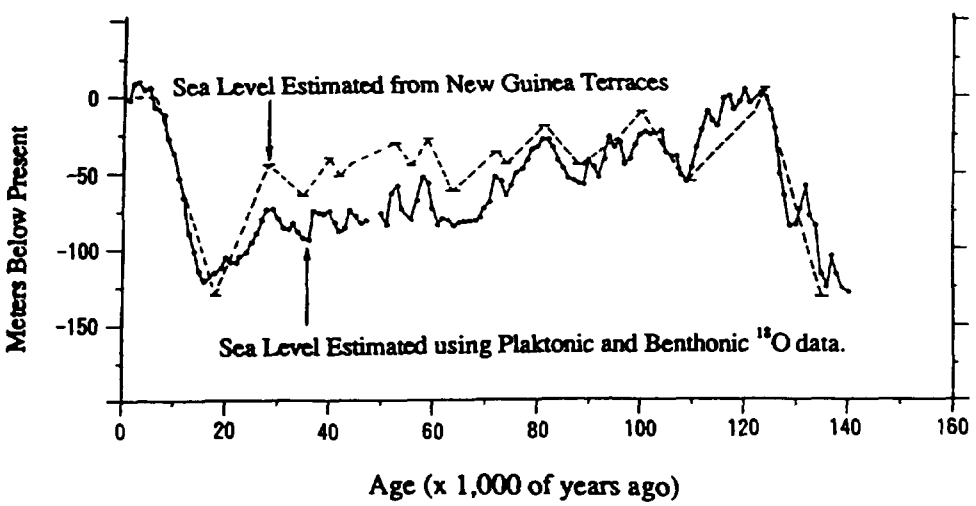

Figure 2.6. Long sea level records: **(Dashed)** Estimated from New Guinea shore terraces. From Chappell & Shackleton (1986). **(Solid)** Estimated from ^{18}O records of Benthic and Planktonic foraminifers. From Shackleton (1987).

2.4 The Interaction Between Glaciers and Local Sea Level

The relative sea level changes recorded in or near glaciated areas are a combination of sea level changes of a more global character, described above; those introduced locally by the ice sheet are mainly from glacio-isostasy and glacio-geoidal change. The evidence of past glacio-isostasy is obtained from uplifted shorelines, today found in Scandinavia up to nearly 300 m above present-day sea level in the areas most affected by glacio-isostasy (Figure 2.8b). The glacio-isostatic downwarp caused a considerable part of present-day Fennoscandia to be below sea level after the deglaciation (Figure 2.7). The maximum level reached by the sea (and the dammed Baltic) is often referred to as the highest coastline, which was normally developed at the onset of the local deglaciation and is, thus, of varying age. The glacio-isostatic uplift began when the ice load started to decrease; thus, a considerable part of the uplift took place before deglaciation and is not recorded by the shore lines.

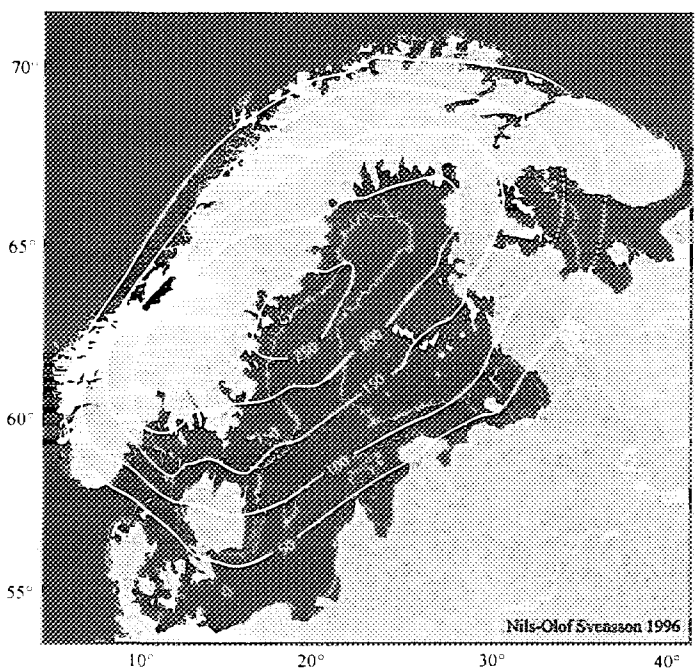

Figure 2.7. Reconstruction of the metachronous highest shoreline of Fennoscandia. From Svensson (1996).

The glacio-isostasy resulting from the last Weichselian glaciation has been modelled by several authors. According to Mörner's (1979) calculations, the absolute Fennoscandian uplift in the centre of the uplift cone in northern Sweden is slightly more than 800 m. The model of Fjeldskaar (personal comm. and Fjeldskaar & Cathles, 1991) gives slightly lower values of the

maximum isostatic deflection, around 700 m, based mainly on a thick ice model and best-fitting earth rheology parameters. In the Stockholm region, Mörner's (1979) uplift model gives values of c.500 m absolute uplift, while Fjeldskaar's model shows larger values around 600-700 m.

The present-day land uplift of Fennoscandia (Figure 2.8a) is generally interpreted as a remnant of glacio-isostasy although a tectonic component could exist. Estimates of remaining glacio-isostatic land uplift are quite varying as they mostly depend on the size of the assumed glacio-isostatically induced geoid depression of Fennoscandia. Assuming a remaining glacio-isostatically induced geoid depression of c.10 m, the remaining uplift was calculated by Bjerhammar (1977) to be 116 m, and by Kakkuri (1987) to be 80-130 m with a relaxation time of 7000-12 000 years. However, large parts of the geoid depression seem to be caused by increased crustal thickness (Andersen, 1984). Thus, the glacio-isostatic part of the geoid low is only c.2 m and calculations based on this value give a remaining land uplift of c.30 m for the uplift centre (Ekman, 1989). An effect of glaciation outside the glacier margin is the forebulge. Its appearance is predicted especially in earth models applying mantle flow in limited layers or channels. Observational evidence of this feature is weak and it is not easy to estimate its timing and extent from published earth rheology models. Thus, the forebulge is not included in the climate change scenario (yet see later sections for further discussions).

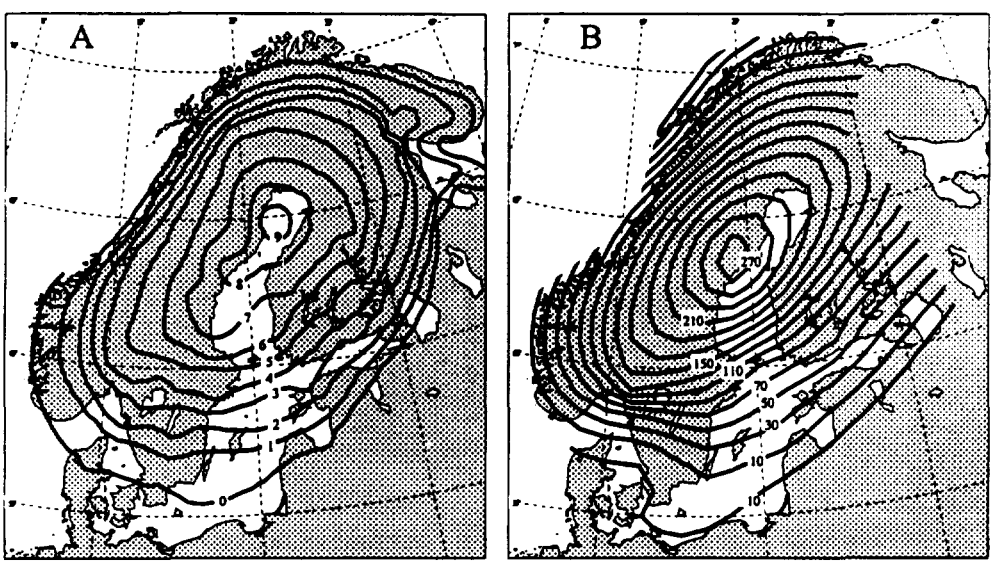

Figure 2.8. **(a)** Present-day relative land uplift of Fennoscandia, in mm/yr. Based on data from Ekman (1977). **(b)** Isolines of the 9 300 BP shoreline in metres above present-day sea level. From Svensson (1996).

2.5 Climate Models

For constructing the scenario, Milankovitch-based climate models were chosen. However, these models have several shortcomings. The worst shortcoming may be that, despite the strong connection between Milankovitch forcing and climate changes during the Quaternary, the reasons for this connection are still obscure. The changes in insolation owing to orbital forcing are not large enough to directly cause the glacial cycles of the Quaternary, but need to be amplified by some other factors such as albedo effects, $C0_2$ variations or ocean response. These effects will be of considerable strength when an ice age has been initiated and ice sheets have grown to some extent, but what will amplify the orbital signal enough to initiate ice growth is not known. In addition, the main glacial frequency of the late Pleistocene is 100 000 years, a very weak frequency of insolation.

A common feature of the Milankovitch-based models is that they are based on insolation changes for the Northern Hemisphere; most orbital parameters give an opposite effect for the Southern Hemisphere. As the Ice Age cycles are simultaneous on both hemispheres there must be other, not fully understood, climate links between the hemispheres.

Despite the uncertainties affecting Milankovitch-based climate models, they have been shown to reproduce past climate changes very well and are the best alternative for reconstructing future climate with the present knowledge.

2.5.1 The Imbrie Model

The model by Imbrie & Imbrie (1980) is a time-dependent model developed to simulate the glacial history for the past 500 000 years. It is based on orbital forced insolation changes for 65°N and is matched to fit the $\partial\ ^{18}O$ deep-sea record RC11-20. The model incorporates two non-linear factors which have been tuned to obtain the best fit with the deep-sea record. The first factor is a slow time constant for the ice sheets to react on changes in insolation (17 000 years). The second factor is that the time constant during ice growth is four times longer than that during times of ice decay. In the model, anthropogenic and other possible sources of variation acting at frequencies higher than one cycle per 19 000 years are ignored. The result of the modelling represents the total volume of land ice in arbitrary units and the climate curve calculated for the next 100 000 years (Figures 2.9 and 2.14c).

2.5.2 The Aclin Model

The Astronomical Climate Index, ACLIN, was calculated by Kukla et al. (1981). It is a model combining the three orbital elements to index curves aimed to be correlated to palaeoclimate records from pollen-data, sea level

and ∂ ^{18}O records. The model gets the best fit with the palaeoclimate records when a time lag of 5000-6000 years is used. Its general agreement with the palaeoclimate records allows a prediction of future climate (Figure 2.14d).

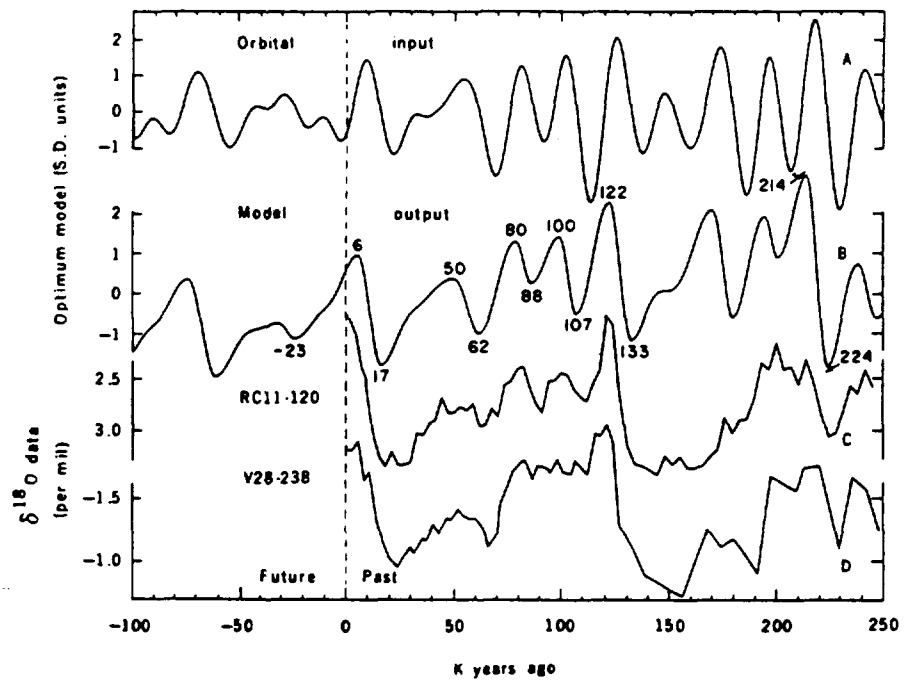

Figure 2.9. Input and output of Imbrie and Imbrie's (1980) response model, compared with isotopic data on climate of the past 250 000 years. **(A)** Orbital input corresponding to an irradiation curve for July at 65°N. **(B)** Output of a system function with a mean time constant of 17 000 years and a ratio of 4:1 between the time constants of glacial growth and melting. Ages of selected maxima and minima are given in thousands of years. According to this model, the influence of orbital variations over the next 23 000 years will be to enlarge continental ice sheets. **(C)** Oxygen isotope curve for deep-sea core RC11-120 from the southern Indian Ocean (Hays et al., 1976). **(D)** Oxygen isotope curve for deep-sea core V28-238 (Shackleton and Opdyke, 1973) from the Pacific Ocean. Curves C and D are plotted against the TUNE-UP time scale of Hays et al. (1976). From Imbrie and Imbrie (1980).

2.5.3 The PCM Model

The PCM model presented by Berger et al. (1990) is a two-dimensional climate model coupled with an ice sheet model. The model takes into account feedbacks between the atmosphere, the upper ocean, sea ice, ice sheets and the lithosphere. The model gives a good fit with the low frequency part of deep sea records and sea level records, however after 6 000 BP, ice volumes of Greenland and N America are overestimated. The model has also given

results for the coming 80 000 years (Figure 2.14f).

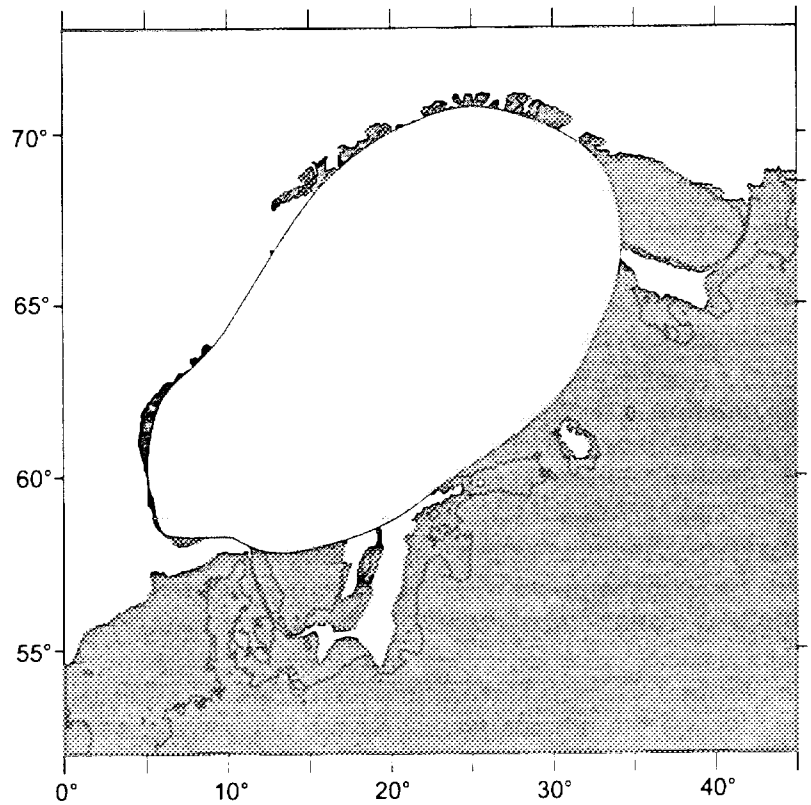

Figure 2.10. Scandinavia during the Mid Weichselian. A eustatic sea level of -60 m is assumed. Elevation data from ETOPO5 is used in the reconstruction. Also based, in part, on reconstructions by Lagerlund (1987), Lundqvist (1992) and Anderson & Mangerud (1989).

2.6 Glaciation, Glacial Isostasy and Sea Level in Fennoscandia During the Weichselian and Holocene

Comparison with the Weichselian glaciation of Scandinavia has been the main tool in constructing the scenario for future glaciations. Unfortunately the knowledge of the onset and evolution of this glacial before its maximum is quite limited. This limited knowledge is mainly because the ice in most parts of Scandinavia during the Late Weichselian has removed or hidden most of the older deposits. Reconstruction of a complete Weichselian record is, thus, to a large extent, based on scattered stratigraphic records. The difficulties in dating and correlating these fragments are large, as they are mostly beyond the limit of ^{14}C dating. Correlation with deep-sea stratigraphies and central European pollen records are thus crucial.

According to a summary by Lundqvist (1992; see top of Figure 2.11), the first Weichselian glaciation in Sweden took place during isotope stage 5d (ages of the isotope stages are shown in the lower part of Figure 2.11). Its ice extent is unknown, but the ice margin possibly was situated in central-northeastern Sweden. Following this was the Peräpohjola Interstadial, probably with only a restricted mountainous glaciation. Later, during isotope stage 5b, a quite extensive glaciation followed with its ice margin possibly extending across south-central Sweden. Afterwards, during the Tärendö Interstadial, the ice withdrew to the mountains. During isotope stage 3+4, the ice advanced to southern Sweden but it was not until isotope stage 2 or c.20 kyr BP that the ice reached its maximum position, covering the whole of Sweden. The southernmost province of Sweden, Scania, was not reached by any Weichselian glaciation until c.21 000 BP and was deglaciated around 13 000 BP (Berglund & Lagerlund, 1981).

As mentioned the Weichselian glaciation in Norrbotten, northernmost Sweden was also interrupted by warmer interstadials. Lagerbäck & Robertsson (1988) and Aronsson et al. (1993) describe the deposits of these interstadials, the Peräpohjola and Tärendö interstadials. According to analyses of plants and insect remains (mainly Coleoptera) in deposits from the Peräpohjola interstadial, the climate was Arctic or sub-arctic with a mean summer temperature of c.8-12 °C (Aronsson et al., 1993).

In Northern Denmark, a continuous marine record exists from the Eemian up to c.20 000 BP, when a glacial advance reached the area (Sörensen-Aaris et al., 1990). In this marine record, a sequence with ice-dropped stones, a drop till with stone material originating from the southern Baltic reveals a Baltic ice advance, the Old Baltic Ice. It is correlated to isotope stage 4, i.e. early Middle Weichselian, and its till deposits are found in Southern Denmark (Petersen, 1984). In Denmark, a considerable number of Mammoth remains have been found. The datings performed mainly on a number of Mammoth tusks indicate ages between 32 000 and 21 000 BP, together with one around 44 000 BP and a few of infinite ages (Sörensen-Aaris et al., 1990). This implies that the period 44 000 to 20 000 BP was ice-free in Denmark and that the last glaciation in Denmark only lasted about 7000 years.

The glacial stratigraphies of Fennoscandia have been compiled into schematic glaciation curves by Lundqvist (1992; Figure 2.11) and Anderson & Mangerud (1989; Figures 2.11 and 2.14h). The Scandinavian glaciation record has shown that glaciation of a large area could be quite a fast process. One process contributing to the fast glaciation observed could be the outlet surges described by Lagerlund (1987). According to Lagerlund's theory, outlet surges occurred when the cold-based Weichselian ice advanced into water-filled deep basins of the Baltic (e.g. the central Baltic). The ice then became warm-based at the front and surged into the basin and filled it with ice with low surface gradient. At this advanced position, the ice thickness was built up and, after advancing to the next basin of the Baltic, a new outlet surge could occur. This process could increase the rate of glacier advance in the

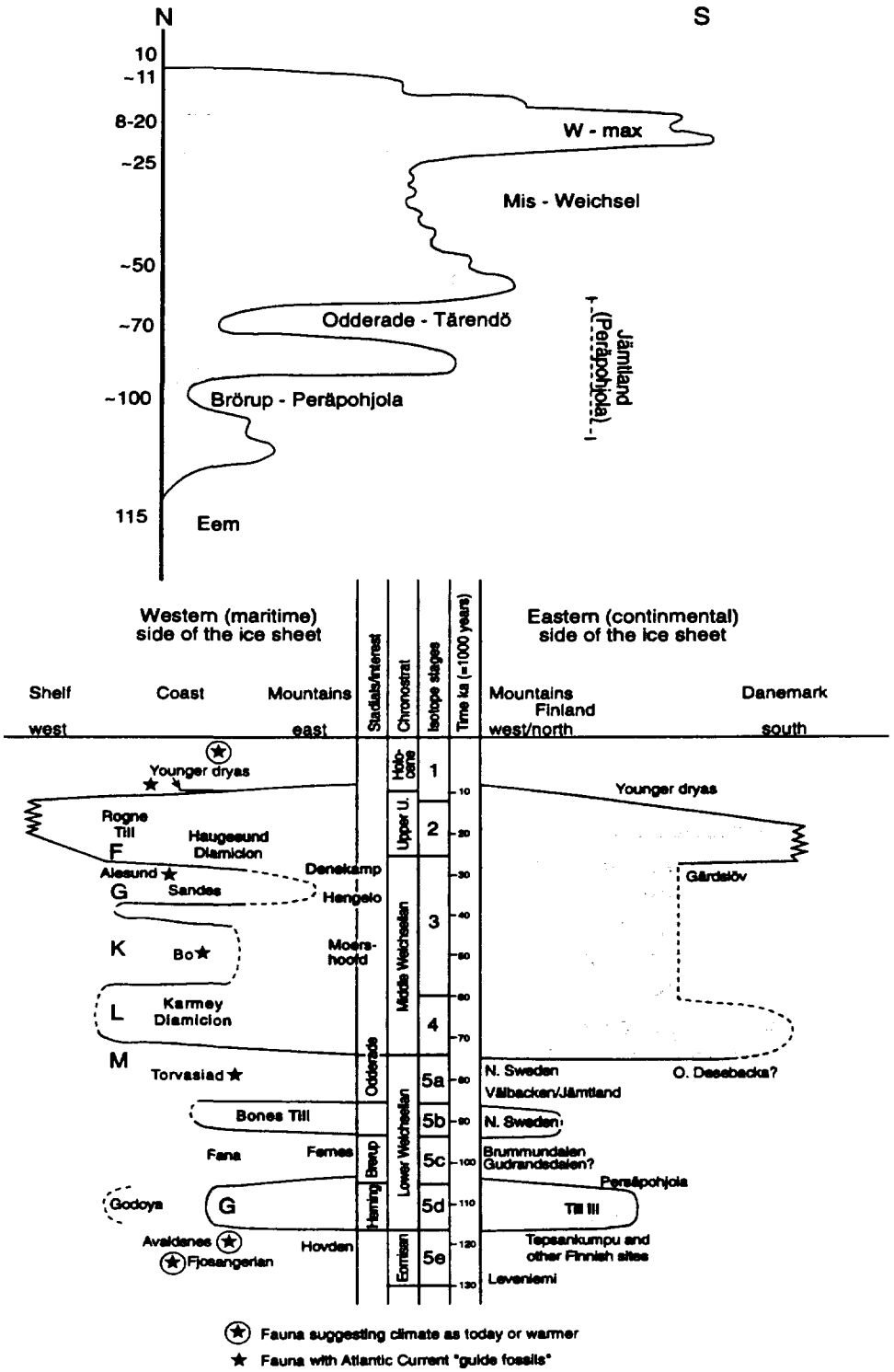

Figure 2.11. Glaciation curves for the Weichselian in Sweden. (**Top**) From Lundqvist (1992), the extent of ice before c.25 000 BP is uncertain. (**Bottom**) From Anderson & Mangerud (1989).

Baltic basin. It also introduces the possibility of Old Baltic Mid Weichselian ice reaching Denmark through the southern Baltic without glaciating Scania.

Records of shorelines and shore displacement for Fennoscandia only exist for the period after the last deglaciation. The only exceptions are some sites in Finland, where deposits related to Eemian sea levels described by Eronen (1989) have been described. These deposits indicate significant differences in the glacio-isostatic pattern between the Saalian (130 000-210 000 BP) and Weichselian glaciations, thus making reconstruction of future glacio-isostasy even more uncertain.

The highest shoreline of Fennoscandia (Figures 2.7 and 2.12), was formed by the sea or by the dammed Baltic. This normally occurs at the time of deglaciation, but the highest shoreline could also have formed during a later transgression. This shoreline is, thus, metachronously formed in different parts of Fennoscandia. Its age is c.13 000 B.P. in southern Sweden and c.8500 B.P. in northern Sweden. The elevation to which this shoreline has been uplifted varies with the extent of land uplift since the time of deglaciation, and its elevation is a few tenths of metres in Scania, increasing northwards to nearly 300 m in Ångermanland. It seems reasonable to expect similar sea levels following a future major glaciation, although the differences in sea levels between the Eemian and Holocene (Eronen, 1989) make this assumption somewhat doubtful. In the Baltic basin, the scenario reconstruction is complicated since the water level may have been higher than the oceans due to periodical damming. The outlet from the Baltic to the ocean was variable and characterised by erosion and deposition. Following the last glaciation, the outlet path has shifted five times before the present-day situation was reached. During the Mid Weichselian, the outlet was probably through the Alnarp Valley in southern Scania (Lagerlund, 1987; Miller, 1977). During early parts of the Eemian interglacial, a connection between the Baltic and the White Sea seems probable (Forsström et al., 1988). Diatom records show higher salinity and more pronounced marine influence during the Eemian than recorded during the Holocene (Forsström et al., 1988).

The amount and rates of Fennoscandian shore displacements are very variable, due to the various extent of the glacio-isostatic uplift (Figure 2.10). Within the Baltic basin, several periods of damming strongly influenced the pattern of shore displacement during the Late Weichselian and early Holocene. Generally, in the Late Weichselian shore-displacement is characterised by a rather rapid regression (Figure 2.12). However, in places close to the Younger Dryas ice margin, distinctly reduced rates of regression or even a transgression are seen. This is due to the increased glacio-isostatic loading of the advancing ice sheet. (Anundsen, 1990; Björck & Digerfeldt, 1991). During the Early Holocene, the rates of glacio-isostatic land uplift in large parts of Scandinavia were still higher than the eustatic rise of the sea. During the first part of this period, the sea level fell far below present-day sea level in southernmost Sweden. Later, in the Holocene, shore displacement was characterised by the eustatically rising sea level, the Post-glacial

transgression (the Littorina transgression in the Baltic). Only in regions of high land uplift was no transgression recorded.

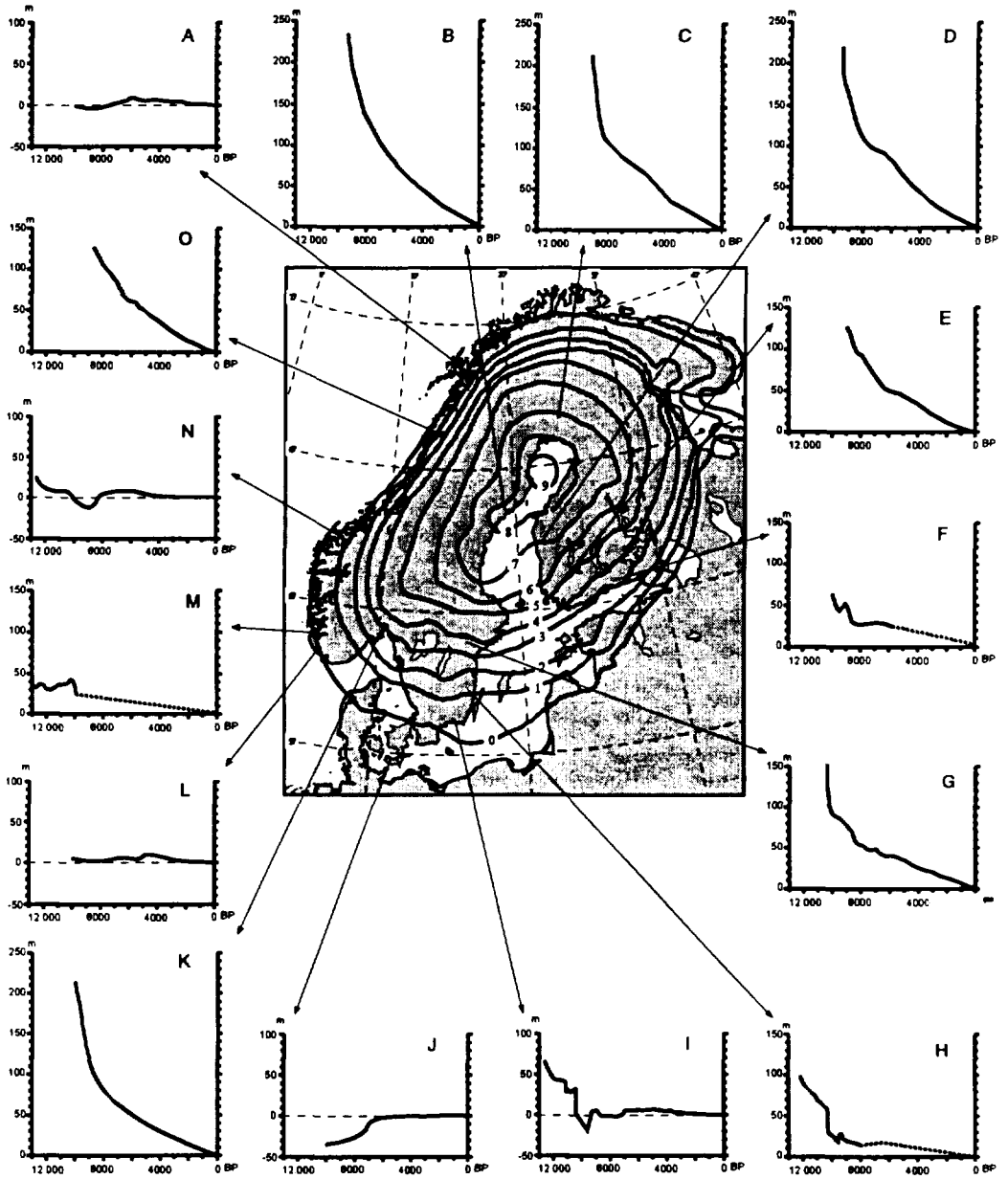

Figure 2.12. Selected Fennoscandian shore-displacement curves for areas with different rates of present-day land uplift (isoline map). From Svensson (1996), where full references are given.

Reconstructing sea level changes after a future major glaciation, assuming similar ice distribution as during the Late Weichselian, could be achieved by

applying a rather straightforward parallel. However, for the period of glacier build-up and for more limited glaciations, larger uncertainties arise. One reason for these uncertainties is the lack of Scandinavian sea level observations for the Early and Mid Weichselian. Furthermore, the global ice volume regulating the eustatic sea level need not to be fully in phase with the Scandinavian ice build-up.

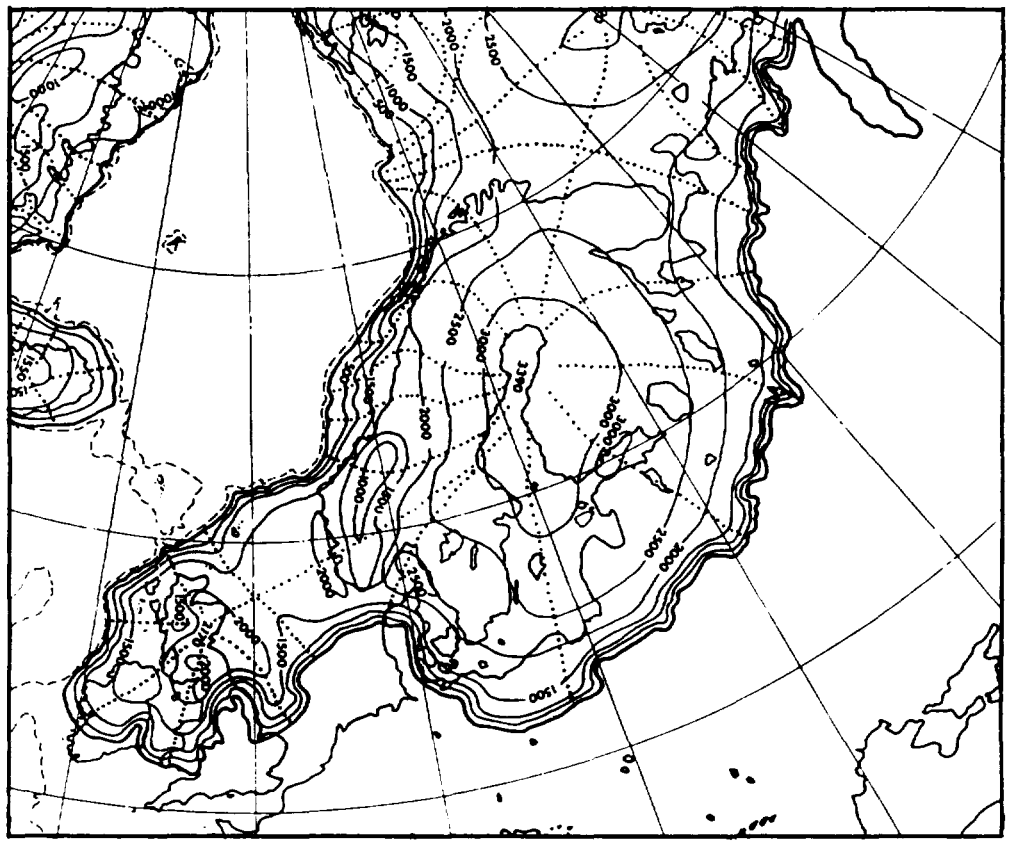

Figure 2.13. Reconstruction of the Fennoscandian ice sheet. From Andersen (1981).

The thickness of the Weichselian ice sheet is an important control on glacio-isostasy. Various ice models have been presented; one of the most frequently used is by Andersen (1981; Figure 2.13). The model describes a Northwest European ice sheet with a maximum thickness of c.3000 m and individual domes for the British Isles, Fennoscandia and Barents sea during the Late Weichselian maximum. The knowledge of ice extent during the Late Weichselian maximum and later recession is considered as rather good but in some areas, especially in the North Sea and Barents Sea, uncertainties exist. A greater uncertainty of much importance to the scenario is the thickness of ice, since there are no direct observations of the ice thickness. Several

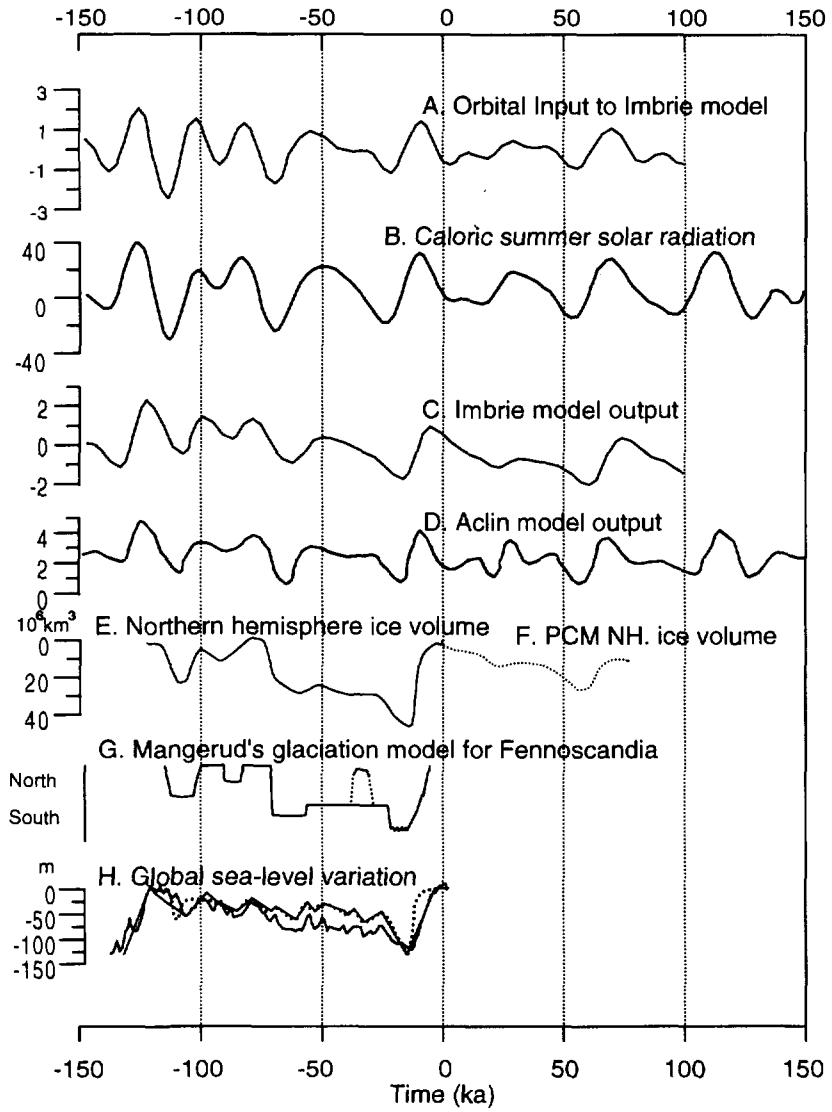

Figure 2.14. Summary diagram of past and predicted climate variables. (**A**) Insolation (July 65°N) calculated by Berger from the Milankovitch parameters. From Imbrie & Imbrie (1980). (**B**) Caloric summer northern hemisphere solar radiation during mid July at 65°N, expressed as deviation of insolation from the year of 1950. From Berger (1978). (**C**) Climate model by Imbrie & Imbrie (1980). (**D**) The ACLIN Climate model. From Kukla et al. (1981). (**E**) Northern hemisphere ice volume Model PAL6NH, calculated by Gallée et al. (1991) red line. (**F**) The PCM climate model (Berger et al., 1990) integrated by Gallée (1989) for the next 80 000 years. (**G**) Scandinavian glaciation curve. From Andersen & Mangerud (1989). (**H**) Weichselian sea level records. Grey line from Chappell and Shackleton (1986), dotted line from Bloom and Yonekura (1985) and black line showing sea level variations based on oxygen isotope records, from Shackleton (1987).

alternatives to the model of thick ice in a single dome over Fennoscandia have been presented, for example by Nesje & Dahl (1990, 1992) and Lagerlund (1987). The ice model by Nesje & Dahl (1990, 1992) is based on observations of block fields with *in situ* weathered bedrock in southern Norway. This model suggests a multi-domed, thin Late Weichselian ice sheet with low surface gradients in the southern Baltic region and the North Sea. Recently, however, the relation between the block fields in South Norway and the maximum Weichselian ice thickness (and thus the Nesje & Dahl, 1992 model) has been criticised (Sollid & Sørbel, 1994). Based on ice movement indicators and till stratigraphy of southern Sweden, Lagerlund (1987) proposes an ice model with marginal ice domes over the southern Baltic.

Applying a model with thinner ice in modelling glacio-isostasy is difficult and the results will not fit the observed pattern of uplift and palaeo shore-line tilt (Fjeldskaar, 1994). Since the evidence of a thin Weichselian ice is questioned, and the earth rheology models seems only to work with a thick ice, the scenario construction has assumed a thick, single-dome model. The occurrence of marginal ice domes during certain stages of glacial development seems probable but, as their occurrence is yet not fully understood, these factors are not accounted for in the scenario constructed here.

2.7 Constructing the Scenario for Future Climate Changes

The scenario is based on the climate reconstructions of the three models described above (Imbrie & Imbrie, ACLIN and PCM; Figure 2.14). The Climate Model output from Imbrie & Imbrie (1980) is used up to 100 000 years, and the ACLIN Model (Kukla et al., 1981) for the period beyond 100 000 years. Both these models apply orbitally-induced changes in insolation as the source of climate changes (the Milankovitch theory). The models ignore human influence on climate and sources of climate variation less than c.19 000 years. From these models, changes in the global amount of ice and corresponding eustatic sea level were estimated. The timing and extent of coming glaciations and sea level variations in Fennoscandia were based on parallels with the last glaciation, guided by the output of the climate models used. Figure 2.15 outlines how the future sea level and climate have been assessed.

In the following sections, important factors contributing to the scenario will be discussed as well as those significant factors not taken into account.

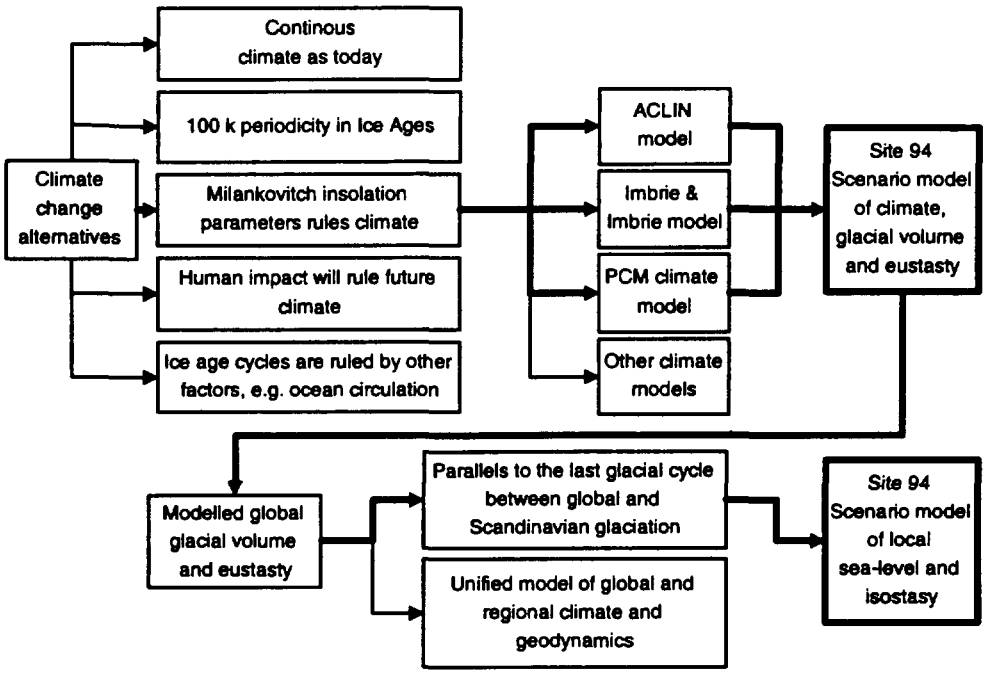

Figure 2.15. Outline of how future sea level and climate have been assessed.

2.7.1 Variables and assumptions contributing to the scenario construction

The following variables and assumptions have contributed to the construction of the climate scenario:

- The presented scenario is based on orbitally-induced changes in insolation, the Milankovitch forcing. These changes have been calculated both for the past and the future (Berger, 1978) and are incorporated and tested in the climate models used. Three such models of future climate and glaciations, the Imbrie & Imbrie Model, ACLIN Model and PCM Model, are used for constructing the scenario.

- For future glaciations, an ice model with a single Fennoscandian dome and a maximum ice thickness of 3000 m is used for a major glaciation.

- The ice volume calculated in the Imbrie & Imbrie Model and PCM Model is used for estimating future global sea level fluctuation. For periods not included in these models, glacial volume and global sea

level are subjectively derived from the ACLIN Model.

- The local sea level is derived directly from the predicted global sea level, only adding the predicted glacio-isostasy.

- The isostasy during glacial episodes is estimated through comparisons with modelling results for the last Weichselian glaciation given by Fjeldskaar (unpublished data; and Fjeldskaar & Cathles, 1991). This model applies a low viscosity mantle (1.6 x 10^{22} poise), a 75-100 km thick asthenosphere (0.7 x 10^{20} poise) and a lithosphere close to 90 km thick.

- The distribution and extent of ice during forthcoming glaciations is derived by direct parallels with the Weichselian. The timing of future Scandinavian glaciations is assumed to be in phase with the global ice volumes of the models used.

2.7.2 Important variables not accounted for in the scenario construction

The following uncertainties and alternatives concerning the global climate development exist:

- It may be the case that future climate will not follow the Milankovitch forcing.

- To explain the dominance of the 100 000 year cycles, other factors such as varying response times, understanding the effects of natural CO_2 variations, glacio-isostatic downwarping, basal sliding of the ice sheets and the feedback between sea level and ice sheets may have to be included in the models. To some extent, this is done in the models used, but more work is needed. The effect of such factors are much less predictable than the insolation; if they are strong enough they might significantly modify the path of climate as indicated by orbital insolation changes.

- It has recently been shown that, during the last glacial, massive iceberg discharges from the North American ice sheet occurred regularly (Heinrich, 1988). These events (Heinrich events) have acted as climate triggers, giving a climatic response of global extent (Broecker, 1994). These events seems to be regular features of a glacial and would, therefore, also be expected in the future.

- A 'Flip-flop' variation of climate. The new results from central Greenland ice cores show that the climate during the last 230 000 years has been unstable, with abrupt climate changes (Dansgaard et al., 1993; Johnsen et al., 1995). These abrupt changes are attributed to

sudden latitudinal displacements of the North Atlantic Ocean current. A displacement of the North Atlantic Ocean current to the south will give a considerable climate deterioration in Europe. The North Atlantic circulation system, although not well understood, seems very sensitive and reacts very quickly. Increased input of freshwater to the North Atlantic Ocean seems to be one possible trigger (Manabe & Stouffer, 1995; Rahmstorf, 1995; Bond, 1995). These findings further emphasise that Milankovitch forcing gives only part of the background for climatic changes.

- Human alteration of climate development through effects by human activities (e.g. greenhouse warming) have not been considered. Due to the limited amount of fossil fuels, global warming due to CO_2 could be expected to be a short-lived feature, considering the time period treated in this scenario. However, a much longer effect on climate could result if warming during this short period were to melt the Greenland ice or trigger some other major climate regulator of long periodicity.

- According to modelling by Berger et al. (1996), the anthropogenic rise of atmospheric CO_2 content may melt the Greenland ice sheet within the next 5000 years. The resulting albedo effect will cause a delay in the onset of major glaciations. The model suggests, for example, that the Fennoscandian ice does not reappear until 50 000 AP and will only reach half the size expected with a Greenland ice sheet present.

The following uncertainties and alternatives concerning the local conditions at Äspö, primarily isostasy and sea level variation, exist:

- The global glacial volume as predicted in the models, and thus global eustasy, need not be in the same phase relation with the Fennoscandian ice volume as during the last glacial. If this is the case, the local sea level changes might reach more extreme values and deviate strongly from the scenario presented here.

- The varying estimates of thickness of the Weichselian ice sheet could give large discrepancies in modelling glacio-isostasy, as well as in making parallels for future glaciations. The ice model applied in the scenario, a thick single Fennoscandian ice dome (Figure 2.13), could have alternatives such as a much thinner ice or an ice sheet with separated domes.

- The scenario applies a simplified picture of local sea level and isostasy, thereby not accounting for the effects of forebulge and hydro-isostasy. In addition, the continuation of present-day land uplift is not included. A more thorough way to predict the response of earth crust during future glaciations and its effect on sea level would be to apply detailed geophysical modelling, although some major

uncertainties, e.g. ice thickness, would still allow considerable variation.

- There is a possibility that large iceberg discharges (Heinrich events) also could affect the Fennoscandian ice sheet. If so, their rapid impact on isostasy and shore-displacement should be considered.

2.8 The SITE-94 Central Scenario—The Climate Change Scenario

The present scenario aims to provide a illustration of future climatic change. The prediction of how the climate will change over the next 130 000 years is limited, however, by substantial uncertainties (as described in the previous sections). It is impossible to give true quantitative values for any parameter during the seven different hypothetical evolution stages described below. Thus, the presented estimations should only be looked upon as rough measures and should serve as comparisons between the stages.

The SKB/TVO scenario (Ahlbom et al., 1991) and the report by Björck & Svensson (1992) follow a similar scenario development approach and have served as a background for the present scenario. Input from McEwen and de Marsily (1991) and Svensson (1989; 1991) were also included. The proposed evolution of the future climate evolution is illustrated in Figure 2.16. The climate models used for this study suggest glaciations at c.5000, 20 000, 60 000 and 100 000 years from now.

0 - 10 000 years. The climate in Sweden will gradually change to cooler conditions with growth of an ice sheet in the Scandinavian Caledonides. Ice sheet thickness in the central mountains will be approximately 1000 m, with no ice in Stockholm or southwards. Crustal downwarping of c.300 m will occur in the central mountainous part. Sea level will gradually drop to 20 to 40 m below present-day sea level in the Stockholm region, as well as in the Äspö region. During the colder parts of this period, permafrost will occur in northern Sweden. The water in the Baltic will gradually become fresher as the connection to the oceans decreases.

10 000 - 30 000 years. After a minor, somewhat warmer period, the climate will get colder and fully glacial conditions will prevail around 20 000 years from now. The glacial peak will last perhaps 5000 years. The ice sheet is estimated to reach the Stockholm area, but probably not the Äspö region. Ice thickness in the central part of the ice sheet will be c.1500 m, while the ice sheet thickness in the Stockholm region will be c.800 m. Crustal downwarping of about 500 m in the central part of the ice sheet and c.60 m in the Stockholm latitude will occur. During deglaciation, when the ice front is located at the Stockholm region, the sea level is estimated to be c.25 m below present-day sea level. At Äspö, sea level will drop to c.50 m below present-

day sea level (Figure 2.17A). The total effect of the glacial loading at Äspö is difficult to evaluate, but will probably not be large. Permafrost conditions may exist down to southern Sweden, including the Äspö area. The water in the Baltic will be fresh, but probably level with the oceans, due to erosion at its outlets.

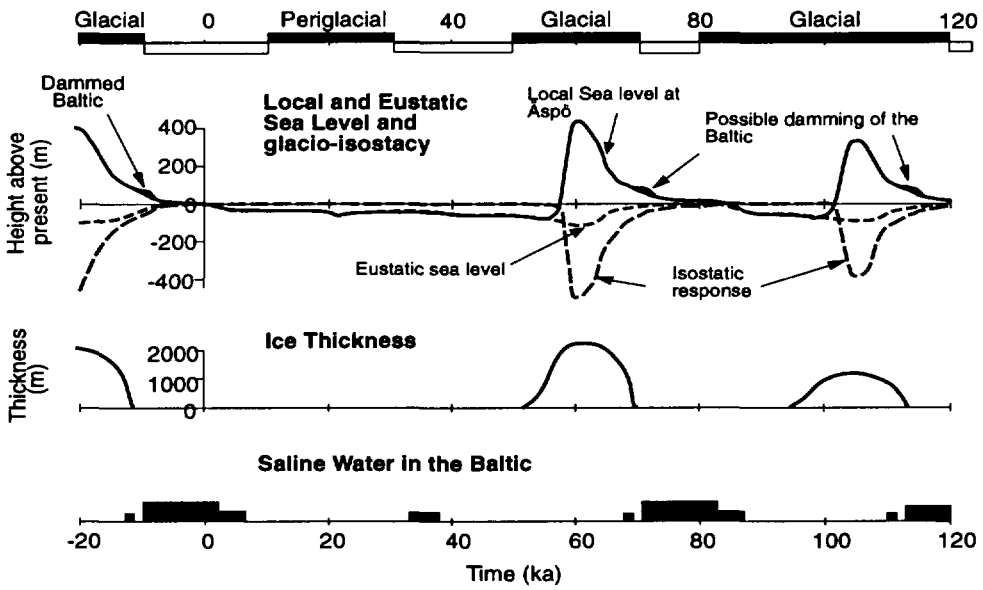

Figure 2.16. Predictions and observations of global eustatic sea level (and locally for Äspö), sea level variations, ice cover, glacio-isostasy and Baltic salinity. The past eustatic record is from Fairbanks (1989) and past shore-displacement is from Svensson (1991).

30 000 - 50 000 years. Interstadial with a dry and cold climate (like the climate today on Greenland). During this phase, periglacial conditions will prevail over all of Scandinavia, with a dry and cold climate, glaciers in the Swedish mountains and permafrost in northern Sweden. Permafrost may be present throughout the period at Äspö, but may be thin and discontinuous during the middle of the interstadial. At Äspö, there will not be significant isostatic uplift during this period. The sea level will therefore be c.30-40 m below the present-day level. However, one or more episodes of damming of the Baltic may occur, such that Baltic lake levels may be closer to or similar to those of present-day sea levels. This may inhibit the development of permafrost. The Baltic will mainly be fresh but some saline water may enter it.

50 000 - 70 000 years. Full glacial conditions. Owing to the previous cold conditions, the ice sheet will respond more rapidly. The glacial culmination

will be around 60 000 years The ice sheet will cover the whole of Sweden reaching down to north Germany, comparable to the maximum of the Weichselian glaciation. Ice sheet thickness in the central part will reach c.3000 m. In the Stockholm region, the ice thickness will be c.2500 m. The Stockholm region will probably be covered by the ice sheet for at least 10 000 years and possibly longer. Downwarping of c.700 m is predicted in the central part of the ice sheet, c.600 m in the Stockholm area and, at Äspö, the downwarping could be c.500 m. During deglaciation, when the ice front is located at the Stockholm region, the sea level is estimated to be c.150 m at Stockholm and c.80 m above present-day coastline at Äspö (Figure 2.17B). There could also possibly be a damming of the Baltic to 10-30 m above ocean level. The Baltic will be mainly fresh, but during deglaciation saline water may enter the Baltic through isostatically depressed areas. Permafrost will be present in large areas of Europe.

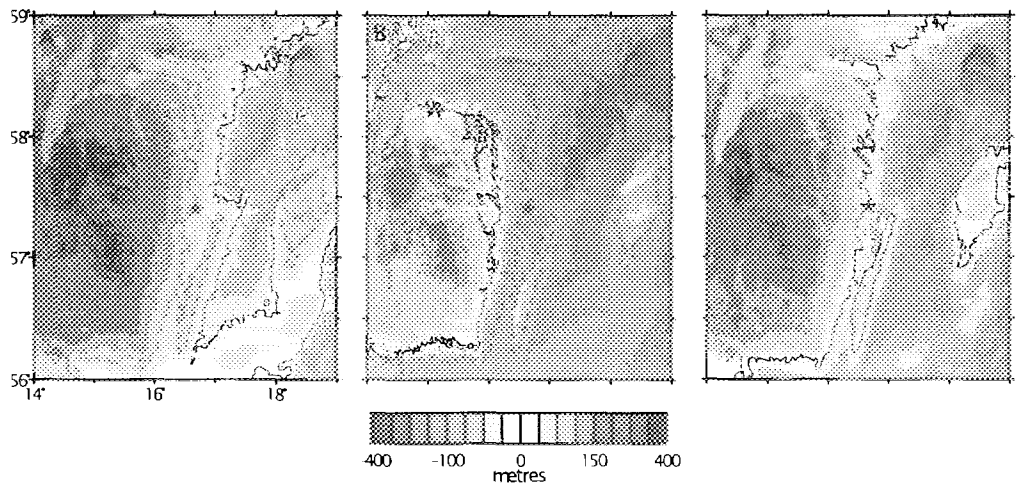

Figure 2.17. Examples of changing land-sea configuration, the Äspö site is indicated by the red star. (**A**) c.20 000 yrs AP, northern Sweden glaciated and a sea level at c.-50 m. (**B**) c.70 000 yrs AP, showing the largest extent of the sea reached during deglaciation. (**C**) c.80 000 yrs AP, late interglacial conditions, sea level as today.

70 000 - 80 000 years. A rapid deglaciation will lead to and culminate in interglacial conditions at 75 000 years. Total crustal uplift is estimated to be c.700 m in the central parts of the previous ice sheet, c.600 m at Stockholm and c.500 m at Äspö. This will be a relatively 'warm' period with a climate in the Stockholm region similar to the present climate in northern Sweden. Small mountain glaciers and permafrost will occur in the very north. Parts of southern Sweden will be resettled and farming might be possible. Sea level and salinity will be similar to the present day (Figure 2.17C) all over Sweden and the land uplift will restore the land-surface to approximately its present

state. Permafrost will only be present in the very north of Scandinavia.

80 000 - 120 000 years. The climate will gradually become colder with maximum glacial conditions at 100 000 years. The ice sheet will be extensive, covering large parts of Fennoscandia. Permafrost could occur in large areas outside the ice margin. In the Stockholm region, maximum ice thickness is estimated to be c.1500 m, and at Äspö c.1000 m. Downwarping of c.500 m at Stockholm is predicted during the main phase of the glaciation. At Äspö, the maximal downwarping will be a little less than at Stockholm, perhaps 400 m. The relative sea level at Stockholm at deglaciation will be c.100 m above present-day coastline. The sea level at Äspö at deglaciation may be c.80 m above present-day sea level, but damming of the Baltic to 10-30 m above ocean-level is possible. The Baltic will be mainly fresh, but during deglaciation, saline water may enter the Baltic through isostatically depressed areas.

120 000 - 130 000 years. Interglacial. The next warm period with a climate similar to the present in the whole of Scandinavia. Sea level and salinity in the Baltic will be similar to the present.

2.9 Permafrost and Subsurface Temperature Model

2.9.1 The Model

In Project 90, scoping calculations were made of the potential depth of the permafrost around a repository as a function of time (McEwen & Marsily, 1991). A simple analytical expression was used, which represented the variation of the surface temperature as a sum of three sinusoidal functions, which approximately described the major harmonics in Milankovitch's theory. The latent heat capacity for freezing the water in the ground into ice was neglected; heat transfer was by pure conduction, with a constant geothermal gradient; and the heat produced by the waste was simply taken by adding the temperature calculated in the ground to the analytical expression of the temperature increase resulting from heat transfer from the waste, calculated numerically by Tarendi (1983). In the present work, a more precise approach was taken, using various assumptions which are described below.

The surface temperature is prescribed from the climate scenario defined in the previous sections. This model predicts the ground surface temperature, approximately at sea level, and is valid as long as no ice is present on the site. As soon as a glacier builds up, it is necessary to take into account the complex effect of the ice on the rock surface temperature. This has been modeled by Boulton & Payne (1992) and, from their results, it is possible to determine the evolution of the temperature at the ground surface (Figure 2.18). However, the Boulton & Payne model is only based on the Imbrie &

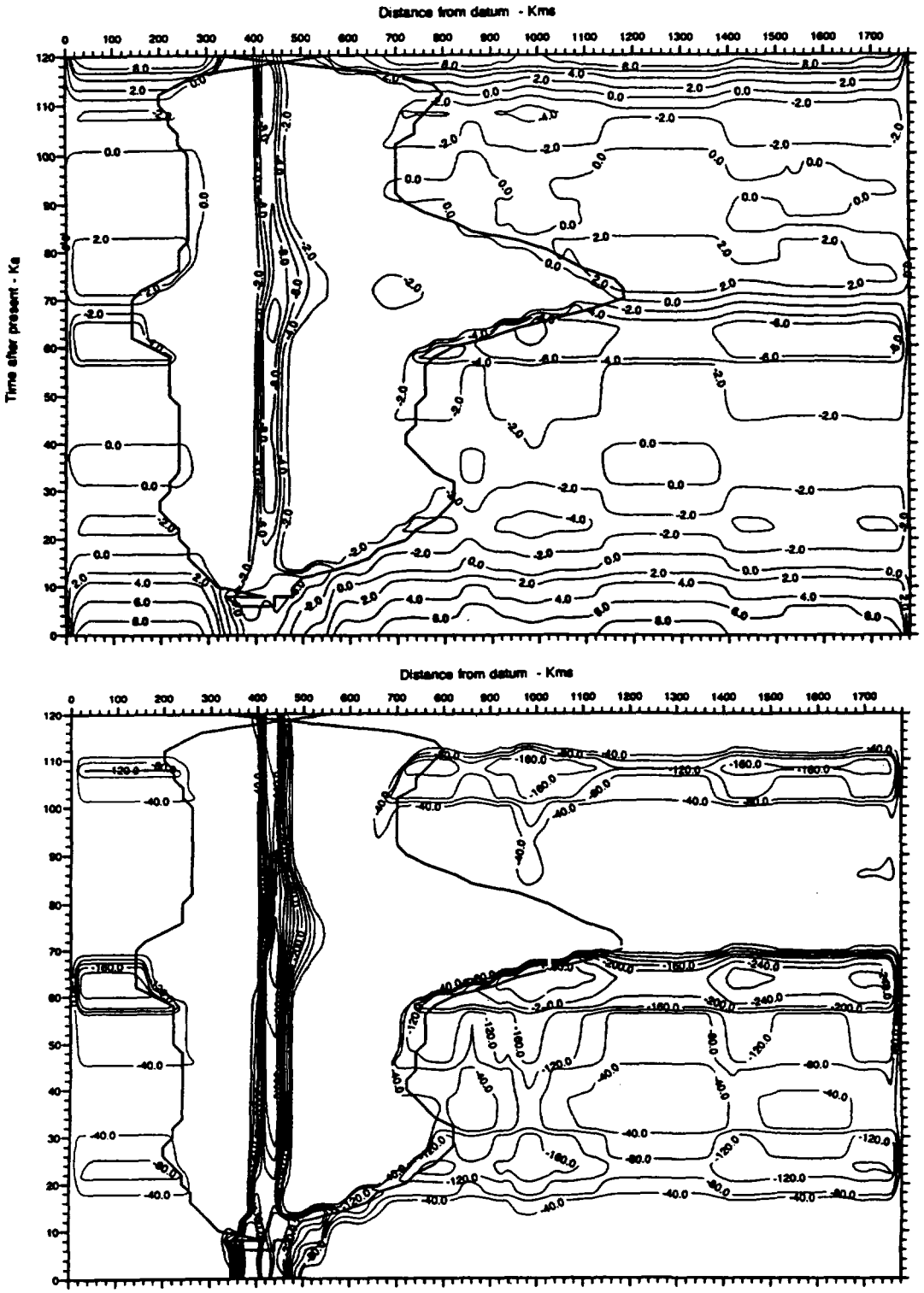

Figure 2.18: **(a)** Predicted ground surface temperature distribution and **(b)** thickness of frozen ground (permafrost) beneath and beyond the ice sheet of future glaciations within the next 120 000 years for a standard sea level of –10° C. Taken from Boulton & Payne (1992). The solid lines represent the predicted extent of the ice sheet along a transect from NW Norway (0 km) to Poland (1700 km). Äspö would apparently be situated at approximately 1000 km on the horizontal axis.

Imbrie climate scenario and does not correspond exactly to the selected climate scenario defined in this study. In particular, it does not predict that second ice sheet will advance as far as the Äspö area around 90 000 years from now. Therefore, some adjustments were made between these two temperature predictions, in order to predict the ground surface temperature as a function of time at Äspö, including the effect of the ice (see Appendix 1 for details). This led to the analysis of three scenarios (Figure 2.19): (i) Corresponding to the SKI Central Climate Change Scenario, where two ice sheets form over the site, around 50 000 and 90 000 years and (ii) Where only one ice sheet forms at 50 000 years, with no ice at 90 000 years, corresponding to the Boulton and Payne (1992) scenario (in the latter case, a colder surface temperature is predicted around 95 000 years, as the ice generally acts as an insulating layer between the cold air temperature and the ground); (iii) As for (i), but with warmer-based ice than for the previous two scenarios (such that the ground surface temperature is approximately zero during ice sheet coverage). The latter scenario may simulate the lowering of effective bedrock temperature as a result of the pressure melting point reduction of the basal ice caused by the ice overburden (see Section 3.3). These three scenarios differ only after 57 000 years.

The initial condition of the system is fixed at 120 000 years BP, in order that the temperature profile at the moment when the repository is built is consistent with the past history of the system, which is still dependent on the abrupt temperature variations that occurred about 10 000 years ago. A steady state has not yet been reached at the present time as shown, for example, by McEwen & Marsily (1991). The ground surface temperature history, as generated by Boulton & Payne (1992), is prescribed at the upper boundary of the model from 120 000 BP to the present. It also has the advantage of making it possible to check the consistency of the calculations between 120 000 BP and the present by comparing them with those by Boulton & Payne (1992), since they also predict the depth of the permafrost in their model from 120 000 years BP. This comparison (not shown here) was first made using the same thermal parameters as Boulton & Payne (1992) and was found acceptable. However, for the actual permafrost depth predictions in this study, slightly different parameters were used, to more closely fit the Äspö data. At 120 000 years BP, a simple steady state initial condition is assumed, with a constant geothermal gradient; any approximation made at this date will not have any residual influence on the calculations from the present time into the future. Note that a slight approximation is made here by using the temperature at the rock surface derived from the calculations by Boulton & Payne (1992), but not exactly the same parameters as they used; their calculated temperature at the rock surface is dependent on the heat flux from the ground. Here, the same geothermal heat flux (0.042 W/m^2) is used, changing only the thermal conductivity from 3.3 to 3 W/m.K, and the rock heat capacity from 3.3×10^6 to 2.16×10^6 $J/m^3.K$. These values are more representative of the Äspö area, and were considered more appropriate, in particular for correctly predicting the thermal effect of the waste.

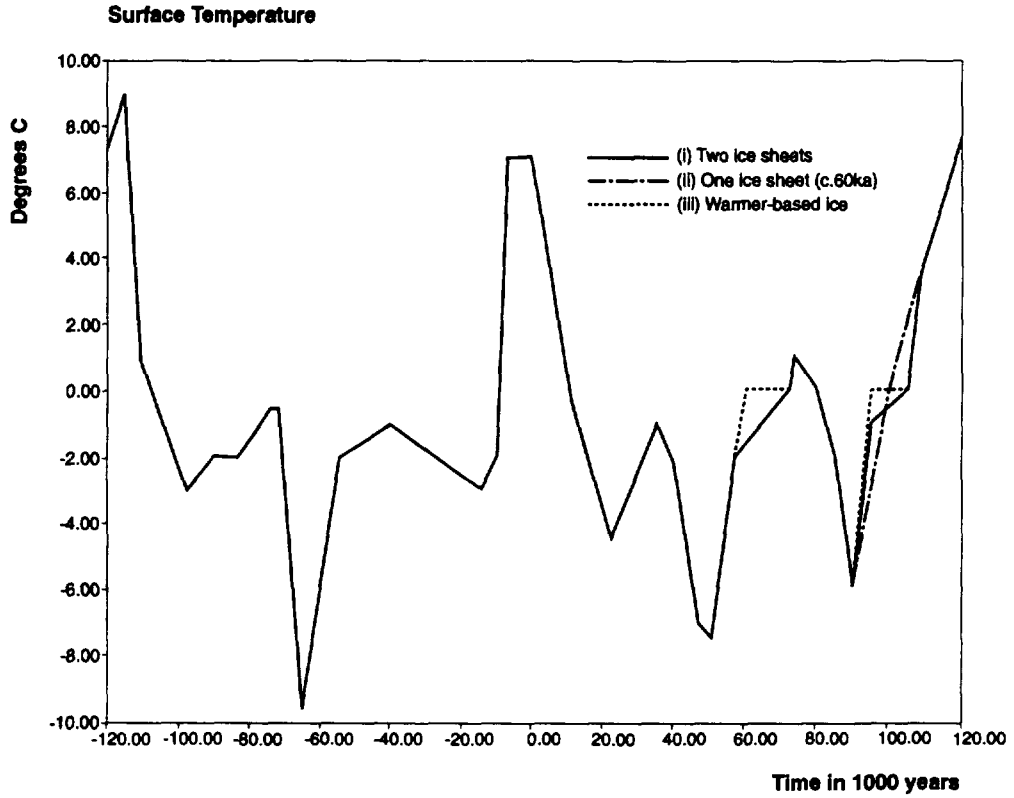

Figure 2.19. Prescribed temperature at the rock surface as a function of time, from 120 ka BP to +120 ka. Adjusted from Boulton and Payne (1992) to fit the SKI climate change model for three different scenarios: **(i)** Two successive ice sheets formed at c.50-70 ka and c.90-110 ka, with moderately warm-based ice; **(ii)** Only one ice sheet formed at 50-70 ka, with moderately warm-based ice; **(iii)** Two successive ice sheets formed at c.50-70 and 90-110 ka, but with warmer-based ice.

It is also assumed that heat is transferred in the ground by pure conduction, but the latent heat for freezing the water in the ground (or for unfreezing) is taken into account in the calculation. Heat transfer by advection with flowing groundwater is neglected, given the low hydraulic conductivity of the rock and the complexities involved with fully describing water flow conditions. It has indeed been shown (e.g. de Marsily, 1988) that convection can be neglected compared to conduction when the hydraulic conductivity is smaller than 10^{-8} m/s. Advective heat transfer would tend to speed up the establishment of permafrost.

A constant geothermal flux is prescribed at a depth of 8 km. This depth is greater than the 2 km used by Boulton & Payne (1992) because it was found in preliminary tests that a length of 2 km was too short to correctly model the thermal effects of the waste on the system. Tarendi (1983) also used about 8 km in his model.

The model is a simple one-dimensional finite difference approximation of the heat transfer equation, in the vertical direction. Horizontal heat transfer is therefore neglected. This is quite acceptable from 120 000 years BP to present and is also used by Boulton & Payne (1992), but it is an approximation when the heat generated by the waste is taken into account, from time zero to approximately +50 000 years. Heat is indeed transferred from the repository to the rock in a three-dimensional pattern. It has, however, been shown by Tarendi (1983) that the one-dimensional solution is an acceptable approximation for predicting the temperature above or below the centre of a full-size repository (a full-size repository may, however, not be feasible on Äspö).

The heat generated at the repository level by the waste is modelled by a source term, decaying over time. The amount of heat, decay rate and density of waste (which is a function of repository design) are taken from Tarendi (1983). A single-level repository is considered, at a depth of 500 m.

The calculation results are presented in the following form, for each of the three scenarios (i)-(iii):

- History of the surface temperature, as prescribed boundary condition of the model. Results are presented from -120.000 to +120.000 years (Figure 2.19; Appendix 1).

- History of permafrost depth, from -120 000 to +120 000 years. For each of the scenarios, two curves are shown, one with waste and one without waste (Figure 2.20; Appendix 1). They, of course, only differ after time zero.

- History of the temperature at the repository depth (500 m); two curves are also shown, one with and one without the repository (Figure 2.21; Appendix 1).

- Temperature profiles as a function of depth, from 0 to 2 km (even if the calculations extend to 8 km). These profiles are given at times 0, 1000, 10 000 and 25 000 years, which are identical for the three scenarios (Figure 2.22; Appendix 1). The case with and without the repository is shown separately.

- Temperature profiles at times 55 000, 70 000, 90 000 and 120 000 years. Six of these profiles are shown, for the three scenarios and for the case with and without the repository (Appendix 1).

The parameters used in the model and the origin of the data are described in further detail in Appendix 1.

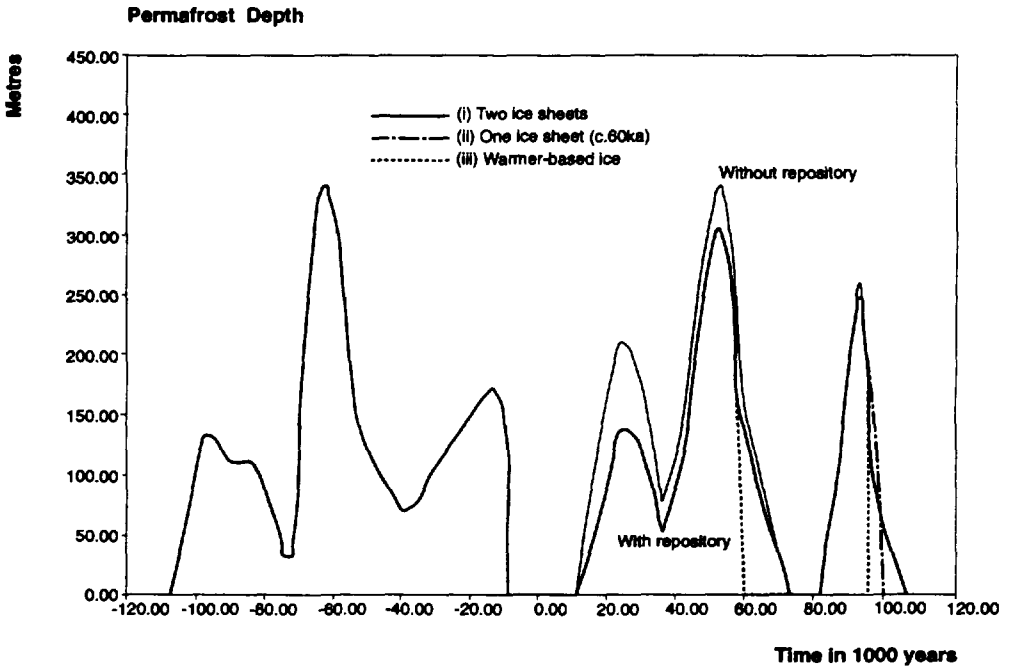

Figure 2.20. Prescribed permafrost depths as a function of time, from 120 ka BP to +120 ka for the three different scenarios: (i), (ii) and (iii) as outlined above.

2.9.2 Permafrost Model results

The permafrost depth as a function of time from -120 000 to +120 000 years is summarised in Figure 2.20 for the three scenarios (i-iii). The depth of the permafrost versus time is presented for the case with and without the repository.

The permafrost depth reaches three peaks at around 25 000, 50 000 and 90 000 years, with values of 210, 340 and 250 m, respectively, for the main scenario with two ice sheets and no repository (model (i)). With no ice sheet at 90 000 years (model (ii)), the permafrost depth is similar, but the permafrost melts faster, at around 100 000 years. With warm-based ice (model (iii)), the permafrost under both ice sheets melts much faster, around 10 000 years in advance.

This latter scenario appears to be more consistent with qualitative descriptions of sub-glacial permafrost development (e.g. Boulton et al., 1993; Ahlbom et al., 1991) and quantitative models (e.g. Boulton & Payne, 1992; Figure 2.16) which consider that permafrost is only present beneath the outer edge and centre of an ice sheet. This may be due to the lowering of effective bedrock temperature as a result of the pressure melting point reduction of basal ice caused by the by the ice overburden (see Section 3.3).

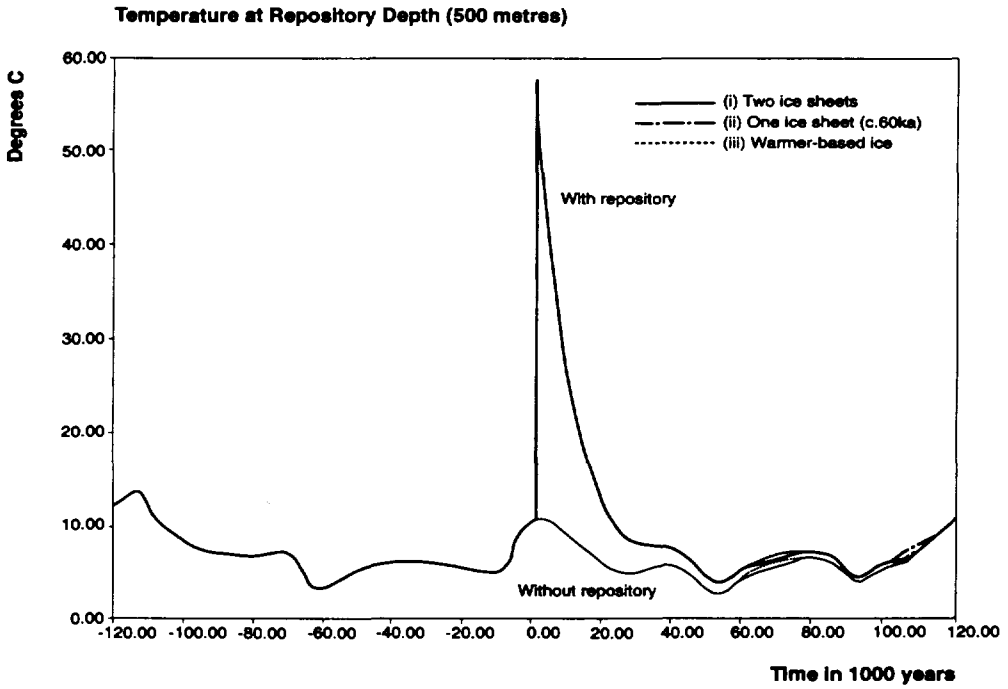

Figure 2.21. Temperature at repository depth, from 120 ka BP to +120 ka for the three scenarios, and for the case with and without the repository. The two curves after time zero (present) correspond to the cases with and without a repository at a depth of 500 m.

Compared to the situation with no repository, the heat generated by the waste reduces the permafrost depth by 75 m for the peak at 25 000 years, and by 35 m and 10 m for the peaks at 50 000 and 90 000 years, respectively.

The temperature at repository depth is shown in Figure 2.23 for the three scenarios and for the case with and without the repository.

The effect of the repository is major at time 1 000 years, of the order of 50°C, and decays to almost zero at 120 000 years. Very little difference can be seen between the three scenarios. Note that the peak temperature at repository depth is probably not very accurate, as it represents an average over 1500 m^3, and neglects three-dimensional effects.

Selected temperature profiles with the repository are shown in Figure 2.22a & b at times 0, 1 000, 10 000 and 25 000 years, for the case with and without the repository respectively. They correspond to the three scenarios, since they only differ after 57 000 years. It can easily be seen that the initial profile at time zero is not in steady state (ie. not a straight line). The heat pulse from the waste is very strong at 1000 years and still considerable at 10 000 years.

(a)

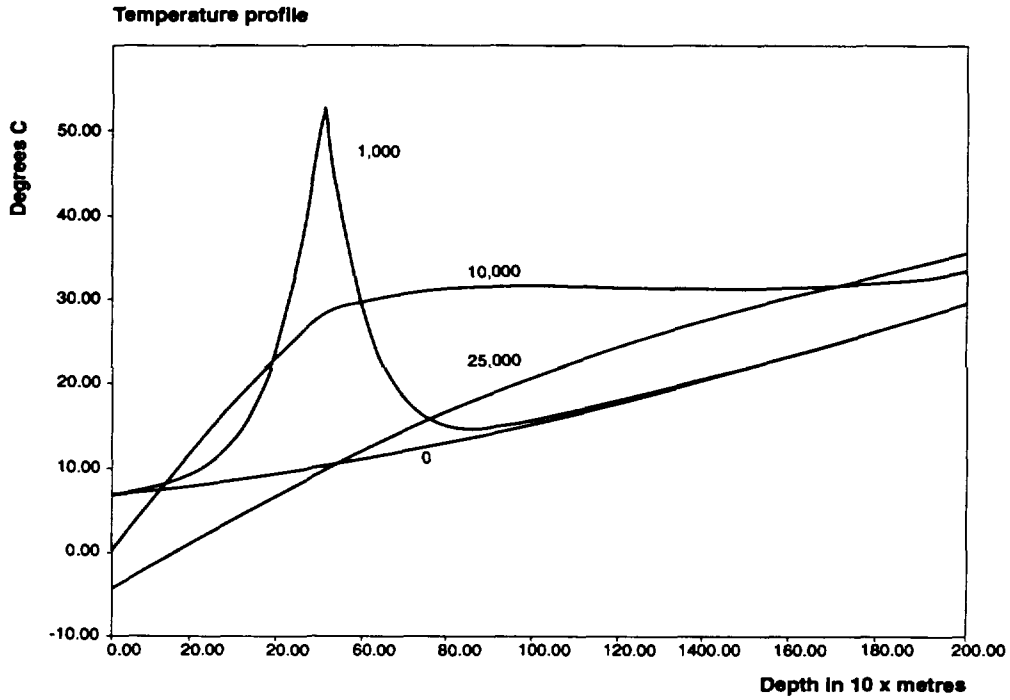

(b)

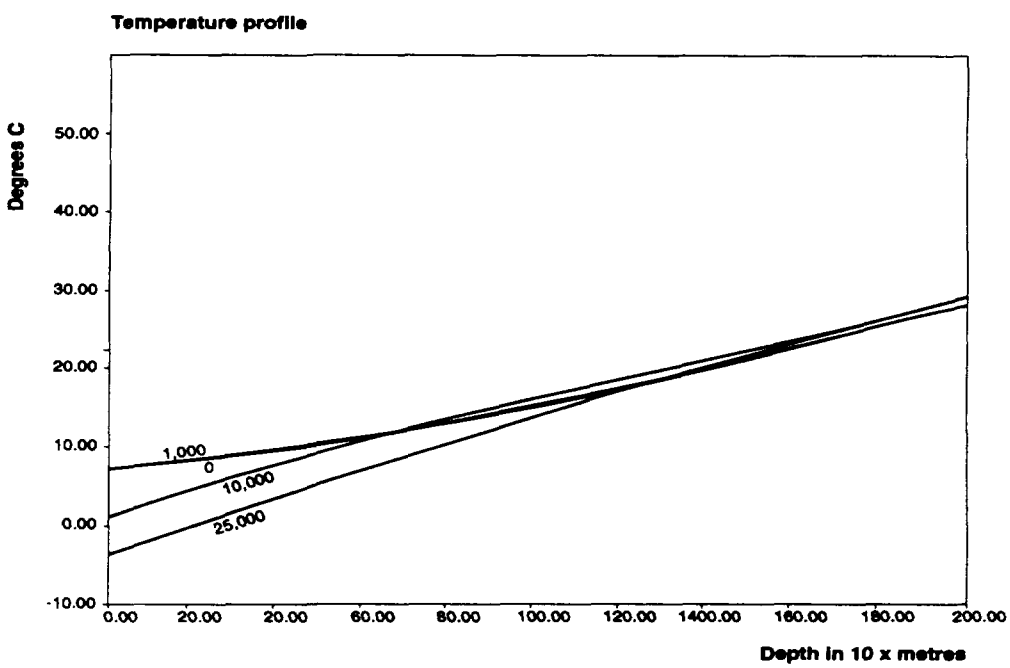

Figure 2.22. Temperature profiles within the bedrock at selected times 0, 1000, 10 000 and 25 000 years, for **(a)** the case with the repository and **(b)** without the repository.

At 25 000 years, which corresponds to the first peak of permafrost penetration, the effect of the waste is still visible at depth. The temperature profiles with and without the repository, at times 50 000, 70 000, 90 000 and 120 000 years, for the three scenarios, are given in Appendix 1. The temperature profiles at 120 000 for all three scenarios are very close to that at time 0 years (Figure 2.22b).

2.10 The Central Climate Change Scenario: Summary

A summary of the climate changes considered to affect the Äspö area over the next 120 ka are shown in Figure 2.23. The permafrost thickness curve is taken to be that of scenario (iii) (Section 2.9).

These changes are used as a basis for the development of the Central Scenario (Sections 6 and 7), although alternatives to this scenario evolution are possible, as discussed in previous sections.

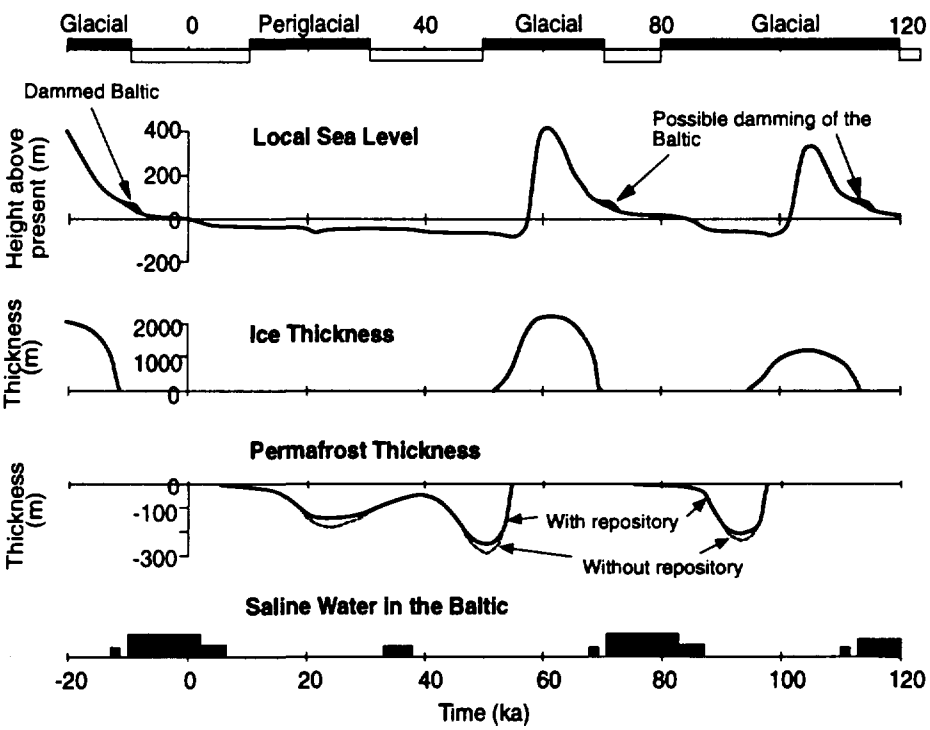

Figure 2.23. The Central Climate Change Scenario for SITE-94 showing selected sea levels, ice thicknesses and permafrost thicknesses at Äspö over the next 120 000 years.

3 General Glaciation and Ice Sheet Review

The following sections describe briefly the main characteristics of ice sheets and glacial conditions, past and present, in order to provide a suitable background for the subsequent formulation of future climate scenarios at the Äspö site (Section 5).

3.1 Introduction and Definition: Ice Sheets

Ice sheets are the largest glaciers on the Earth, a glacier being defined as a body of ice, consisting largely of recrystallised snow, that shows evidence of downslope or outward movement due to the pull of gravity (Skinner & Porter, 1987). Ice sheets may be defined as continent-sized masses of ice thick enough to flow under their own weight and which overwhelm nearly all land within their margins (Skinner & Porter, 1987). Modern ice sheets are confined to Greenland and Antarctica although, during past glacial ages, ice sheets also covered extensive areas of North America and Eurasia. Such ice sheets are predicted to return during future glacial episodes. However, it must be recognised that the present-day polar or sub-polar ice sheets may behave in a different way to those predicted to affect mid-latitudes in the future (e.g. Boulton et al., 1985).

3.2 Morphology / Geometry

Ice sheets may rest on land that lies above sea level (land-based ice sheets such as the East Antarctic Ice Sheet; Figure 3.1) or they may rest on land below sea level (marine ice sheets, such as the West Antarctic Ice Sheet). While land-based ice sheets generally lie directly in contact with the land surface, such that they are grounded, marine ice sheets may be partially grounded and partially afloat. Floating ice sheets are termed ice shelves. However, grounding is likely where the topographic slope is low and the sea is relatively shallow (Oerlemans & van der Veen, 1984).

Ice shelves occur in many places along the margins of the Greenland and Antarctic Ice Sheets, as well as locally in the Canadian Arctic islands. Ice shelves are mainly located in large coastal embayments and are attached to land on one side; their seaward margin generally forms a steep cliff, or ice cliff, rising as much as 50 to 300 m above sea level (Figure 3.1). The largest ice shelves extend hundreds of kilometres seaward and can reach a thickness of 1000 m, such as the Ross Ice Shelf which has formed off West Antarctica. Land-based ice sheets may also terminate in the sea or a lake, where they are likely to have an ice cliff margin (Skinner & Porter, 1987), although they are likely to remain grounded in water depths of less than 500 m (Thomas, 1977). For example, reconstructions of the Fennoscandian ice sheet based on geological evidence indicate that the marine margin of the ice sheet never

extended past the continental shelf, probably ending in a short shelf of floating ice (Lehman et al., 1991). Calving of icebergs is a common feature of ice cliff margins. Land-based ice sheet margins are generally modelled as having a curved, lense-shaped, parabolic geometry with the surface steepening towards the margin (e.g. Ahlbom et al., 1991; Boulton & Broadgate, 1992; Boulton & Payne, 1992; Figure 3.1) although more complex morphologies may occur owing to the formation of moraines at the ice margin (e.g. Hooke, 1970; 1973), the formation of ice cliffs and the development of ice streams, ice lobes and interlobate complexes.

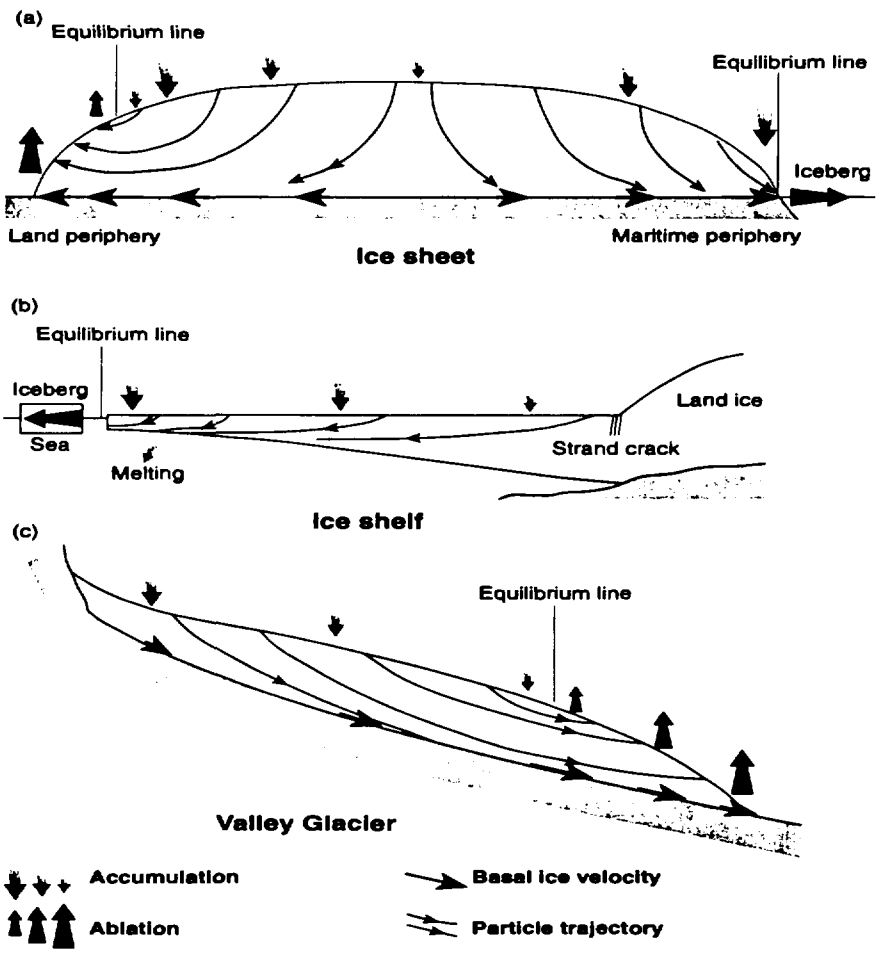

Figure 3.1. Models of **(a)** ice sheet **(b)** ice shelf and **(c)** valley glacier, showing the distribution of accumulation and ablation and related flow characteristics. From Sugden & John (1976).

The geometry and dynamics of an ice sheet are intimately related via the interaction of bedrock temperature, internal ice temperature, internal velocity of the ice, isostatic response and mass balance (e.g. Boulton & Payne, 1992).

The form of an ice sheet may also be related to conditions during the advance, and particularly the retreat, of an ice sheet. For example, the nature of the substratum underlying the ice sheet, with regards to its hydraulic and strength properties, has been shown to have a very significant control on the movement and surface profile of the ice (e.g. Boulton & Jones, 1979; Holmlund & Fastook, 1993). Many theories developed to account for the surface profiles of ice sheets assume that the ice sheet rests on a rigid surface and that the profile depends primarily on the rheological properties of the ice and the thickness of the lubricating film between the glacier and its bed (e.g. Nye, 1976; Weertman, 1966). A model has been developed such that the ice sheet is underlain by potentially deformable materials such as relatively poorly lithified sedimentary units (e.g. Boulton & Jones, 1979; Holmlund & Fastook, 1993). If these materials have a high hydraulic transmissibility, meltwater is readily discharged sub-glacially, the bed is stable and the profile is a normal parabolic one, governed by the rheologic properties of ice. However, if the potentially-deformable bed transmissibility is low, for example densely packed bottom moraines, water pressures build up, the bed begins to deform and a lower equilibrium profile will develop, so that in the extreme case the ice sheet approximates a flat sheet, similar to an ice shelf. For the last glaciation to affect northern Europe, it is considered that deformable sediments were most likely to have occurred within the Baltic basin and the low-lying European plain to the south of the Baltic (Boulton & Jones, 1979; Holmlund & Fastook, 1993).

The deforming-bed model is therefore most likely to describe the surface profile of the Weichselian ice sheet during its maximum development, but not during the early stages of advance and later stages of retreat where the ice sheet only overlays the relatively undeformable rocks of the Caledonides and surrounding areas (including SE Sweden). The potential change in the profile of an ice sheet with changing substrate is shown in Figure 3.2.

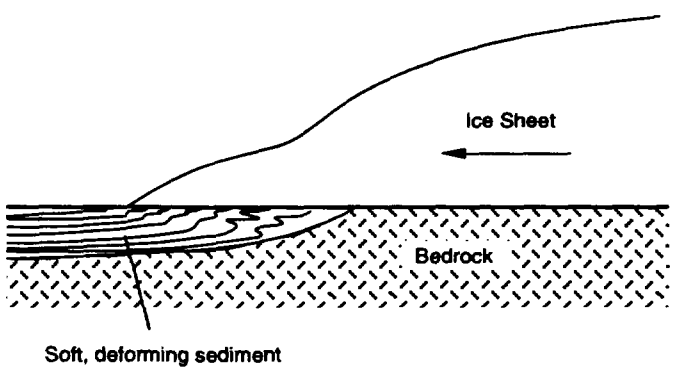

Figure 3.2. Reduction of surface slope of a glacier in its terminal zone where it has flowed over soft, deformable sediments. From Duff (1993).

Most ice sheets appear to be modelled with overall surface gradients of less than one degree. Embleton & King (1975) derived an expression which describes the geometry of an ice sheet:

$$H=4.76\sqrt{R},$$

where H is the thickness of the ice sheet and R is the horizontal extent of the ice sheet from its centre. This assumes that the profile of the ice sheet is in steady state resting on a horizontal base of even roughness, with mass balance and temperature constant and a basal shear stress of 1 bar. This expression was found to fit fairly closely measured values in Antarctica and Greenland. The Greenland Ice Sheet, for example, has a surface slope of 0.001 (0.06°) towards its centre and 0.01 (0.6°) within a few hundred kilometres from its margins. However, reconstructions of ice extent and thickness for the Weichselian and future glaciations in Scandinavia do not appear to be described by this expression (e.g. Boulton & Payne, 1992) and require a value much lower than 4.76 (nearer 3). This disparity may be due to the simplifications made by Embleton & King (1975) in deriving the expression with regard to temperature distribution and shear stresses, etc. and errors involved in predicting past and future ice sheet geometries.

The typical terminal gradient of a land-based ice sheet is likely to be in the order of 0.4 (20°) with a parabolic front (G. Boulton, pers. comm.). It appears that such a high gradient could only exist over a short distance, probably less than a few kilometres, before rapidly decreasing towards the centre of the ice sheet. An ice sheet which terminates in the sea is likely to have a lower marginal gradient (perhaps even negative) which abruptly ends in a 80 to 90° sloping cliff.

3.3 Temperatures and Melting

The temperature may vary significantly within an ice sheet or glacier (Figure 3.3) and is a function of ice thickness, flow rate and accumulation of cold ice (snow). The pressure melting point, the temperature at which ice can melt at a particular pressure, in a thick ice sheet is slightly below 0° C in certain places (e.g. -1.6° C at a depth of over 2 km at the base of the Antarctic ice; Sugden & John, 1976; Figure 3.4). Glaciers can therefore be cold-based, warm-based, or both (Hooke, 1977), such that under certain conditions ice and water can exist in equilibrium. Present-day ice sheets are generally of the cold-based type for the most part (Sugden & John, 1976; Hooke, 1977; Drewry, 1986) although warm-based parts of the Antarctic Ice Sheet have been recognised (e.g. Embleton & King, 1975; Gow et al., 1968). A borehole that penetrated the full 2164 m thickness of the inland Antarctic ice sheet (Gow et al, 1968) recorded a lowest temperature of -28° C at 800 m and at 1800 m, the temperature was -13° C. Liquid water indicative of pressure melting was encountered at the bottom of the ice, possibly as a basal water layer of the order of 1 mm thick. More recent boreholes have also penetrated

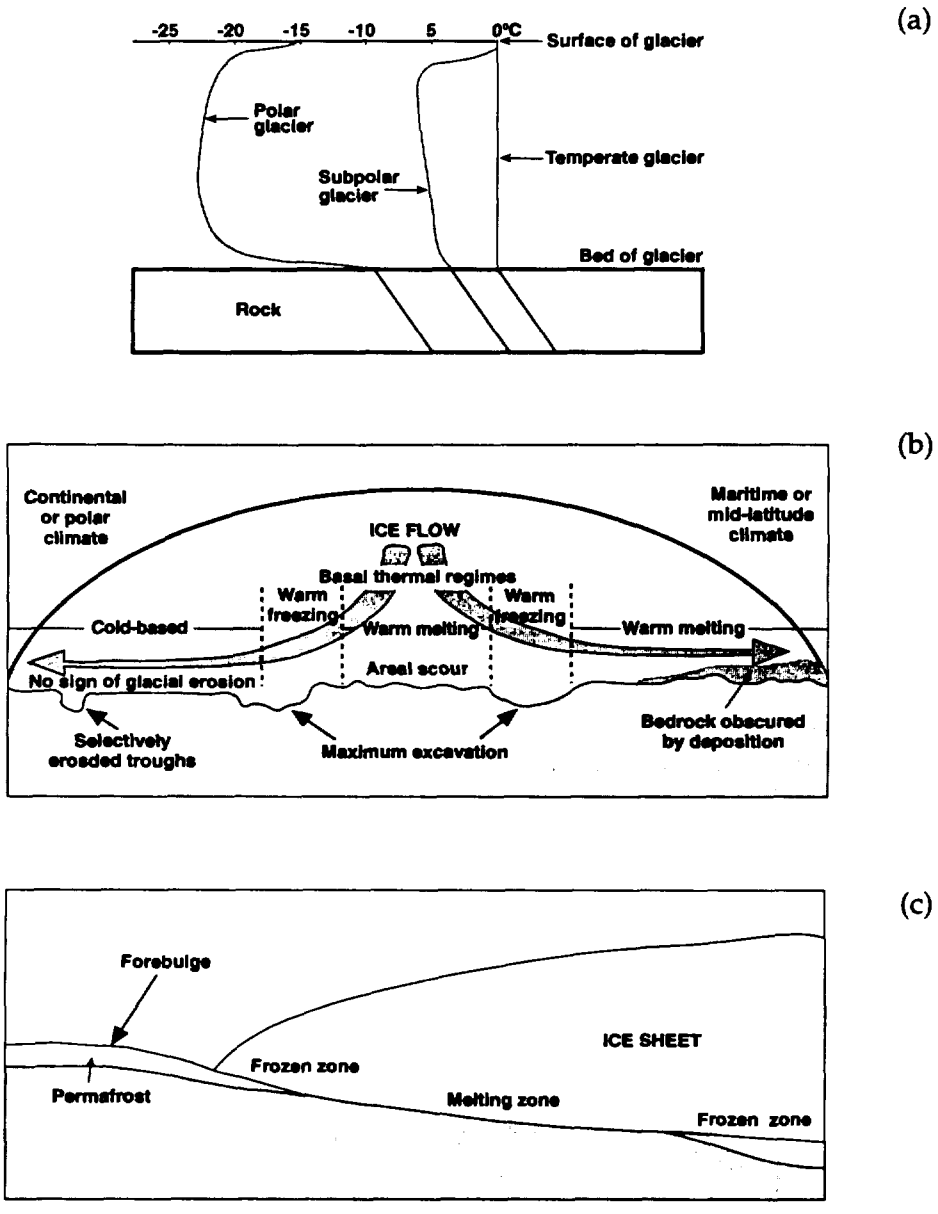

Figure 3.3. Temperature distribution within ice sheets and glaciers. **(a)** Temperature profiles for polar, sub-polar and temperate glaciers (from Skinner & Porter, 1987). **(b)** Cross-section showing the basal thermal regimes within a continental ice sheet. Left, a cold-based glacier; right, a warm-based glacier. From Skinner & Porter (1987). **(c)** Model of the hydraulic conditions to the base of an ice sheet and forebulge uplift; no scale inferred (modified from Ahlbom et al.,1991; Skinner & Porter, 1987; Boulton et al., 1993).

the Greenland Ice Sheet, reaching a depth of 3028.8 m, penetrating several metres of silty basal ice and 1.5 m into the bedrock (e.g. Dansgaard et al., 1993; Gow et al., 1996). Areas at the base of the Antarctic Ice Sheet, where the basal ice is at pressure melting point, are shown on Figure 3.4. There appears to be a close correlation between basal pressure melting and proximity to ice shelves.

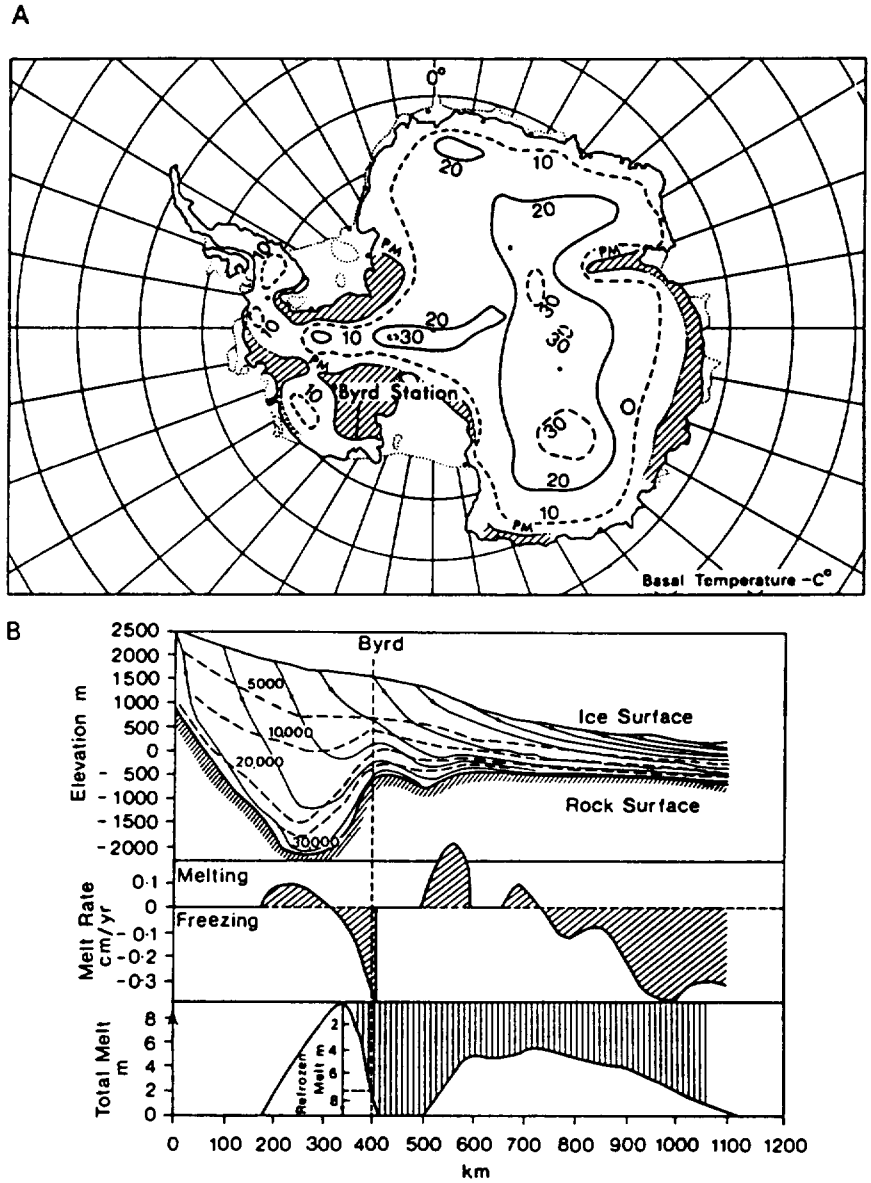

Figure 3.4. **(A)** Calculated basal temperatures for the Antarctic Ice Sheet, contoured for each 10° below pressure melting point. The shaded areas are at pressure melting point. The dotted lines represent the margins of ice shelves. **(B)** Flow-line profile in West Antarctica with ice paths and particle ages (top); calculated rates of melting and freezing (middle); and total amount of melt assuming no migration of meltwater. From Embleton & King (1975). Extent of melting may be underestimated (Sugden & John, 1976).

A warm-based glacier, or warm-based part of an ice sheet, will be capable of moving over the surface of the ground by virtue of the thin basal meltwater layer (Sugden & John, 1976; Gow et al., 1968) or by deformation of the substrate (e.g. Boulton & Jones, 1979). Cold-based glaciers, on the other hand, will move extremely slowly. Ice sheets and glaciers may also be referred to as being either temperate (predominantly warm-based), sub-polar (often both warm and cold-based) or polar (generally cold-based).

Modelling of past and future sub-polar ice sheet basal temperatures has predicted temperature and melting zonation within the ice (e.g. Huybrechts & Oerlemans, 1988; Hindmarsh et al., 1989; Boulton & Payne, 1992). The zonation is caused by the large amount of strain heating near the margin (in the rapid ice flow zone) and the increased rate of cold ice advection near the ice divide (Boulton & Payne, 1992). The central part of the ice sheet has basal temperatures beneath the melting point and, thus, has little or no erosion (e.g. Hindmarsh et al., 1989 *versus* Skinner & Porter, 1987; Figure 3.3b & c). This part is fringed by a broad zone of melting with associated erosion. The outermost part of an ice sheet, (modelled to be a few tens of km for the Greenland Ice Sheet at 70°N; Boulton, Smith & Morland, 1984) is more likely to be associated with a zone of deposition. Irregularities in the ice substrate in the basal melting zone cause pressure variations which force the temperature to drop below the pressure melting point (e.g. Sugden & John, 1976) and hence cause the base of the ice to freeze temporarily, sticking to the ground surface before melting again, with a powerful abrasion effect.

3.4 Glacial Evolution

3.4.1 Periglacial

Land areas beyond the limit of glaciers or ice sheets, where low temperatures and frost action are important factors in determining landscape characteristics, are called periglacial zones and are characterised by a tundra climate state. A common feature of periglacial regions (such as in Spitzbergen and Siberia at present) is perennially frozen ground, known as permafrost. Permafrost is defined as ground, soil or rock, with temperatures which remain continuously below 0°C for two or more years. It occurs in areas with mean temperatures below 0°C and is generally overlain by an active layer, which is subject to seasonal freezing and thawing (Figure 3.5). Permafrost can have a major influence on the recharge and discharge of groundwater (see Section 4.2).

However, the influence of permafrost on groundwater flow will depend on its depth and whether it is continuous or discontinuous. The depth of permafrost is a function of mean annual temperature, thermal conductivity of the ground, the depth of snow and its thermal conductivity with time. The circumpolar permafrost zone in the Northern Hemisphere, which moves south during glacial periods, can be subdivided into two principal subzones: a

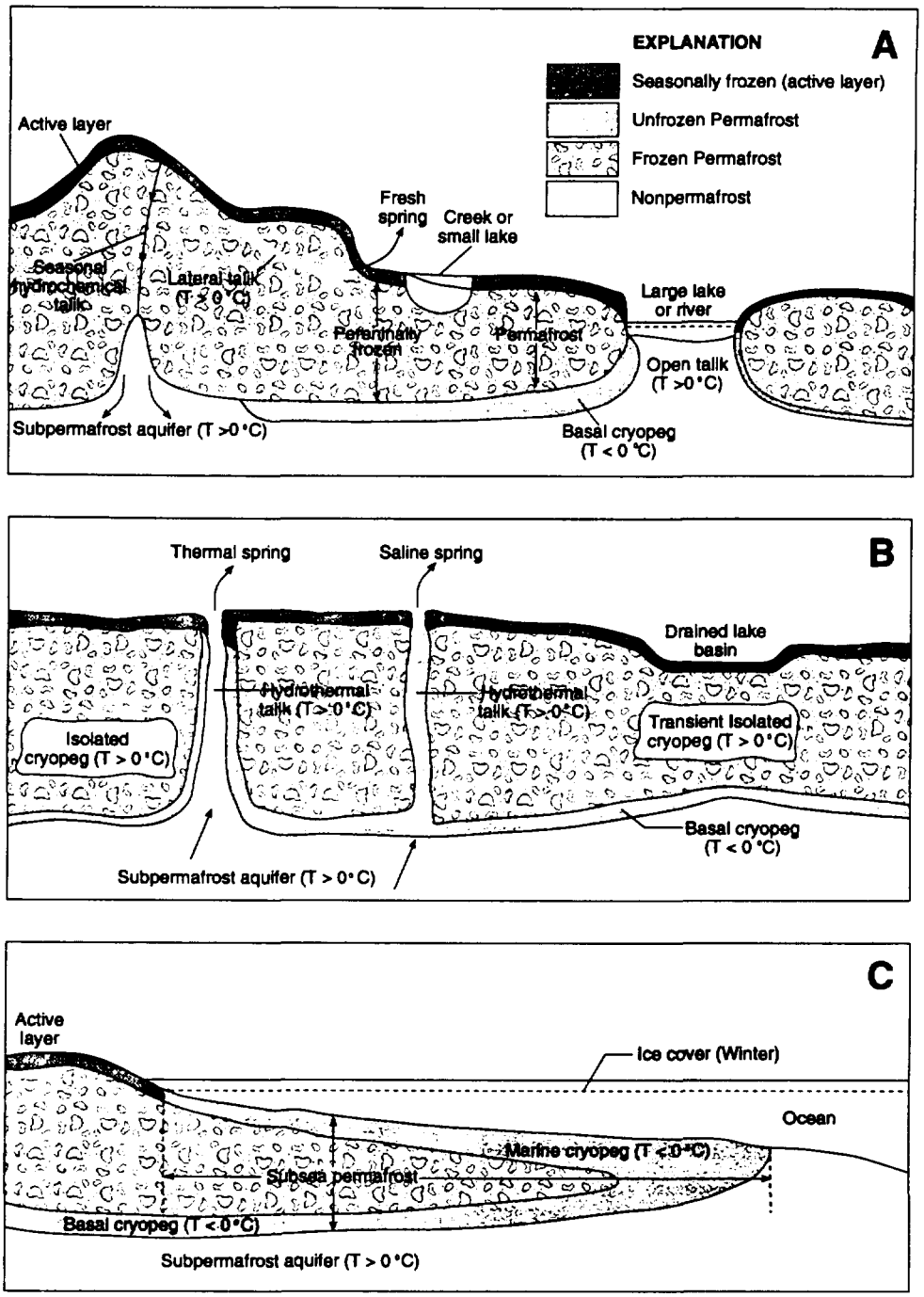

Figure 3.5. Aquifers and water conditions in permafrost areas. **(A)** Suprapermafrost: active layer, closed taliks. **(B)** Intrapermafrost: open taliks (lake, river, hydrothermal, hydrochemical); lateral taliks; transient isolated taliks; isolated, marine and basal cryopegs. **(C)** Subpermafrost. From Sloan & van Everdingen (1988).

zone of continuous permafrost in the north, and one of discontinuous permafrost further south (Washburn, 1980). The junction between the two coincides with the boundary between the tundra and boreal forest zones.

Thaw lakes, rivers and springs may be related to taliks (unfrozen openings in the permafrost). The maximum reported depth of permafrost is about 1400-1500 m in Siberia. Thicknesses of about 1000 m have been reported in the Canadian Arctic and at least 600 m in northern Alaska. Permafrost thicknesses of up to 400 m below the centre of the ice sheet and up to 250 m in front of the ice sheet have been calculated for the next major Scandinavian glaciation (Boulton & Payne, 1992; this study, Section 2.9).

3.4.2 Glacial advance

Relatively little information is available on what happened at the beginnings of past ice ages as the continental ice sheets were advancing. However, it is likely that, as a continental ice sheet grows and extends over frozen ground, the base of the ice will initially be cold. Geothermal heat will gradually raise the temperature at the base of the thick sheet such that the pressure melting point may be exceeded eventually, creating a basal water layer typical of a warm-based ice sheet.

If permafrost has been buried beneath the ice sheet, it will begin to melt gradually from the bottom upwards because of the increased thermal gradient and will completely melt if the ice sheet is warm-based (e.g. Skinner & Porter, 1987; Boulton & Payne, 1992).

Predictions of future Scandinavian glaciations by Boulton & Payne (1992) and others suggest that permafrost may be present beneath the outer cold-based zone of an ice sheet before it completely melts away beneath an expanding melting zone.

Due to the temperature and basal shear stress zonation at the base of an ice sheet, the basal melting regime and the pattern of erosion and deposition at any geographical location will undergo a complex evolution with time as the ice sheet grows and thins (Section 3.3). An advancing ice sheet will bring about some deposition, followed by glacial erosion, although the majority of the erosional, transportational and depositional activity of a continental ice sheet will take place at the melting stage, when the ice margins are retreating (see below).

Loading of the lithosphere and local deformation of the bedrock will take place as an ice sheet advances across an area. A forebulge (an area of elevation) will develop on the margins of the ice-loaded depression and is considered to migrate in the direction of the advance of the ice sheet (Figure 3.4c). There is a great deal of controversy concerning forebulge size, the distance at which it occurs away from the glacier margin and the speed at

which it migrates and collapses during deglaciation. For example, the maximum forebulge upwarping for the Weichselian Glaciation has been modelled to be as low as 18 m about 280 km from the ice front (Walcott, 1970) or, alternatively, the forebulge may have reached a speculative height of 170 m (Mörner, 1979). Several intermediate forebulge models also exist. For example, Boulton (1991) has modelled a forebulge elevation of approximately 80-90 m at a distance of 200 km away from the ice front for a maximum ice sheet thickness of 2000 m. Depression of the lithosphere will occur soon after the forebulge has migrated onwards and will affect an area before the ice front reaches the region (Figure 3.4c).

3.4.3 Glacial maximum

During the peak of a glacial episode, the ice sheet will have obtained its maximum thickness and maximum loading of the lithosphere will take place. Ice sheets provide loads of relatively high magnitude but of such short duration that they do not often reach complete isostatic equilibrium and may involve a time-lag of as much as 15 000 to 20 000 years. As a rule of thumb (Eronen & Olander, 1990), the maximum crustal downwarping beneath an ice sheet is estimated to be 25-30 per cent of the maximum ice thickness, although the downwarping would be considerably less for ice sheets of short duration. Load-induced downwarping will naturally be less towards the margins of the ice sheet. Beneath the centre of the ice sheet, it is likely that basal ice temperatures will be below the pressure melting point and permafrost may be therefore developed (e.g. Boulton et al., 1993; Boulton & Payne, 1992).

3.4.4 Glacial retreat

The most powerful erosional and depositional effects are delayed until the end of each glaciation. As the climate and the ice mass become warmer, a large proportion of the ice sheet in the melting-freezing zone will become warm-based and the ice will move by sliding over the substrate and erode by freeze-thaw plucking of the bedrock (e.g. Sugden & John, 1976). As the ice sheet retreats, the lithosphere begins to rebound. The surface rebound decreases exponentially following the release of the ice-load from the bedrock.

Retreat of a grounded, land-based ice sheet may occur in a different way to that of an ice shelf or even a continental ice sheet which has its margin as ice cliffs at the sea. For example, fjord glaciers may display very rapid retreat, in comparison to the slower retreat of a land-based glacier, owiing to the process of frontal calving from the ice cliff at the glacier margin (e.g. Glacier Bay, Alaska; Skinner & Porter, 1987). Indeed it is suggested by Skinner & Porter (1987) that the final retreat of the interior of the ice sheets of eastern North America and Europe during the last glaciation probably involved the

retreat of calving margins which rapidly cut back into the ice sheets and caused them to collapse. However, if the ice sheet is fully grounded on land (above sea level), retreat will tend to be slower, with ablation at the margin by simple melting of the ice (Sugden, 1982).

3.4.5 Ice sheet growth and decay

Glaciers and ice sheets grow when snowfall exceeds melting and they shrink when melting exceeds snowfall. Ice flow is also important, since it transports the ice from regions where it builds up (accumulation) to regions where it melts away (ablation) or breaks off into marginal seas to melt (calving). Ice flow will be greatest where the ice sheet is warm-based.

Ice sheets may be considered to advance and retreat at relatively constant rates over geological timescales. Estimated rates of retreat of the Weichselian Scandinavian ice sheet are in the order of 150-200 m/year from reconstructions by Boulton et al. (1985) and Holmlund & Fastook (1993; Figure 3.6). Rates of advance may be very different to those of retreat. For example, an advance rate of 50 m/year and retreat rate of 1000 m/year have been modelled for the Weichselian glaciation by Boulton & Payne (1992). However, present-day observations have shown ice margins to display variable rates of movement. For example, ice surging is relatively well documented in upland glaciers (e.g. Skinner & Porter, 1987). Surging is defined as periodic, very rapid movements of large quantities of ice within a glacier, alternating with much longer periods of near stagnation. Surging is frequently accompanied by major advances of the glaciers terminus. Recent surges of the Bering Glacier have involved an advance of part of the terminus of more than 1,500 m into Vitrus Lake at a velocity approaching 200 m/day with other parts in stagnation or retreat (EOS article, Nov. 9, 1993). Recentrly, ice surging has also been suggested as the cause of polar ice streams which move rapidly through the more sluggish mass of ice sheets such as the West Antarctic Ice Sheet (Lingle & Brown, 1987). Calculations by Lingle & Brown (1987) have suggested that high porewater pressures in sub-glacial sediments beneath Ice Stream B would facilitate the rapid motion of the ice stream which is effectively decoupled from its bed. Their model is consistent with direct geophysical measurements indicating the presence of a porous, saturated sub-glacial till layer. Surges within ice sheets, such as those in West Antarctica, are often channelled down valleys and feed into ice shelves. Stress-related features, such as intense crevassing, displaced moraines and extensional fractures, are commonly formed during surges. The Scandinavian glaciation record has shown that glaciation of a large area could be quite a fast process. One process contributing to the fast glaciation observed could be the outlet surges described by Lagerlund (1987; see Section 2.6).

Generalised models for the growth and decay of ice sheets are simplified and, therefore, may not represent local margin geometry at any one point owing to

(a)

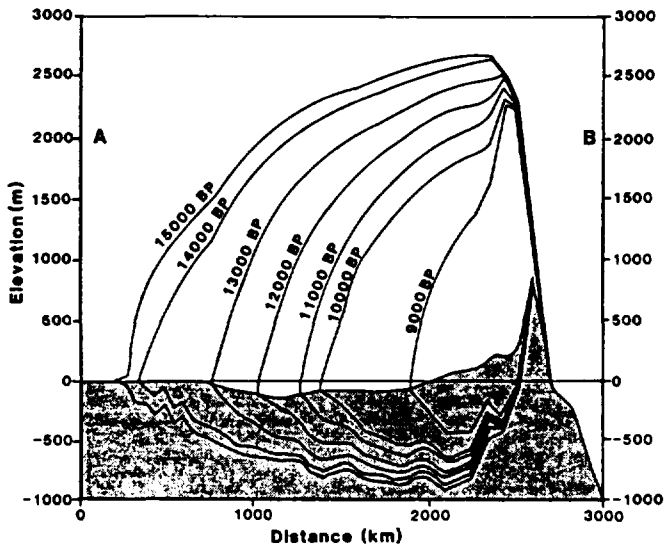

(b)

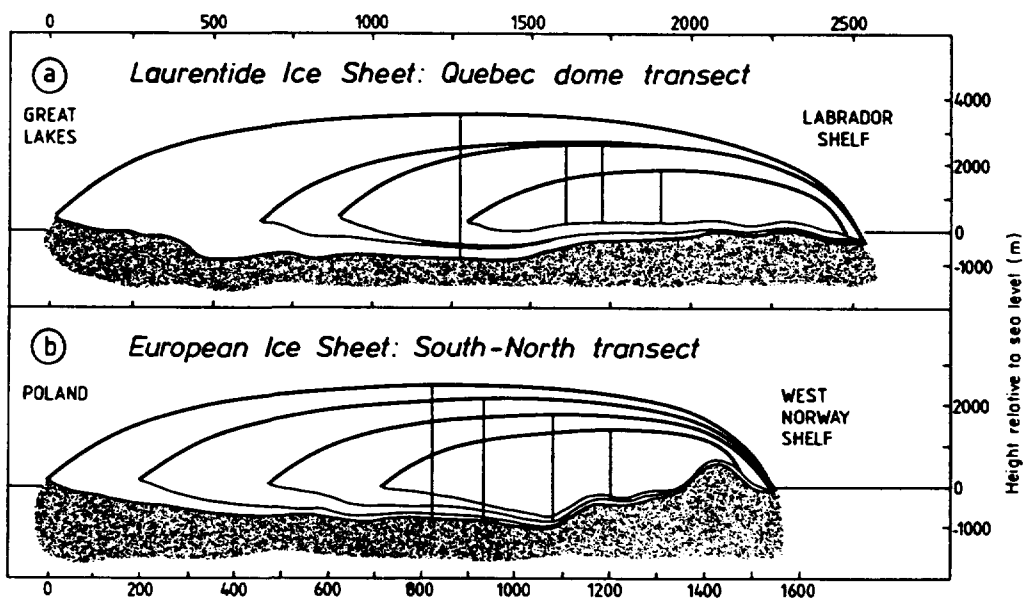

Figure 3.6. Two-dimensional transects of the European ice sheet at different stages of its decay. **(a)** Across the Scandinavian continent from the west Norway shelf to Poland. From Boulton et al. (1985). **(b)** From the west Norway shelf along the Baltic Sea to Denmark. From Holmlund & Fastook (1993).

factors such as termination in the sea or on land and local ice activity. It is likely that a glacial cycle spanning, say, tens of thousands of years, may comprise several smaller scale periods of localised advance and retreat. Boulton & Clark (1990) have shown that the Laurentide Ice Sheet was characterised not only by fluctuations at the margins, but also by lateral shifts of as much as 2000 km in the centres of maximum thickness and flow. Modelling of the last glacial cycle in Europe (Boulton et al., 1985; Boulton & Payne, 1992), in conjunction with reconstructions (e.g. Böse, 1990), has described irregular growth of the ice sheet with relatively rapid on-land expansion of the central south-eastern sector of the ice sheet during advanced stages of growth, in comparison to calving-inhibited growth along the north-western margin. Dating of depositional features suggests that wastage of the last mid-latitude ice sheets was not characterised by unchecked headlong decay, but that well-defined and substantial halts in the processes of mass loss occurred even during the early interglacial period (Boulton et al., 1985).

Various high-frequency climate changes have been recognised in the recent geological record, including the Younger Dryas cold period of NW Europe, the 'Dansgaard-Oeschger' oscillations in the Greenland ice cores (e.g. Dansgaard et al., 1989), and the 'Heinrich layers' in North Atlantic sediment cores (Heinrich, 1988; Broecker et al., 1992). The latter two types of change have durations of a thousand years or so with recurrence intervals of a few thousand years. Six Heinrich events have been identified in the last 60-70ka. All of these phenomena have been associated with the sensitivity of thermohaline circulation to the influx of freshwater and ice (e.g. Stocker & Wright, 1991).

During the Younger Dryas cooling event in central Scandinavia during Weischselian deglaciation, the ice sheet has been found to respond to cooling in different ways and at different rates in different places. These differences have been interpreted to reflect both mass balance and substrate effects (Holmlund & Fastook, 1993). Fluctuation of an ice sheet margin is, therefore, not merely a function of climate and mass balance but also a function of the change in hydrogeologic and strength properties of the substrate (e.g. Boulton & Jones, 1979).

4 Overview of Ice Sheet Impacts on Surface and Sub-surface Conditions

4.1 Introduction

Now that the main events and processes that are considered to occur during a glacial cycle of a continental ice sheet have been introduced, these features are considered in detail, in terms of their effects on the far-field of a potential repository situated at a depth of c.500 m within a fractured crystalline bedrock. The following sections describe the potential impacts, both observed and modelled, of a glacial episode on rock stress, hydraulic conditions, groundwater chemistry and surface conditions of the local bedrock.

4.2 Rock Stress and Rock Mechanics

The advance and retreat of an ice sheet will exert stresses on the bedrock. Most information on these stresses is derived from examination of unloading effects such as glacial rebound and reactivation of faults which have been described in the literature. Stresses on the bedrock during a glacial cycle may be a function of both the direct loading by the ice sheet (e.g. Muir-Wood, 1993) and the suppression of regional tectonic forces by the confining effect of large ice sheets (e.g. Johnston, 1987).

4.2.1 Loading and deflection of the crust

As described in the previous chapter, loading and unloading of the lithosphere occurs during a glaciation cycle. Both increased horizontal and vertical stresses have been related to glacial loading and rebound in Scandinavia (Muir-Wood, 1993; Chen, 1991). The stress-state in Fennoscandia prior to the accumulation of the last ice sheet has been inferred to be one in which the maximum horizontal stress was NW-SE and the minimum principal stress vertical (Muir-Wood, 1993), although it may also have been the case that intermediate principal stress was vertical (Ove Stephansson, pers comm, 1994). The imposition of the ice sheet would have served to increase the vertical stresses far more than the horizontal stresses. Loading by an ice sheet causes downwarping, characterised by lithospheric radial compression, as the underlying mantle is forced towards the surrounding forebulge. However, for the duration of the ice sheet, it is likely that the increase in vertical stress significantly exceeded any increase in horizontal stress and, as a result, the area covered by the ice sheet was almost aseismic (Johnston, 1987, 1989). During glacial unloading, the vertical stress returns to its pre-glacial state, but horizontal stresses take longer to respond to the slow inward flow of mantle material. While the rebound dome

may experience crustal subsidence and compression (Muir-Wood, 1993).

The form of the ice sheet, sub-glacial topography and the rheology of the lithosphere are important in determining the response of the bedrock stress to glacial loading (Muir-Wood, 1993). On a larger scale, crustal stresses will be affected by the thickness of the lithosphere and by the centre(s) of maximum ice thickness. Rates of deglaciation will also have an effect on the spatial distribution of rates of uplift and, hence, local stress regimes. On a smaller scale, a grounded ice-cliff margin would be expected to have a greater loading effect on the local bedrock than a tapering, hence thinner, land-based ice margin, although the larger scale isostatic loading effect would not be significantly different (Figure 4.1).

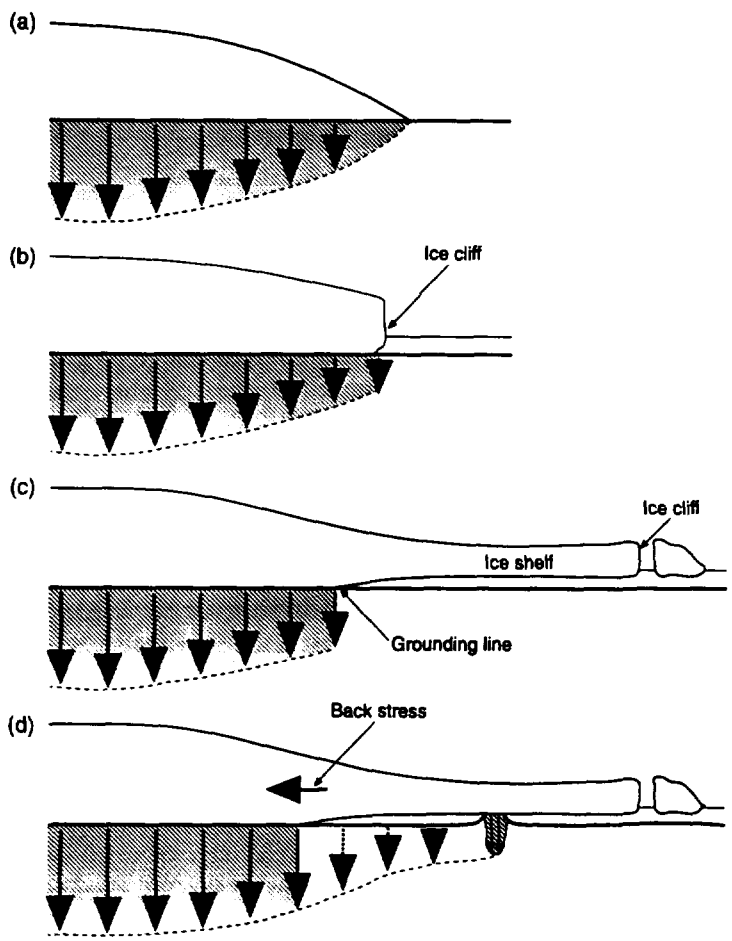

Figure 4.1. Simplified cartoons showing the general distribution of vertical loading by ice sheets of variable morphology. **(a)** Land-based ice sheet; **(b)** Grounded ice sheet terminating in water; **(c)** Grounded ice sheet continuing in water as an ice shelf; **(d)** As for (c) but with the ice shelf partially grounded (solid arrows, shaded area) and/or trapping water beneath it (dashed arrows, unshaded).

In addition, a floating ice shelf would have very little or no direct stress effect on the sea or lake bedrock unless it were temporarily grounded due to irregularities in the sea or lake topography. An ice shelf that has run aground or is restricted in its movement would be expected to exert considerable horizontal stresses on the grounded ice sheet behind it (Oerlemans & van der Veen, 1984). Considerable stresses may also be exerted on the bedrock beneath an isolated inland sea or lake which is overlain by an ice sheet, because of the low compressibility of the water relative to the bedrock.

As well as affecting the lithosphere directly below the ice, stress effects will also be felt ahead of the ice sheet, as far as the forebulge upwarp. Hence, through a glacial cycle, a particular site will experience a sequence of changing stress states as the forebulge upwarps and downwarps pass through the area (Figure 4.2), increasing as the ice sheet directly impinges in the bedrock and thickens, causing maximum horizontal and vertical stresses during the maximum development of the ice sheet. During retreat of the ice sheet, loading stresses will decrease and will continue to decrease even once the ice sheet has retreated away from the area. It is during glacial unloading that tectonic activity may be maximised (see below).

It is considered likely that the current stress-state of Fennoscandia is fairly close to the stress-state that existed prior to glaciation, except for regions in which there has been large scale stress release in fault displacement and, consequently, permanent strain (Muir-Wood, 1993). However, the disparity between the pre-glacial tectonic stress-state and that encountered today (taking into regard the fact that rebound is not yet quite complete) could provide a measure of the degree to which there has been local strain release within the glaciation/deglaciation cycle (Muir-Wood, 1993).

Preliminary modelling has given some insight into the nature and distribution of stresses during glaciation. Shen & Stephansson (1990) have shown that glaciation is likely to have a large influence on the magnitude of principle stresses but a relatively minor influence on principle stress orientation. Only while an ice wedge overlies a site may there be a significant reorientation of principle stresses. The stress increase at the location of a 500 m deep repository is about 6 MPa for the horizontal stresses and about 28 MPa for the vertical stress (Shen & Stephansson, 1990). More recent modelling of the Äspö site has shown that similar stress changes occur (Stephansson & Håkan, pers comm., see Section 8.3)

4.2.2 Reactivation of fractures and seismicity

The possibility of reactivation of fractures is obviously of great importance to the hydrogeology and long-term stability of a potential repository site. Fractures may be potentially reactivated both during and subsequent to ice sheet development.

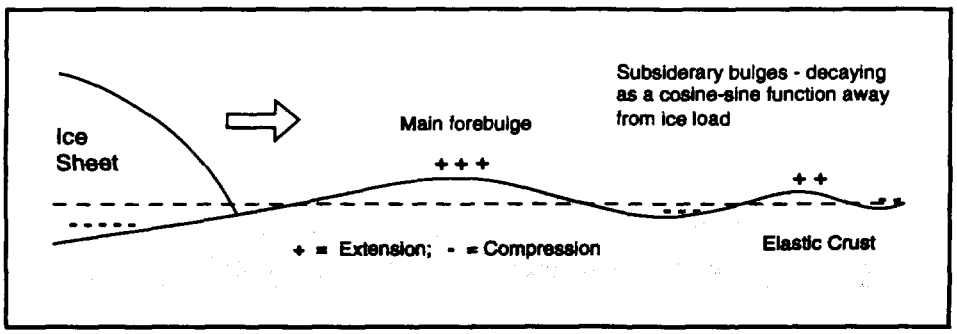

Figure 4.2. Simplified representation of the theoretical pattern of forebulge uplift and downwarp ahead of an advancing ice sheet. From Ove Stephansson (pers comm, 1994). No scale inferred.

Evidence of postglacial fault movements has been reported from several parts of northern Sweden and Finnish Lapland, notably in the northern regions such as the Lansjärv area (Lundqvist & Lagerbäck, 1976; Lagerbäck, 1988; Bäckblom & Stanfors, 1989). The supposed postglacial faults in northern Scandinavia seem to reveal a major component of thrust-fault movement along ancient NE-SW trending structures. Studies have found that postglacial fault movements occurred within major zones of older faulting, shortly after the ice sheet left the area during a time when the postglacial sea covered the area. For example, the Lansjärv Fault is considered to have formed within a few years or, at most, a few decades, of being uncovered by the ice sheet. Both strong postglacial uplift (Muir-Wood, 1989, 1993) or release of suppressed tectonic forces by the load and insulation of large ice sheets (Johnston, 1987) have been suggested as causes of the faulting. Johnston (1987), among others, has argued that the crust is supressed and stabilised by the ice load so that crustal movements that would otherwise take place more or less continuously are delayed. All the movement that has added up during the glaciation will take place over a short period of time after deglaciation. Muir-Wood (1993) has argued that the recent and present seismotectonics of mainland Sweden are predominantly a result of rapid deglaciation and postglacial rebound and that regional tectonics play a minor role, although this is a matter of some debate. Despite evidence for reactivation, there appears to be no evidence that new faults have formed as a result of glaciations. Numerical modelling of rock mass response to future glaciations (e.g. Rosengren & Stephansson, 1990; Dames & Moore, 1992) show that future displacements caused by glaciation and deglaciation are most likely to occur in pre-existing fracture zones.

It has been suggested that sub-glacial water pressures generated during ice sheet loading (see below) may induce extensive hydrofracturing in the bedrock (e.g. Muir-Wood, 1989; Boulton et al., 1993). Hubbert & Rubey (1959) first considered the role of fluid pressure in the mechanics of

overthrust faulting. They showed clearly that the shear resistence along a horizontal or gently-dipping fault plane will approach zero if the porewater pressure on the fault plane approaches the total overburden pressure. Hydrofracturing may, therefore, be expected to be most likely in the proglacial zone where porewater pressures may build up beneath the permafrost (Boulton et al., 1993).

During erosional unloading of rocks, joints may form owing to the greater ease with which decompressed rock expands normal to, rather than parallel to, the free surface (e.g. Hobbs et al., 1976). It is possible that similar joints may form as a response to the removal of an ice overburden. These types of joints are generally restricted to within a few hundred metres of the rock surface and are not as well developed in anisotropic rocks. Reactivation of pre-existing joints, particularly if they have low dips, may also be likely.

4.2.3 Fracture volume changes and displacement

Under glacial conditions, a number of factors may affect fracture volume. If a thick permafrost layer forms, the formation of ice within a fracture and the resulting expansion of the fracture water volume will exert stresses that tend to propagate the fracture (e.g. Davidson & Nye, 1985). During a glacial advance, it has been suggested that high porewater pressures and the increasing weight of ice acts to reduce the volume of fractures in the bedrock (Nurmi, 1985). However, the response of fracture systems to loading is likely to be more complicated. Owing to the overburden from the ice sheet, the bedrock is compressed and horizontal and subhorizontal fault planes are likely to be forced together and/or sheared. On the other hand, vertical or subvertical fracture zones may undergo some increase in compression due to horizontal stresses, shearing due to vertical stress, or even slight horizontal expansion as a result of the excess porewater pressures which may build up beneath a thick ice sheet (see Section 4.3). The determination of hydrogeological properties of the rock mass is therefore complicated (see Section 4.3.7). Modelling by Shen & Stephansson (1990) has provided estimates of fracture deformation. They predict that 3 km of ice loading will result in 1.9 cm of closure along the horizontal fracture zones and almost 6 cm of shearing along inclined major fractures for their modelled block (11 x 10 x 7 km). Most of the fracture deformations are elastic and are recovered during deglaciation. Up to 12 cm of post-glacial joint movement has been observed in Scotland (Davenport et al., 1989). A complicated fracture zone geometry will result in a complicated stress distribution in the rock mass. Hence, non-uniform fracture volume changes are likely to occur within anisotropic bedrock overlain by ice. Fracture volume changes and movements will have an effect on the transmissivity of fracture zones as well as the fractured bulk rock (Section 4.3.7).

4.3 Groundwater Flow

Groundwater flow rates, hydraulic gradients, groundwater flow directions and the size of groundwater catchments may all be affected significantly by a continental ice sheet and periglacial conditions. The presence of hydraulic connections between water bodies at the surface, within and to the base of an ice sheet, may also affect the rate and volume of groundwater flow in the underlying bedrock. Field data on the hydraulic conditions at the base of an ice sheet, or in the underlying bedrock during major glaciations and deglaciations, are still generally lacking. Observations and interpretations of water movement and storage within and at the base of present and past ice sheets must, therefore, be utilised to infer how the bedrock groundwater may be affected. Palaeohydrogeology can also provide some information concerning past glacial water movement.

4.3.1 Permafrost

The hydrogeology of permafrost areas is not very well understood and recent advances have only been made because of increased development in areas such as Alaska, northern Canada and Siberia. Knowledge is generally confined to observations of groundwater discharge phenomena, observations of karst recharge and data on a small number of shallow wells distributed over a very large area (e.g. Michel & Wilson, 1988).

Since permafrost is defined solely on the basis of temperature, it may not necessarily comprise completely frozen ground. Therefore, it should not be considered as totally impermeable, but rather as a confining bed with a very low permeability (Sloan & van Everdingen, 1988). With decreasing temperature below 0°C, the hydraulic conductivity of the soil (or rock) decreases. The presence of segregated ice, as layers or lenses, may decrease hydraulic conductivity to the point where the ground becomes effectively impermeable (Sloan & van Everdingen, 1988).

The presence of muskegs (peat bogs) and numerous lakes and ponds in areas where the rainfall is not high (e.g. in the Canadian arctic) illustrates that infiltration and recharge are severely restricted by permafrost, especially in areas of low relief (Roulet & Woo, 1986; 1988). Many of the larger lakes and rivers, however, are underlain by taliks of variable horizontal and vertical extent. If these taliks completely penetrate the permafrost, pathways are available either for recharge or discharge of sub-permafrost water. The concentration of recharge in smaller areas and fewer points can lead to increased recharge and discharge rates. Measurements are only available from karstic regions of Canada where, during snowmelt, inflow into individual sinkholes in permafrost near the Great Bear Lake exceeded 1 m^3/s (van Everdingen, 1981).

Lateral movement of groundwater in permafrost areas (van Everdingen,

1976) is confined to :

- seasonal flow in the active layer during the frost-free season,
- flow in taliks and
- flow in unfrozen rock below the permafrost.

At sufficient depths below the permafrost, the groundwater flow regime remains relatively unaffected, except that the volumes of water could be retricted if the permafrost is continuous and lasts for considerable periods of time. Groundwater flow cells within crystalline rock, which do not normally have a great lateral extent, are likely to be widened because of restricted recharge and discharge. However, this effect may not be considered to be too significant, as gradients may perhaps be halved, and transit times perhaps doubled (McEwen & de Marsily, 1991).

Research in Canada (according to McEwen & de Marsily, 1991) has shown that most springs in permafrost areas derive their water from subpermafrost regions via open taliks. Base flow measurements from rivers have also suggested that the groundwater contribution to base flow in drainage basins in the discontinuous permafrost zone generally ranges between 1 and 5 l s^{-1} km^{-2} in Canada and Alaska (Sloan & van Everdingen, 1988).

Fractures, which tend to dominate groundwater flow in crystalline rock, may become sealed by ice within the permafrost zone, but if flow is relatively significant prior to permafrost development, a major fracture or fracture zone may form an open talik with subsequently increased flow (Figure 3.4).

The distinction between continuous and discontinuous permafrost is important in consideration of the hydrogeological regime of an area, since there is no (or very little) hydraulic connection between groundwater and surface water flow in the case of continuous permafrost. Continuous permafrost beyond an ice sheet will tend to act as a seal which maintains glacially-generated porewater pressures (Boulton et al., 1993; see subsequent discussions) and does not allow sub-glacial groundwaters to be discharged. On the other hand, if the permafrost is discontinuous, glacially-generated porewater pressures will be reduced and discharge of sub-glacial groundwaters will be permitted, albeit through restricted taliks.

4.3.2 Observations of ice sheet hydrogeology

There appears to be a general paucity of hydrogeological data on the movement of groundwater beneath glaciers and particularly continental ice sheets. The only observational information found during this study is that of Sigurdsson (1990), who describes groundwater patterns beneath glacial areas in Iceland.

Sigurdsson (1990) has demonstrated that glacial groundwater constitutes a

major component in some shallow aquifers extending for some kilometers away from the glaciers and fracture zones extending for tens of kilometers away. His studies also indicate that the dilution of the glacial groundwater is less the higher the anisotropy of the aquifers. On highly permeable ground, with a sufficient supply of precipitation and glacial melt, the infiltration through the glaciers was estimated to reach 1500-2000 mm yr^{-1}. Observations by Sigurdsson of flow channels and conduits at the margins of the glaciers indicated that the permeability structure of the glaciers is characteristed by few but wide conduits. This indicated that infiltration into the ice was rapid, but may have been limited, the storage was restricted and the release was also rapid. However, where the permeability of the bedrock was lower, the glacial meltwater was forced to flow off the glacier as surface water. The total groundwater infiltration rates under two glaciers in Iceland were estimated as 50-80 $m^3 s^{-1}$ (for a glacier area, 1000 km^3) and nearer 10 $m^3 s^{-1}$ (for a similar glacier area). Sigurdsson (1990) estimated that the groundwater component of river discharge from the glacial basins (300-350 $m^3 s^{-1}$ for each glacier) was perhaps 70% in the first case, but only 15% in the latter case. This was attributed to the different permeabilities of the glacial basins.

4.3.3 Sub-glacial Hydrology

The location and flow of internal and basal glacial water is of considerable interest and importance for potential groundwater recharge as well as sub-glacial erosion. Several modes of basal water flow have been proposed:

- in thin sheets or films;
- through interlinked cavities;
- in various types of channel or conduit;
- in ponded water bodies (lakes).

These features are discussed below.

Water layers and films

Weertman (1966, 1972) has argued that, where the bed of a glacier is impermeable, basal water will discharge in a thin film only a few 10^{-6} m thick. The glacier surface slope is the main control on the direction of water flow. However, the likelihood of sheet flow over substantial areas of real, rough glacier beds is open to question (e.g. Nye, 1976).

Cavities

Water may be considered to be located in and flow through cavities connected by thin channels. Walder & Hallet (1979) have described cavities from the recently deglaciated beds of the Blackfoot Glacier, Montana and Castleguard Glacier, Alberta which have a vertical relief of between 0.1 and

1.0 m and make up to 20-24% of the ice-rock interface. Weertman (1972) modified his sheet flow theory by allowing the film of water to thicken to form minor pools but his theory has not gained wide acceptance and is considered as one particular case of basal water flow.

Channels and conduits

Two fundamental types of channel are recognised in present-day glacial regimes (Weertman, 1972; Röthlisberger, 1972; Nye, 1976), as confirmed by dye-tracer experiments (Drewry, 1986):

- Röthlisberger (or 'R') channels
- Nye channels

'R' channels comprise a series of conduits or pipes at the base of a glacier incised upwards into the ice (e.g. as found in the margin of the Schuchert Glacier, East Greenland; Drewry, 1986). Tunnel melting is due to frictional heating of turbulent water flow.

Nye channels are incised into the bedrock beneath a glacier. These canals consist of many wide, shallow, channels which do not form an arborescent network but comprise short, often unlinked segments, which may have been eroded out along the lines of abrasional features such as striations or gouges. Discharges of 10^4 to 10^5 m^3y^{-1} have been calculated for a channel of average size carrying surface-derived meltwater from the Blackfoot Glacier (Walder & Hallet, 1979), which is equivalent to the total discharge produced by basal melting alone.

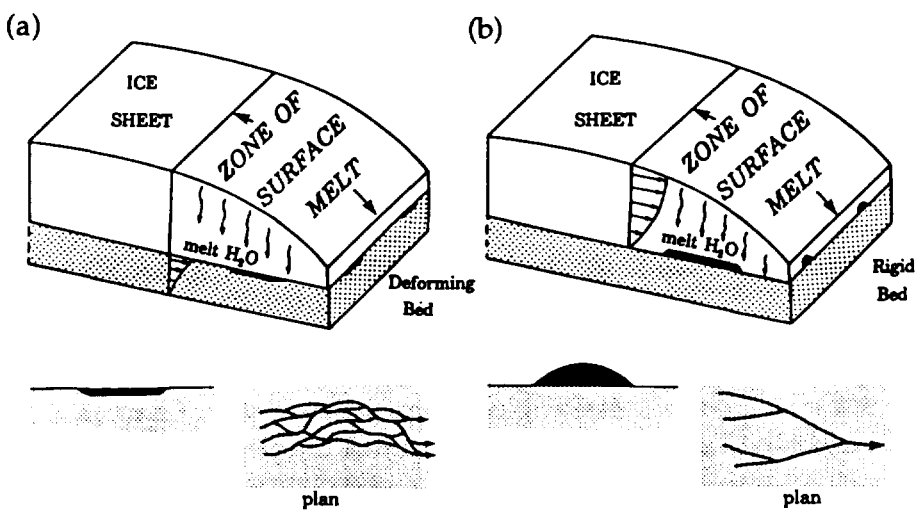

Figure 4.3. **(a)** Schematic illustration of drainage over a deforming bed via a system of canals (Nye-channels?). **(b)** Schematic illustration of drainage over a rigid bed via a system of tunnels (R-tunnels). From Clark & Walder (1994).

Glacial theory predicts that the sub-glacial drainage network at the base of gently sloping ice sheets resting on deforming sediment should consist of braided shallow canals (perhaps similar to Nye channels) rather than an aborescent network of a relatively few large tunnels, as would develop over a rigid substrate (Figure 4.3). A corollary prediction has been examined by Clark & Walder (1994) that eskers, which form in large sub-glacial tunnels, should be rare where sub-glacial bed deformation occurred, but they may be relatively common where the bed was rigid. They have observed that the distribution of eskers in areas of the Laurentide and Eurasian ice sheets during the last glaciation coincides reasonably well with the presence of high-permeability till overlying crystalline bedrock, thus matching the theoretical predictions. The orientation of sub-glacial channels would be expected to reflect the overall topographic slope imposed by the ice sheet, as appears to be confirmed by the distribution of eskers for the Laurentide and Eurasian ice sheets (Boulton et al., 1985; Clark & Walder, 1994).

Sub-glacial Lakes

In favourable locations, meltwater may be ponded to form large bodies of water or lakes. Such reservoirs may occur:

- on the surface of a glacier,
- where a glacier dams a suitable topographic depression (e.g. Graenalon, Iceland), or
- as accumulations in hollows or under favourable pressure gradients a t the glacier bed.

The latter are well known beneath the East Antarctic Ice Sheet (e.g. Drewry, 1981), where they occur in areas of low surface slope, low ice velocity, low surface accumulation and where bedrock hollows exist. Although most sub-glacial lakes have small horizontal dimensions in the order of a few kilometres, several very large lakes (up to 8000 km^2) have been observed (Drewry, 1986).

4.3.4 Erosional and depositional features in Scandinavia

Erosion is considered to have been of minimal extent at the centre of the glaciated area in Fennoscandinavia during the Weichselian glaciation, as indicated by the discovery of organic material in Lapland and northern Sweden dating back beyond the peak of the glaciation (e.g. Lundqvist, 1986). However, both erosion and glacial transport were more pronounced nearer the ice margin, as indicated by lack of organic deposits and erratics in Estonia sourced from the Precambrian bedrock of Finland (Donner, 1989). This is consistent with the calculations of Hindmarsh et al. (1989) which predict the presence of a melting zone associated with greater erosion of the bedrock. Even so, it is still considered that average erosion was only in the order of a few metres in Finland over the last glaciation (e.g. Okko, 1964),

Figure 4.4. (a) The pattern of glaciogenic longitudinal, radial lineations (primarily drumlins and striae) and frontal morrains (concentric, transverse features) over Fennoscandia. From Boulton et al. (1985). (b) Distribution of eskers deposited by the Eurasian ice sheets (margins shown by the heavy line). Intermediate line separates crystalline bedrock from sedimentary bedrock. From Clark & Walder (1994).

perhaps because the landforms and deposits most susceptable to erosion had mostly been removed by earlier glaciations.

Meltwater depositional formations, such as eskers, sandurs and glaciofluvial deltas, are more common in glaciated areas of Scandinavia than are erosional landforms of glaciofluvial origin (Boulton et al., 1985; Clark & Walder, 1994). It is the study of these features which give insight into the histories of past ice sheets in terms of their advance, retreat and discharge, since the morphology and orientation of the features is considered to be directly related to the evolution of the ice sheet (Boulton et al., 1985; Clark & Walder, 1994).

For example, such features have been described for the southern and central parts of the South-Swedish Highlands (e.g. Persson, 1974; Boulton et al., 1985; Figure 4.4). Glaciofluvial canyons in Sweden, of a few metres to 100 m depth, have also been described by Olvmo (1989) who interprets them as having been formed by glaciofluvial streams flowing subaerially, along the ice margin, in open crevasses behind the margin, or by supraglacial streams superimposed on the ground. Olvmo (1989) only recognised a single canyon which was likely to have formed sub-glacially. He has interpreted the lack of canyons in the low areas of Sweden to be related to the restriction of canyons to areas characterised by deglaciation above sea level.

The presence of depositional features such as eskers would indicate, therefore, that water movement occurred at the base of the ice sheet of the last glaciation to affect Sweden, at least partially in the form of 'R' channels. Sub-glacial flow along incised canals was probably rare, as indicated by the lack of sub-glacial meltwater canyons (Olvmo, 1989). Similar features may be likely, therefore, to control sub-glacial water movement in future glaciations, with orientations governed predominantly by the thickness distribution of the ice sheet (Figure 4.3).

4.3.5 Rates of glacial discharge of meltwater

Water which has travelled through or across the surface of a glacier is discharged in one or several large melt outwash streams (Drewrey, 1986), which are generally restricted to the summer melting season. Much work has been undertaken on the study of glacier discharge but ice sheet discharges have received less observation. Lingle & Brown (1987) have calculated sub-glacial discharge of 3-18 m^3/s at the ice sheet grounding line of Ice Steam B of the West Antarctic Ice Sheet.

Boulton et al. (1993) have investigated glacial melt rates, particularly regarding the sensitivity of sub-glacial melt rates to glacier dynamics, variations in geothermal flux and topography. Changes in ice sheet dynamics were found to strongly influence the rate of basal melting, whereas geothermal flux and topography had less influence on the meting rates. According to their calculations, melt rates at the base of an ice sheet are likely to fall within a

range of 2-100 mm/year. In contrast, surface melting rates are likely to be one to two orders of magnitude greater than sub-glacial rates (Sugden & John, 1976; Boulton & Payne, 1992). Boulton & Payne (1992) have calculated that sub-glacial meltwater flux may reach 2000 m^2y^{-1} during the next glacial cycle, in comparison to only about 320 000 m^2yr^{-1} surface meltwater flux, for an ice sheet with areal dimensions of approximately 1500x1125 km.

Sudden, high magnitude discharge events, or jökulhlaups, have been recognised in Iceland, occurring about twice each decade (Björnsson, 1974), with an average volume discharge of 3 to 3.5 km^3. Numerous streams and rivers discharging from glaciers show sudden flood events which result from heavy rainstorms or strong ablation on the glacier. Larger floods, however, are usually caused by the rapid emptying of glacial water bodies. The 1922 jökulhlaup was one of the largest ever recorded, discharging c.7.1 km^3 water with a maximum flow of 5.7×10^4 m^3 s^{-1}. Nye (1976) remarked that this is more than the flow of the river Congo. Meier (1972) summarised many of the hypotheses for the triggering of jökulhlaups including:

- vertical release of an ice dam by floatation consequent upon raised water levels;
- overflowing of an ice dam (especially in ice margin locations);
- destruction or fissuring of an ice dam by earthquakes;
- drainage at the ice-bed interface through pre-existing tunnels due to enlargement of the tunnels by increased water pressures or frictional melt enlargement;
- sub-glacial melting by heat from volcanic activity.

4.3.6 Sub-glacial water pressures

The very weight of the ice above the bedrock will exert a pressure on the underlying bedrock and, hence, any groundwater contained therein. As a rule, the water will only support some fraction of the weight of the ice, the solid substrate supporting the remainder. In other words the total stress is composed of the fluid pressure and the so-called 'effective stress' exerted by the solid, with the latter not being zero in general (A. Provost, pers comm, 1994). Only if the rate of glacial discharge were high enough, and the permeability of the substrate low enough, would the water pressure rise to support the full weight of the ice.

The precise form of the piezometric surface for groundwater flow beneath an ice sheet can only be calculated if local geohydrological parameters are known. In the absence of such information Boulton & Broadgate (1992) took a limiting case, in which, over a significant area, groundwater heads were expected not to exceed ice pressure (thickness) values. As a first approximation, they suggested that the form of the piezometric surface should be taken to be the form of the glacier surface, giving both heads and pressure gradients. Hence, discharges and hydraulic gradients are expected to

increase towards the margins of an ice sheet. The ice will exert pressure on any sub-glacial water equivalent to approximately one tenth less than the equivalent height of water, since the density of ice is only 0.92 g cm^3. For example, for a glacier 1000 m thick, the maximum ice head would be 920 m. However, it must be stressed that this approximation is likely to result in an over-estimation of hydraulic head values.

Calculations by Hindmarsh et al. (1989) indicate that the basal temperature in the central part of a thick ice sheet will probably be beneath the pressure melting point. Thus, no groundwater recharge or flow would be expected in this region and groundwater will be stagnant. In the basal melting zone, however, melting rates may be in the range of 2-100 mm per year (Ahlbom et al., 1991; Boulton et al., 1993). If the potential pressure in sub-glacial water rises to equal the value of ice pressure, the water will be expelled either directly into the underlying bedrock via conductive fracture zones or aquifers, or will flow in channels (such as 'R' or Nye channels) at the glacier-bedrock interface finally to emerge at the ice front as glacial outwash. If the transmissibility of the bedrock is low, the total sub-glacial discharge may not be able to occur by groundwater flow alone and tunnels will form at the ice/bed interface enabling transport of a significant part of the total meltwater discharge. On the other hand, if the transmissibility of the substrate is high, it may have the capacity to discharge all the melt by groundwater flow and there will be no tunnel flow (Boulton et al., 1993). Particularly high water pressures would be expected to occur within ice-loaded sub-glacial water bodies such as sub-glacial lakes. Sub-glacial meltwaters, if expelled into the bedrock, will both increase the volume of groundwater flowing through the rock mass and increase the groundwater flow rates.

Hence, over the relatively impermeable bedrock of much of Sweden, tunnel flow is likely to dominate the sub-glacial discharge, but over the thick, permeable aquifers of Scania, Denmark, Germany and Holland, all the melt flux could be accomodated by groundwater flow (Clark & Walder, 1994; Boulton et al., 1993).

However, an additional effect of the development of sub-glacial tunnels is that they may affect local hydraulic pressures and hydraulic gradients. It is likely that a tunnel will be associated with a lowering of the local hydraulic head at the bedrock surface and associated increases in the local hydraulic gradients (result of discussions at the Workshop on Glaciation & Hydrogeology held in Stockholm, April 1996; King-Clayton et al., 1997). Thus, local groundwater flow patterns may be rather more complicated and less predictable than one may initially expect.

4.3.7 Sub-glacial hydraulic connections

The presence of hydraulic connections from the top surface of an ice sheet to the base of the sheet may have an effect on the sub-glacial discharge of meltwater into the groundwater system. At a sub-polar glacier surface, water is usually confined to a network of streams and in places ponded in surface lakes. Flow also takes place in near-surface layers of permeable snow and firn (compacted snow). The downward percolation of meltwater is usually slow and complicated owing to the presence of many inhomogeneities, such as ice layers, lenses and fractures which will divert the meltwater (Drewry, 1986). At the firn/ice transition, ice becomes impermeable as pores in the ice are sealed off. Saturation of the overlying firn occurs above this level and a continuous piezometric surface (water table) is usually present. The piezometric surfaces within the Grosser Aletsch Gletscher and the Findelengletscher Glacier, Switzerland and the South Cascade Glacier, Washington are found at depths of 14-32 m, 70 m and 25-75 m respectively, approximately 20-50 percent of the glacier thickness (Drewrey, 1986; Figure 4.5). Downward percolation continues largely via cracks, fissures and crevasses which coalesce with depth. Raymond & Harrison (1975) and Berner et al., (1977) found percolation rates of 7.6×10^{-8}m s^{-1} for water penetrating to a glacier sole. It is generally considered that water descends rapidly to the bed, taking the shortest possible route without being stored in any considerable volume nor for any considerable time (Drewry, 1986). Models of meltwater flow above, within and to the base of glaciers have been attempted by Sugden & John (1976) as shown in Figure 4.6.

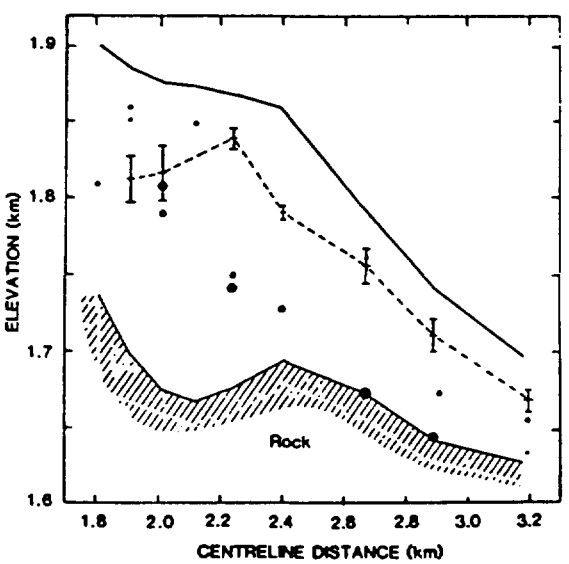

Figure 4.5. Water within the South Cascade Glacier, Washington. Water is located in cavities encountered during drilling (solid circles proportional to cavity size). The dashed line represents the piezometric surface (water table). From Drewry (1986; after Hodge, 1976).

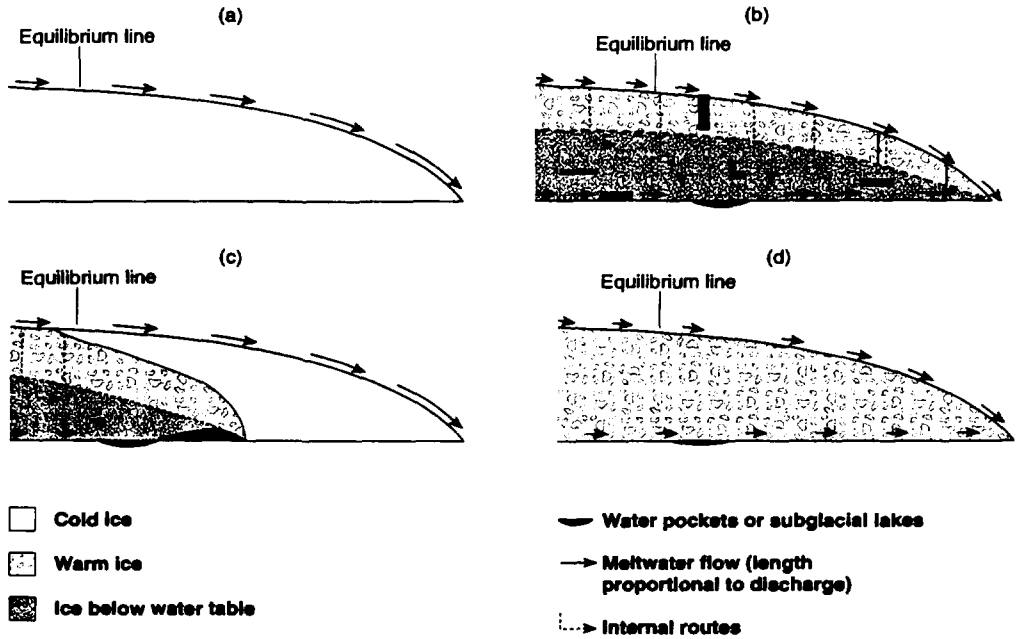

Figure 4.6. Meltwater models for glaciers and ice sheets of different temperature regimes: **(a)** cold ice, **(b)** warm ice, **(c)** combination of warm ice in the accumulation zone and cold ice in the ablation zone, **(d)** high altitude glacier. From Sugden & John (1976).

If crevasses and fissures extend to the base of an ice sheet they would, thus, provide an open hydraulic connection from the top of the ice mass to the bedrock. However, such connections are only likely to develop at the unstable margin of a mid-latitude ice sheet where calving of the ice occurs into the sea or a lake, or at the edges of a surging ice stream or glacier. Surface meltwater generated during the summer season may drain into moulins (vertical pipes formed by plunging, rotating water) and crevasses which penetrate to the surface. However, during the winter, any cavities which developed during the previous summer by the action of meltwater would tend to close at a shallow depth of 100 to 150 m by the flow of ice (Boulton & Payne, 1992). Further towards the centre of an ice sheet, more than a few 100s of metres away from the margin, it may be more likely that fissures and crevasses in the ice will self-heal due to freezing of water and flow of ice.

In the absence of hydraulic connections such as crevasses, glacial discharge into the bedrock will be supplied exclusively by basal melting. However, towards the margin of an ice sheet, particularly an unstable, crevassed ice cliff margin, hydraulic connections may occur. These will allow supraglacial water to penetrate to the base of the ice sheet, hence increasing the potential glacial discharge into the bedrock by up to two orders of magnitude, since the rate of surface melting may be considered to be two orders of magnitude greater than that of sub-glacial melting (Sugden & John, 1976; Boulton & Payne, 1992).

4.3.8 Glacial stress effects on hydrogeology

The stresses induced during a glacial cycle (Section 4.2) will have an effect on the transmissivity of both individual fracture zones and on the bulk rock transmissivity. However, such changes are likely to be extremely complicated owing to the complexity of fracture systems, the tectonic state of stress, differential horizontal and vertical stresses induced during ice loading and porewater pressure effects. Little work, therefore, has been undertaken to determine glacial effects on bedrock transmissivity.

Wallroth & Gustafson (1993) have proposed a general conceptual model for the depth-dependence of bulk hydraulic conductivity due to the change in overburden stress during ice loading, but they make it clear that the model only accounts for vertical stress change and neglects any excess porewater pressure effects.

In very general terms, it may be expected that, owing to the overburden from the ice sheet, the bedrock will be compressed; therefore, horizontal and subhorizontal fault planes are likely to be forced together and/or sheared. This will tend to decrease their transmissivity due to the decrease in fracture apertures, and increase in the area of contact points between asperities on the fracture surfaces which results in longer and more tortuous flow paths. Vertical or subvertical fracture zones may undergo some closure or shearing because of vertical and horizontal stresses. However, excess sub-glacial porewater pressures may cause the fracture to open (Section 4.2.3). This will lead to a slight decrease, or even an increase, in the transmissivity of the fractures. Changes in bulk rock transmissivity are even more difficult to estimate, since the geometry of the fracture systems may be very complicated. However, it is likely that overall compression of the bedrock during ice loading will cause bulk rock transmissivity to decrease, whereas lithospheric rebound will cause overall extension of the rock mass and an increase in bulk rock transmissivity. Once stress states have returned to their pre-glacial values, rebound having finished, transmissivity values may also be expected to return to their pre-glacial values. However, if stress changes have been accomodated by fracture movement during deglaciation, more permanent changes in fracture transmissivity may result which are not able to revert to pre-glacial values before the next glacial cycle resumes.

Crustal rebound predominantly involves crustal expansion and an associated increase of crustal porosity can be predicted across Sweden over the past 10 000 years (Muir-Wood, 1993). It has been calculated that, for a crust with a flowing porosity of 0.1 percent, a cumulative post-glacial strain of 10^{-4} since deglaciation, distributed down to a depth of 10 km, would draw surface groundwater to an average depth of 1000 m (Muir-Wood, 1993). This depth is, of course, very sensitive to the flowing porosity of the rock mass. Conversely, during loading, or during forebulge collapse, a reduction of

fracture apertures would be expected during compression, which would tend to expel water from the bedrock, particularly beyond the margins of the ice sheet. The coseismic strain associated with seismicity is also expected to affect crustal porosity (Muir-Wood, 1992). Elastic rebound following normal faulting is compressional and, hence, causes crustal porosity to decrease and results in increased groundwater discharge. On the other hand, rebound is extensional following reverse fault movement, causing increased crustal porosity and drawdown of surface waters.

4.3.9 Glacial groundwater flow predictions: summary

Modelling of the subsurface reponse to ice sheets has been complicated by the coupling of ice sheet dynamics and groundwater flow; melt rates both influence and are influenced by the effective pressure at the sole of the ice sheet. The following features are likely to have a significant effect on the hydrogeology of a glaciated site:

- climate,
- nature of the substrate,
- geometry of the ice sheet (partly a function of substrate),
- orientation of the ice front,
- basal ice temperature and pressure,
- permafrost development, and
- loading and stress effects

Local groundwater flow patterns are likely to be re-organised on a continental scale during a glaciation, as determined by the ice sheet pressure gradient (Boulton & Payne, 1992). In contrast to normal hydrogeological drainage basins (of the order of 10's of km) which are driven by local topography, in a glacial environment it is the ice sheet surface slope which is likely to define the piezometric surface controlling groundwater flow patterns. Groundwater flow rates are expected to increase, particularly where high permeability exists in either aquifers or within transmissive fractures in crystalline rock of overall low permeability. Modelled potential gradients, groundwater discharge rates and groundwater velocities are typically two orders of magnitude greater in the distal zones of the ice sheet than in a non-glacial case (Boulton & Payne, 1992). A net downward flow vector beneath the ice sheet, and a strong upward flow beyond it, may be expected due to basal meltwater overpressuring and ice loading effects (Boulton et al., 1993; Figure 4.7).

According to Figure 4.7, in the central, cold-based zone of an ice sheet where permafrost is expected to exist, sub-glacial melting will not occur and and the groundwater will be stagnant. Beneath the zone of melting, groundwater flow will occur, with piezometric gradients defined by the surface slope of the ice sheet as a first approximation, increasing outwards. Meltwater tunnels are expected to form under these conditions, particularly where bedrock

transmissivity is low. Beneath the outer cold-based zone underlain by permafrost, sub-glacial discharge will decrease outwards as the permafrost thickens. Here, sub-glacial water pressures may build up, leading to instability and surging of the ice sheet or extensive hydrofracturing at the glacier/bed interface. In the proglacial region, permafrost may seal off potential sub-glacial aquifers or fault zones which would otherwise allow groundwater discharge. Excess pore pressures are likely to exist which will tend to cause hydrofracturing in the permafrost and pressure release, or even 'pingo'-like growths so as to release pressure (Boulton et al., 1993; Ahlbom et al., 1991).

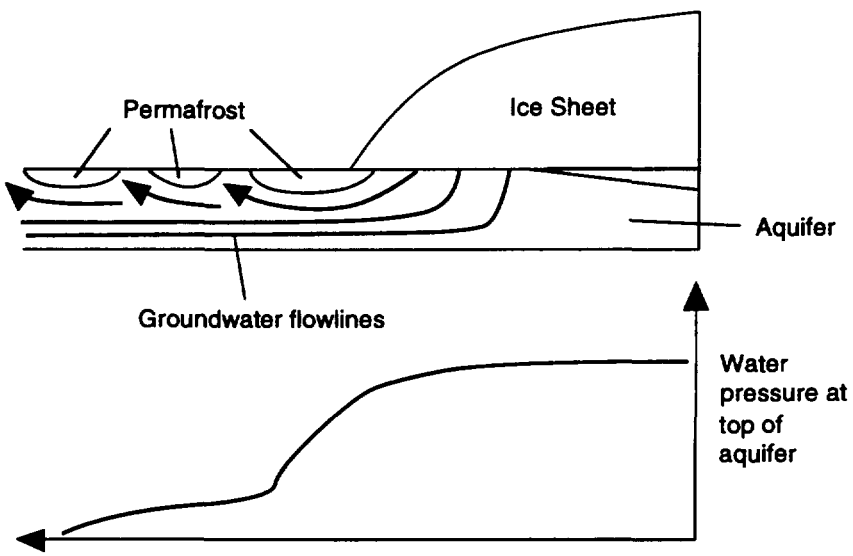

Figure 4.7. Schematic diagram of groundwater flow and water pressure beneath an ice sheet. Potential pressure gradient is zero beneath the inner permafrost zone, and has an increasing gradient beneath the melting zone and a constant gradient beneath the outer permafrost zone. After Boulton (1991).

Groundwater recharge and discharge will also be modified considerably during a glacial cycle, predominantly as a function of stress, seismicity, permafrost development and sub-glacial melting rates. Recharge will tend to be enhanced during glacial advance and retreat when basal melting of the ice sheet occurs, but will be restricted when permafrost is developed during early stages of glacial advance. Groundwater discharge, on the other hand, will be constrained to periods when the ice front is located close to a particular site and where permafrost is either absent or is punctuated by taliks which will allow discharge of glacial meltwaters.

The loading effect of an ice sheet will influence the pattern of groundwater flow both below (as described above) an ice sheet as well as in the areas

surrounding the ice sheet. For example, it is likely that the upwarping and adjacent downwarping of the forebulge area will alter the regional topographic gradients and, hence, will influence regional head gradients and groundwater flow patterns. Loading effects ahead of the ice sheet may even result in temporary reversal of groundwater flow directions as suggested in Figure 4.8.

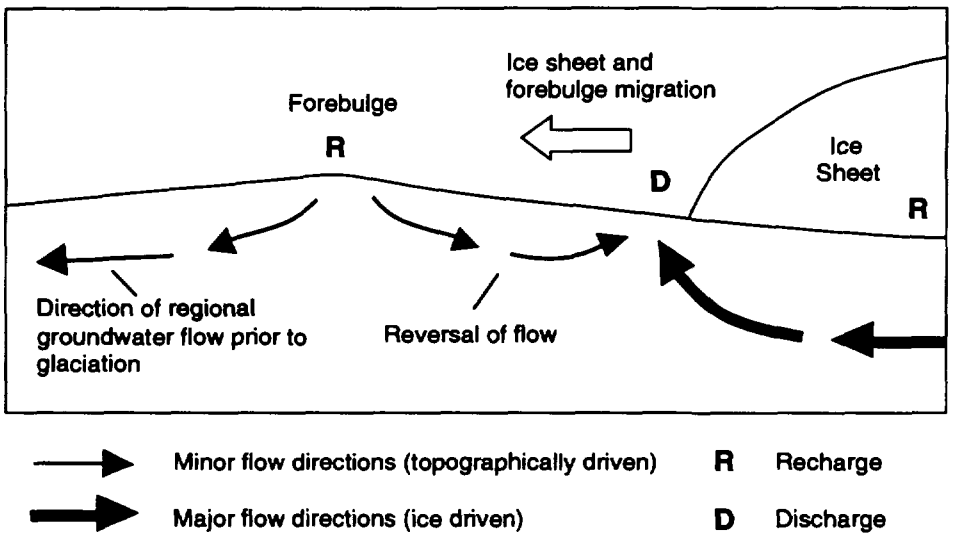

Figure 4.8. Schematic representation of the effect forebulge development may have on the groundwater flow patterns adjacent to an ice sheet, assuming a low regional topographic gradient prior to glacial advance.

Thus, the presence or not of permafrost and the geometry of the ice sheet margin may be expected to influence the groundwater flow beneath and close to the ice sheet. Some examples of how the groundwater flow pattern could vary according to different glacial marginal regimes, according to Boulton Hulton & Wallroth (1996), are shown in Figure 4.9. Similar discussions are summaried in King-Clayton et al (1997).

In addition, the presence of sub-glacial tunnels may also complicate local patterns of groundwater flow (Section 4.3.6). Thus, although it may be considered that the major control on groundwater flow is on the scale of the ice sheet, local groundwater flow patterns may be rather more complicated and less predictable owing to more local controls such as forebulge development, sub-glacial tunnel development and substrate properties.

It is considered in most models that the groundwater recharge during glacials will be entirely provided by basal melting of the ice sheet (e.g. Boulton et al.,

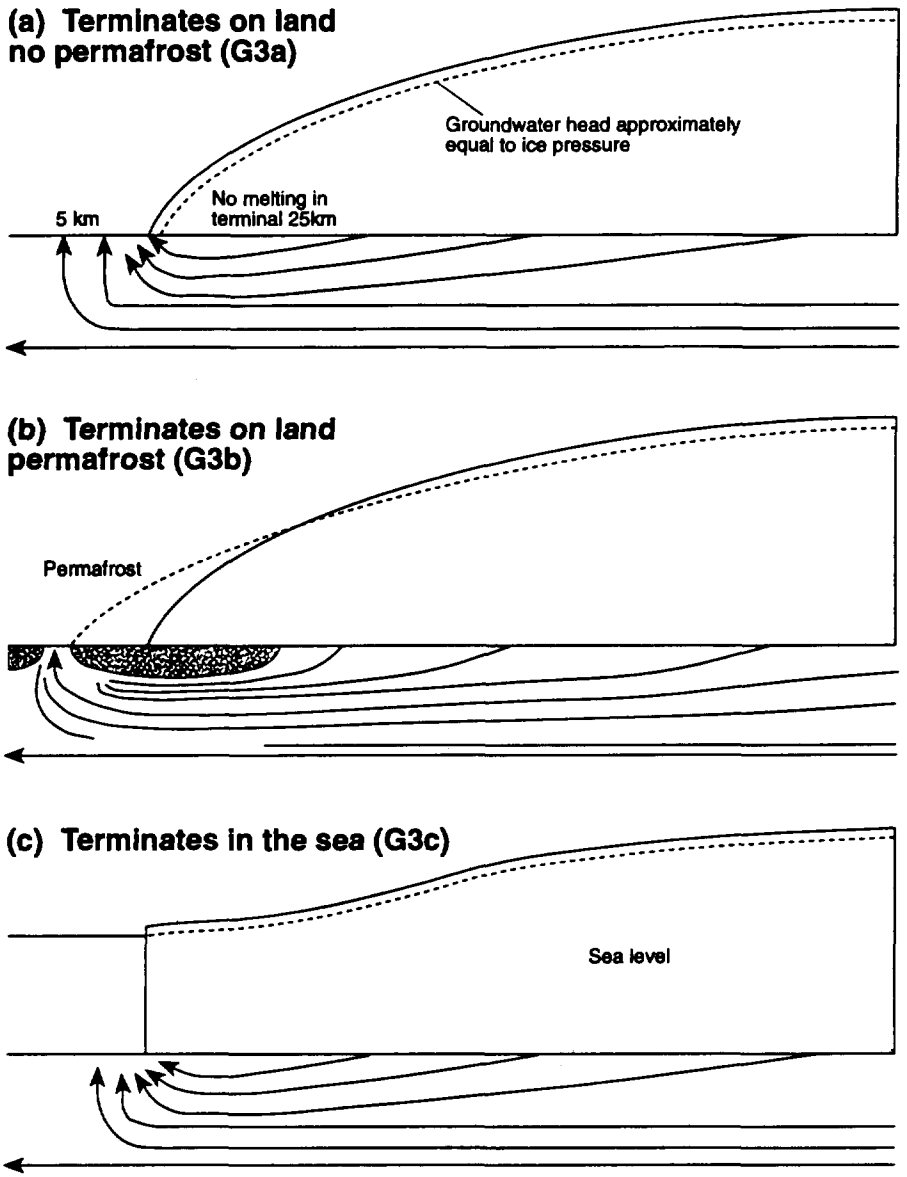

Figure 4.9. Schematic representation of glacial margin regimes, according to Boulton, Hulton & Wallroth (1996) and similar to those discussed in King-Clayton et al (1997). **(a)** The ice sheet terminates on land without proglacial permafrost. Groundwater head values are approximately equivalent to ice pressures. Glacially-driven groundwater flow rises strongly towards the surface in the immediate proglacial zone. **(b)** The ice sheet terminates on land that has proglacial permafrost. Glacially-driven groundwater flow is sustained beneath the permafrost, thereby elevating the head above the surface and generating strong buoyant forces in the permafrost zone. Stong upward groundwater flow occurs at the edge of the permafrost or in holes/taliks within the permafrost. **(c)** The ice sheet terminates in the sea. There is no proglacial permafrost. Glacially-driven groundwater flow rises strongly towards the surface in the immediate proglacial zone.

1993; Boulton & Payne, 1992). The presence of hydraulic connections with the surface of the ice sheet could increase recharge to the underlying bedrock by providing additional surface water input. This may be significant, since the rate of surface melting may be considered to be two orders of magnitude greater than that of sub-glacial melting (Boulton & Payne, 1992). However, hydraulic connections between the surface and base of an ice sheet, such as crevasses, are unlikely to occur more than a few kilometres away from the ice margins. Melt rates at the base of the ice sheet have been calculated to fall within the range 2-100 mm/year, (Boulton & Payne, 1992; Boulton et al., 1993). Taking an average melt rate of 5 mm/year Boulton et al. (1993) estimated that groundwater at 500 m depth may be driven to the surface over periods of the order of 10^3-10^5 years.

In additon to the overriding controls on sub-glacial water movement, such as sub-glacial melting rates, flow may also occur rather more episodically, or fluctuate throughout a glacial cycle as a result of smaller scale seasonal fluctuations and events such as sub-glacial tunnel development or enlargement and jökulhlaups. Such events would have the effect of intensifying flow at any one point in time although the average flow at a site may be lower.

4.4 Groundwater Chemistry

Relatively little appears to be known about changes in groundwater chemistry as a result of glacial activities. Many of the following features or processes are, therefore, predictions based upon observations of glacial meltwater compositions. It may be envisaged that the following conditions may have a significant control on groundwater chemistry:

- permafrost development
- glacial meltwater discharge
- sea level changes

4.4.1 Permafrost

Permafrost can produce changes in groundwater chemistry owing to a fractionation-type freezing process and longer residence times. These processes result in the formation of more saline waters, especially at the base of the permafrost zone (Boulton & Spring, 1986; McEwen & de Marsily, 1991). This may produce a downward-migrating saline front which could extend to greater depths, particularly along large-scale fracture zones, over a time period of thousands of years (Ahlbom et al., 1991). Permafrost may also result in a concentration of radionuclides, if they have already been released from a repository, in the groundwater beneath or within the permafrost zone, or to the base of chemically stratified lakes. These may be subsequently released as a concentrated pulse when thawing takes place (McEwen & de

Marsily, 1991).

The chemical composition of groundwater lying above the permafrost is more likely to reflect the influence of precipitation and a relatively short residence time with low dissolved components, but a relatively high organic component (McEwen & de Marsily, 1991).

4.4.2 Glacial meltwaters

The chemical analysis of glacial meltwaters collected either directly at the glacier bed or upon discharge at the glacier terminus, show them to be rich in numerous dissolved chemical species (Drewry, 1986). The principal contributions to glacial meltwater come from:

- precipitation at the ice surface,
- ice and firn,
- groundwater and surface runoff, and
- exchanges between meltwater and the atmosphere and bedrock.

Bulk meltwaters which drain from beneath Alpine glaciers consist of at least two components (Collins, 1979; Tranter & Mills, 1989). The first component, the englacial component, is dilute and represents waters which are produced by diurnal melting cycles on the glacier surface and which flow rapidly through the hydrological system. The second, sub-glacial component is more concentrated and represents water which flows at or near the base of the glacier, in contact with the comminuted glacial debris. The residence time of the sub-glacial component in the hydroglacial system is longer, which promotes solute acquisition. However, these sub-glacial waters are still likely to be considerably more dilute than the non-glacial groundwaters at depth within the underlying bedrock. In additon to simple mixing of these two components, post-mixing weathering reactions may also occur which modify the chemistry of bulk meltwaters draining from alpine glaciers (Tranter & Mills, 1989).

Meltwater has been found to contain a large number of inorganic chemical species whose concentrations vary considerably from glacier to glacier and through time (e.g Todd, 1980; Freeze & Cherry, 1979). Six principal ions (Na^+, Mg^{2+}, Ca^{2+}, Cl^-, HCO_3^- and SO_4^{2-}) make up greater than 90 % of the total dissolved solids. Dissolved gases (e.g. O_2, N_2, CO_2, CH_4, H_2S and N_2O) are also present in meltwater, as well as organic substances. The concentration of dissolved gases is expected to increase with depth within the ice, owing to the decrease in partial pressure (Berner et al., 1977).

The work of Sigurdsson (1990) has shown the chemistry of Icelandic sub-glacial groundwaters to be characterised by low concentrations of dissolved species, especially such mineral components as are normally dissolved from the host rock in the groundwater systems. The concentration of dissolved

species in the groundwater is apparently less (i.e. the dilution by glacial meltwater is greater) the lower the anisotropy of the bedrock.

It is expected, therefore, that glacial meltwater would be characterised by:

- low ionic strength (owing to the high precipitation and ice input),
- oxygen saturation with low O-isotope values, and
- low carbonate content (due to a virtual absence of microbial activity).

The latter point would not hold if the bedrock was of carbonate composition since, during its passage over carbonate rocks, sub-glacial water readily takes up carbonate (e.g. Hallet, 1976). During winter, when melting and glacial water flow is at a minimum, interaction between the meltwater and groundwater may be of decreased importance (Drewry, 1986).

These non-saline, oxidising, alkaline waters may penetrate the bedrock owing to high hydraulic gradients and porewater pressures induced beneath an ice sheet, facilitated by deeply penetrating conductive fracture zones. The depth to which oxidising conditions may penetrate is not certain, but scoping calculations suggest that, under high ice-induced flow rates in granitic rocks, a redox front could reach repository depths (500 m; Arthur, 1996).

4.4.3 Lakes and restricted inland seas

Lakes in permafrost areas often display chemical stratification. Hypersaline waters sometimes fill the deepest parts and are overlain by meteoric waters, with an intermediate mixed layer (McEwen & de Marsily, 1991). Such lakes are likely to desalinate with time, owing to increasing glacial melt input.

Dammed lakes and restricted inland seas in glacial environments may be hypersaline, brackish or dilute, depending on the origin of the water body and the amount of glacial meltwater input. Breaching of such lakes (because of those reasons outlined above) would be likely to result in a large increase in non-saline glacial water discharge or a brine-rich discharge. Saline waters are more likely to penetrate the local bedrock owing to their high density. Dilute waters may only affect the bedrock to very shallow depths.

4.4.4 Sea level changes

During a glaciation cycle, with both lowering and rising of sea level, groundwater of both marine and non-marine origin may be expected to infiltrate the bedrock causing a mixing of groundwater types (Ahlbom et al., 1991). During a lowering of sea level, non-saline water would successively replace saline water, with an associated increase in alkalinity owing to the influence of clay minerals previously in contact with seawater (Ahlbom et al.,

1991). Subsequent sea level rise would tend to cause seawater intrusion to be re-established. Transmissive fractures in the bedrock would tend to enhance any mixing processes, whereas the less transmissive rock matrix would tend to retard mixing.

4.4.5 Glacial erosion

Where glaciation removes older, oxidised surface deposits, the fresh and unweathered rock surface and subsequent glacial deposits are generally unoxidised. This will affect the redox-potential of the groundwaters, which will tend to be more reducing at shallow depths (Ahlbom et al., 1991).

4.4.6 Scandinavian palaeohydrological investigations

Site-specific investigations on the Fennoscandian shield in the circum-Baltic area have shown the present state of groundwater mixing to be highly complicated, with water components resulting from a variety of glacial and non-glacial sources (e.g. Wallin, 1995). The present day nature of groundwaters beneath Äspö has been attributed to the modification of deep saline waters by infiltrating rain and glacial meltwaters prior to, during and subsequent to the Weichselian ice sheet and to more recent marine transgressions (Smellie & Laaksoharju, 1992; Glynn & Voss, 1996; Laaksoharju & Skårman, in press; Wallin, 1995). The fracture systems appear to have provided zones of deeper meteoric and meltwater flushing than the surrounding unfractured rock. It is difficult to determine how many glacial cycles may be represented by the present-day groundwater compositions.

The freezing of seawater and deep landward intrusion of the resulting brines has been suggested as a source of saline water in the Baltic region (Bein & Arad, 1992). However, Glynn & Voss (1996) have highlighted the general lack of waters with a clear marine signature in the Äspö groundwaters. In addition, glacial waters are generally only found at greater depths (Laaksoharju & Skårman, in press). This may be due to a flushing away of both marine and glacial waters during isostatic uplift by near-surface meteoric waters and deep saline waters. Some glacial waters may be locally preserved in bedrock areas of low hydraulic conductivity which were less conducive to flushing out during isostatic recovery. Glynn & Voss (1996) attribute the majority of the deep saline waters to deep (possibly fluid inclusion) sources.

From a review of currently available palaeohydrological data in coastal areas of the the circum-Baltic area, there appears to be a multiple source for saline waters, although it is apparent that most of the groundwaters found in the coastal areas below the highest marine transgressions during the Holocene suggest that saline water intrusions, during isostatic downwarping and transgression of the sea, may have been responsible for the groundwater

formation at intermediate depths, between 150 and 500 m (Wallin, 1995). For example, fracture water at a depth of 400 m at Outokumpu in SE Finland has been found to possess an exceptionally light ^{18}O isotope values, indicating distinctly colder conditions during recharge of that water. This fracture-controlled water is interpreted as a mixture of glacial meltwater with the local dominant chloride water implying that recharge of glacial fresh water reached a depth of about 400 m (Vuorela, Äikås & Blomqvist., 1996).

It is apparent that palaeohydrogeological data may hold the key to answering many of the uncertainies regarding the impact of past glaciations on groundwater flow, chemistry and rock mechanical behaviour (see sections 8.3 and 8.4).

4.5 Biosphere and Surface Conditions

The advance and retreat of an ice sheet and the associated proglacial conditions will have a major effect on the biosphere, the zone of the earth's surface in which organisms live. This section does not aim to comprise an exhaustive review of glacial climatic effects on biosphere conditions and surface conditions, but only to identify and describe changes which may be significant for far-field (geosphere) Performance Assessment modelling.

4.5.1 Temperate conditions

In areas such as Äspö at the present day, there is little vegetative cover; bare rock comprises about 90 percent of the ground surface and the remainder is covered by thin moraine/soil located within small depressions and valleys (Smellie & Laaksoharju, 1992).

4.5.2 Boreal conditions

Coniferous forests represent the climax communities of the boreal climate. Due to the high percentage of bare rock at Äspö at present, under boreal conditions there will be little opportunity for climax communities to develop. In poorly drained, lowland areas of boreal climates, decaying plants may accumulate and bog-mosses are common. Peat, shrubs and heaths may form on top of the mosses (e.g. Selby, 1971). Boreal geomorphological processes are influenced by frost action, resulting in increased redistribution by erosional processes and mass movement. Soils are characteristically acidic and nutrient deficient owing to mineral leaching (Watkins et al., 1994).

4.5.3 Periglacial conditions

Tundra or periglacial environments are characterised by barren ground dominated by heath, lichens and mosses and few trees, although the type of vegetation is largely controlled by the topography and groundwater conditions (e.g. Selby, 1971). The presence of permafrost and frequent freeze-thaw cause disruption of root systems and redistribution of soils and sediments. Low-lying, poorly-drained areas typically form tundra marshes dominated by thick mosses, grasses, sedges and rushes. Organic accumulations can be deep within these marshlands and may therefore have a significant, but local, effect on near-surface groundwater chemistry. Erosion and sedimentation may be affected by periglacial conditions. Estimates of increases in runoff rates during snowmelt for Britain in periglacial times by Pitty (1988) suggest that between 25 and 100 times the current mean annual discharge of a major river would occur during these events. Extensive erosion of any superficial sediments is likely to take place, with deposition of these sediments in areas of low relief. Similar differences may therefore be expected in SE Sweden during the next glaciations. Soils in tundra areas are often acidic (pH 3 to 5.8; e.g. Watkins et al., 1994) and the active layer of tundra soils varies between 0.3 and 1.2 m (Larkin et al., 1992).

4.5.4 Glacial and post-glacial conditions

True glacial environments are so cold and dry that only the most hardy vegetation can grow and large areas of ground are devoid of plant growth. The presence of an ice sheet will obliterate all forms of vegetation and will cause erosion and deposition to varying degrees at the ground surface. Subsequent to the retreat of an ice sheet away from an area, the terrestrial biosphere will begin to re-establish itself, particularly once sea levels or lake levels have dropped. The plant community may take several hundred years to re-establish climax development (forest). Biosphere conditions will also be dependent on the nature of the glacial soils which were formed. If glacial soils are thin, rocky or absent, vegetation will be poorly developed even after several thousands of years (e.g. Selby, 1971). Soils exhibit poor nutrient status, owing to low decomposition rates and a low pH and are also often waterlogged (Watkins et al., 1994). After glaciation, strong winds can result in wind-blown silt (loess) being deposited over wide ares (Coughtrey, 1992). Surface run-off, river discharges and sediment loads are high as with periglacial conditions (Thorne, 1992).

5 Äspö Glacial Cycle Scenarios

5.1 Conceptualisation of the Scenarios

The following sections discuss a sequence of scenarios at Äspö for a single glacial cycle, based on the glaciation which is predicted to climax at c.60 000 years from now. It is the intention that the sequence of scenarios represent the most significant features, events and processes (FEPs) for analysis of the future safety of a repository for spent fuel. However, it is clear that the described scenarios can only provide an *illustration* of potential FEPs and their impacts and do not constitute a unique prediction of the future evolution of the Äspö region.

The location of the lines of section used to construct the scenarios are shown in Figure 5.1. The scenarios have been described at two scales; firstly, at a Scandinavian scale (1000s km; Figure 5.2) and, secondly, at a more detailed site scale (c.10 km; Figure 5.3). The larger scale is used to put the more detailed site descriptions into the context of the development of the Fennoscandian ice sheet as a whole. The scenarios described below are summarised in Appendices 1-7 and in Figure 5.1. Values have been estimated for many of the important parameters such as ice thickness, permafrost thickness, hydraulic head, hydraulic gradient and fracture transmissivities (see Section 7). Alternatives to the scenarios described in the following sections are discussed in Section 8.

(a) (b)

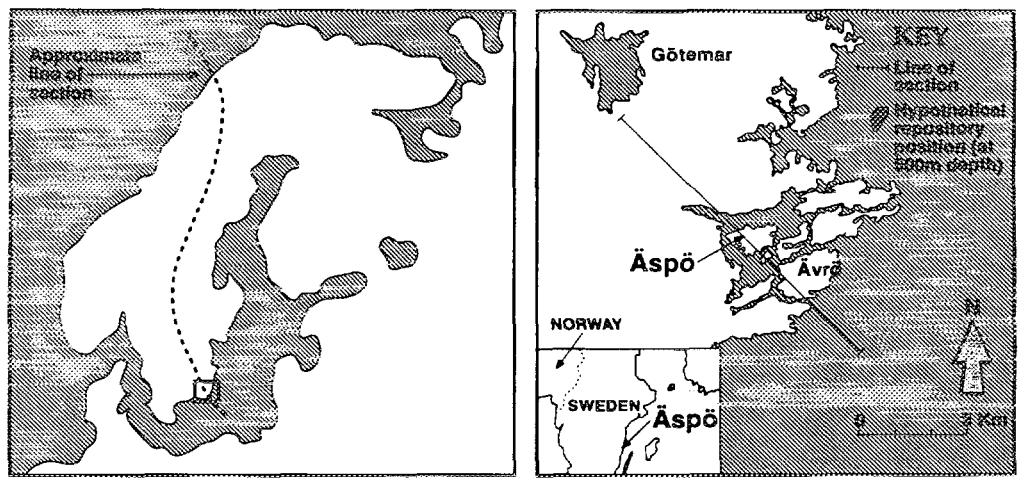

Figure 5.1. The location of Äspö with the lines of sections used to construct the glacial cycle scenarios. **(a)** Regional scale (see Figure 5.2). **(b)** Local scale (see Figure 5.3).

The following assumptions have been made in the development of the scenarios (see Section 5.9 for futher discussion):

- The Äspö region is covered by an ice sheet during the 100 ka glacial and permafrost melts beneath the ice sheet by a few ka after ice advance (scenario (iii) of Section 2.2).

- The topography and substrate of the Äspö region and area is assumed to be unchanging throughout the glacial cycle. Although some modification may take place owing to both deposition and erosion, it is considered to be unlikely to be changed significantly.

- Only three fault zones (EW-1, NE-1 and the Ävrö Zone) are considered. Obviously, further transmissive and non-transmissive zones will be present throughout the Äspö region and area. Flow within the regional bedrock is assumed to occur predominantly along hypothetical fault zones of average to high transmissivity, although these are not specified. The flow paths shown within the bedrock are therefore only intended to display approximate flow directions.

- The geometry of the ice sheet has been assumed to be that of a single ice dome covering Scandinavia and northern Europe. As discussed in earlier sections, this may not have been the case for the last glaciation to affect Scandinavia which may have involved the formation of several coalescing domes (e.g. Anundsen, 1993), but it must suffice as a first approximation in the light of insufficient data to predict a more detailed distribution of ice thicknesses. Such an approximation will tend to lead to over-estimations of the ice sheet thickness at Äspö for future glaciations.

- The possibility of the development of localised ice streams/lobes at the margins of the ice sheet have not been considered although similar features are considered to have been possible during the Weichselian Glaciation (e.g. Holmlund & Fastook, 1993).

- The morphology of the ice sheet during different scenario stages has been determined by assuming that the ice sheet develops over a predominantly non-deformable substrate during the early and later periods of the glacial cycle (over the majority of Norway and Sweden), but that the ice sheet may advance and retreat over more peripheral deformable substrate, such as that of inland Europe and the Gulf of Bothnia, during the glacial maxima.

- Surface profiles have been determined by consideration of maximum ice thickness estimates and the horizontal extent of the ice sheet (Section 3.2), modelling by Boulton & Payne (1992) and by comparison with the Antarctic and Greenland ice sheets (e.g. Embleton & King, 1975; Skinner & Porter, 1987).

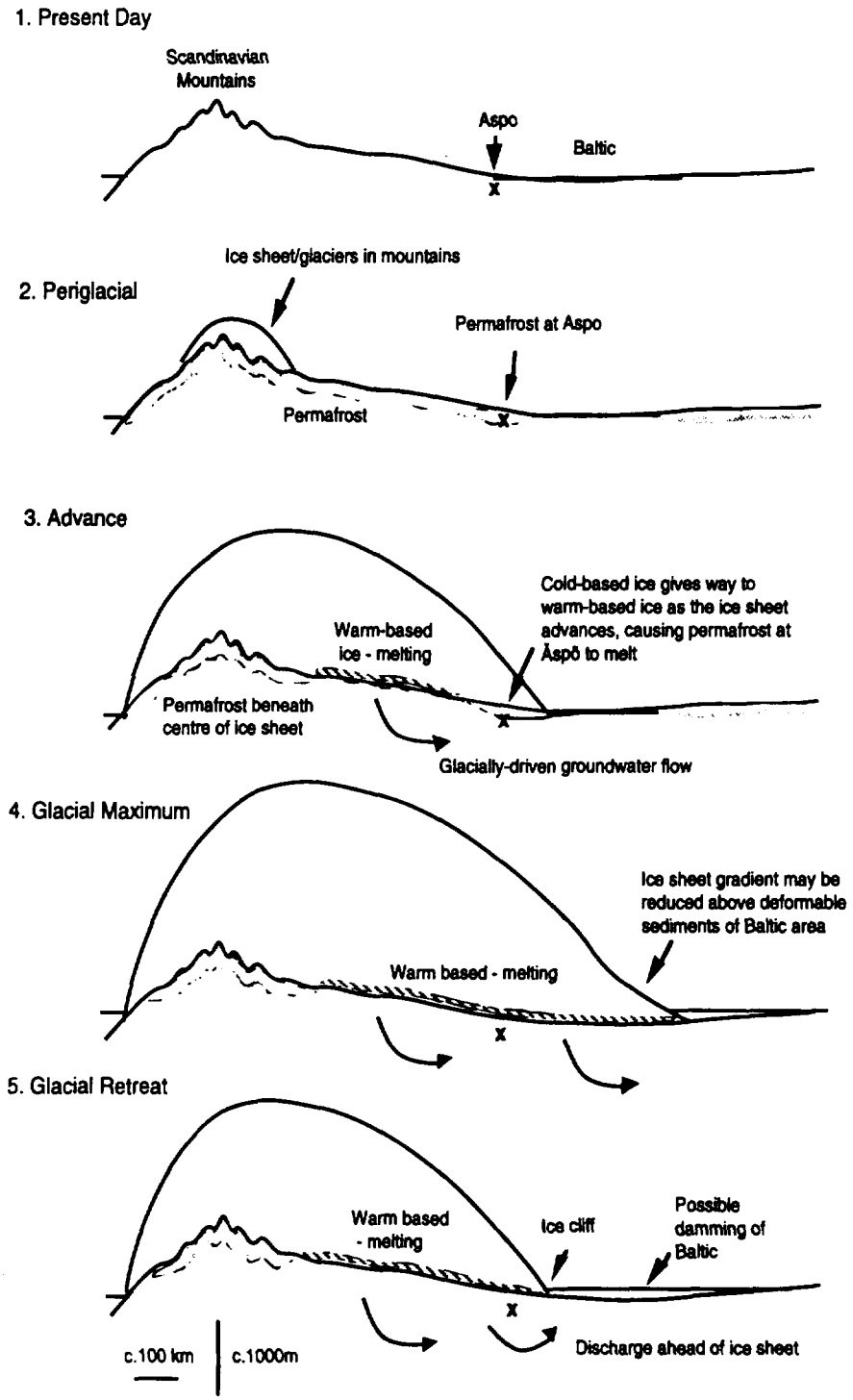

Figure 5.2. Continental scale scenarios for the Scandinavian ice sheet through the glacial cycle predicted to occur from 50 000 to 70 000 years from now.

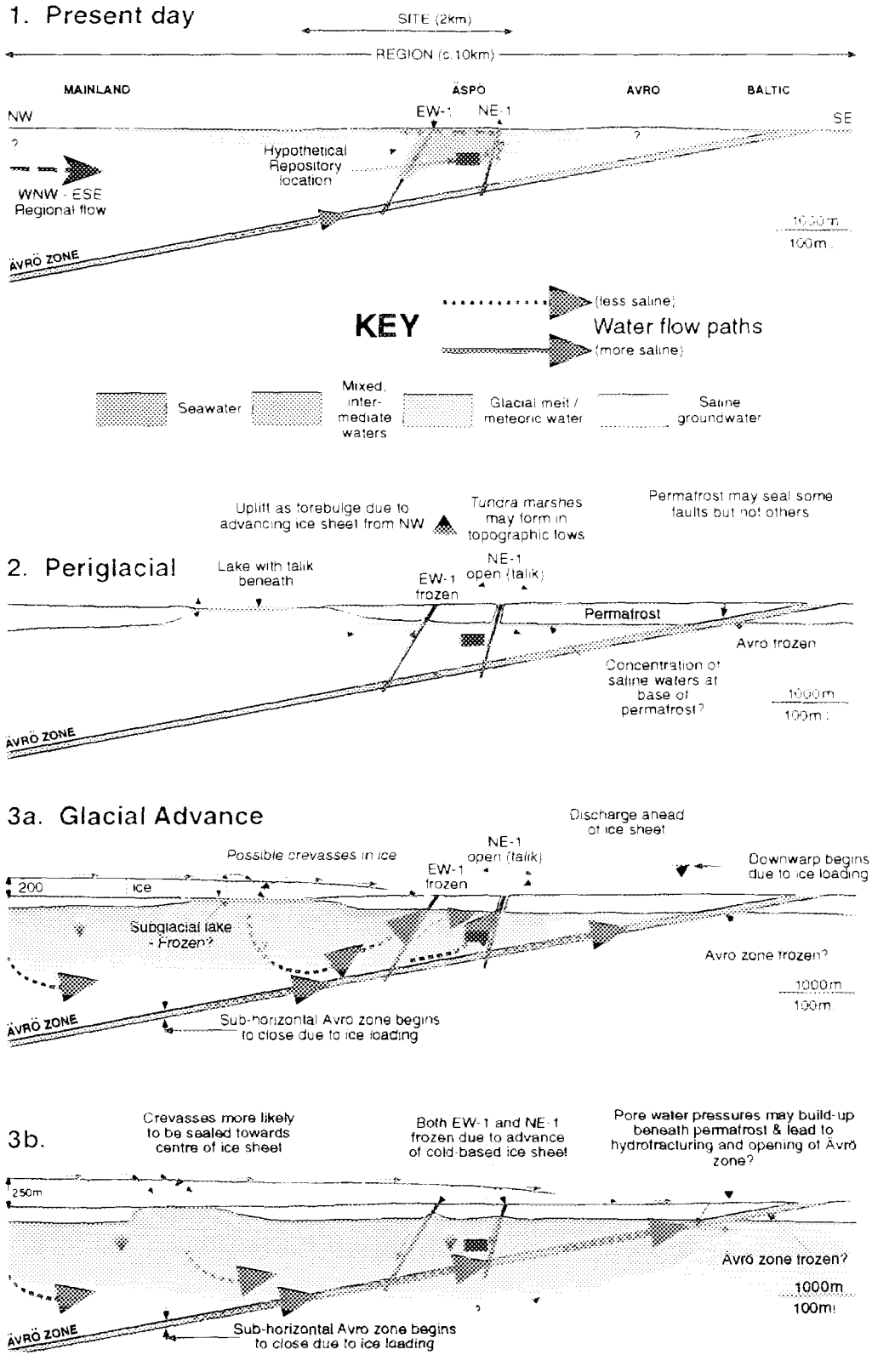

Figure 5.3. Local scale scenarios for the Aspö site and area through the glacial cycle predicted to accur from 50 000 to 70 000 years from now.

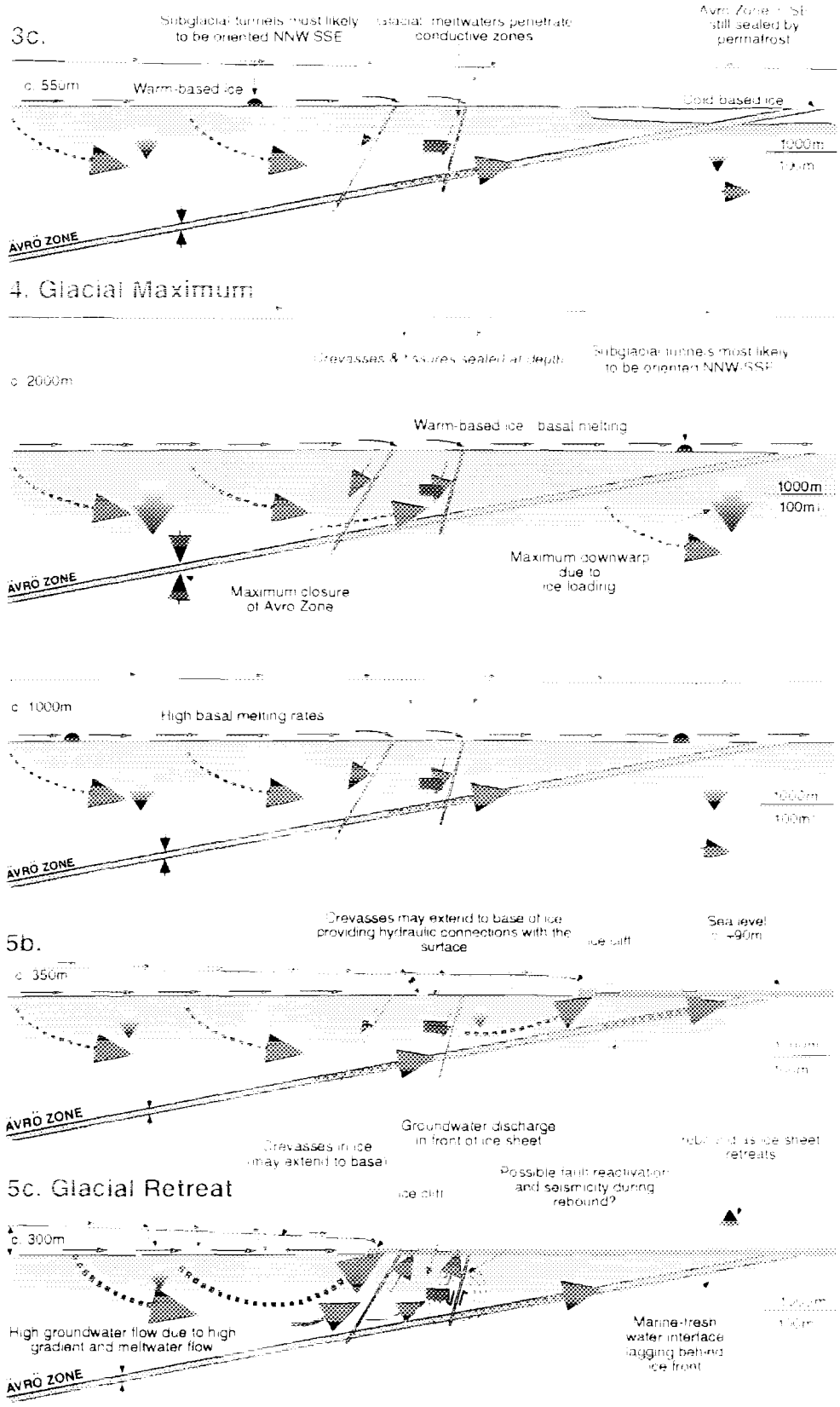

Figure 5.3 (continued)

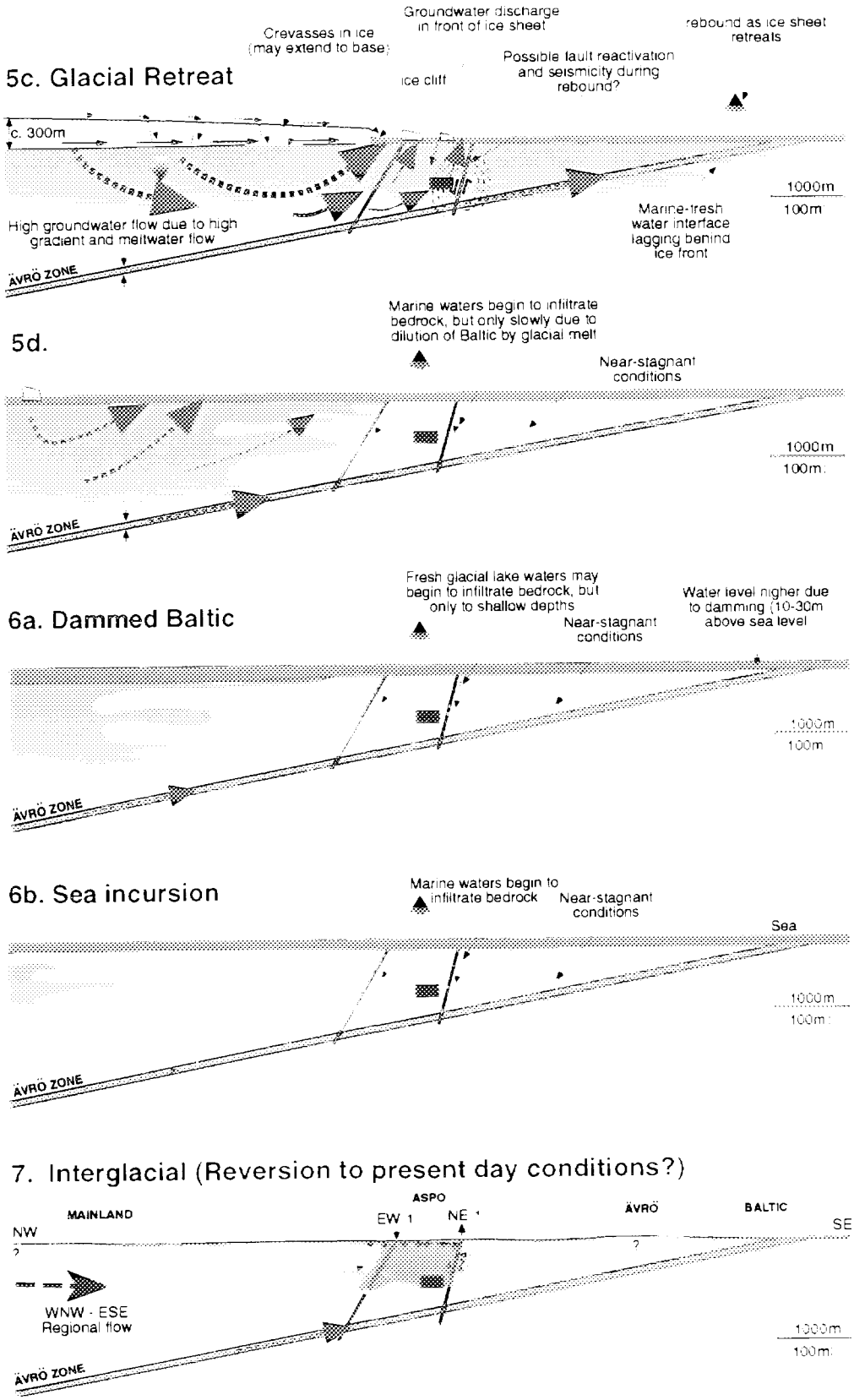

Figure 5.3. (continued)

- The approximation has been made whereby excess hydraulic heads at the ground surface are given by the thickness of ice above that point (see Section 4.3.6 for discussion).

- Seasonal effects and repetition of phases, such as multiple advance and retreat due to ice surging or climatic changes within the glacial cycle, have not been considered (see Section 8).

- Groundwater compositions and flow paths have been very generalised such that the complexities of different degrees of mixing and flow along transmissive fracture zones and within the generally less transmissive rock matrix are not considered in detail.

5.2 Present-Day Interglacial Base Case (Scenario 1)

5.2.1 Scenario

The Base Case scenario is that of an interglacial period with relatively warm conditions, free from the influence of permafrost or ice. Such conditions are considered to be akin to those at the present day at Äspö. For the purposes of this study, the present-day scenario has been taken to be a Base Case to which all subsequent scenarios are compared. For example, hydraulic heads and gradients have been assumed to be zero at the ground surface which is taken to represent the water table (except for beneath the sea).

The areal and site-scale scenarios are depicted in Scenario 1 (Figure 5.3) and have been modified from Smellie & Laaksoharju (1992), particularly by the addition of the subhorizontal Ävrö Zone. It is assumed that the potential repository for spent fuel is situated at a depth of 500 m, in the SE of Äspö, and that it has been closed just prior to this scenario. For the purposes of the modelling, the repository is considered to be one tenth of the size of an actual repository, comprising 400 canisters.

5.2.2 Rock stresses

The tectonic setting of Äspö is considered to remain constant throughout the glacial cycle, such that only glacial loading or glacio-isostatic effects are considered. The regional maximum principal stress is known to be in a predominantly NW-SE direction at the present day. Glacio-isostatic stresses are considered to be zero for this Base Case (although isostatic rebound may still be occurring over Scandinavia, e.g. Anundsen, 1993).

5.2.3 Groundwater flow

The nature of present-day groundwater flow in the Äspö area and region has been simplified in order to accommodate modelling. Fracture Zone NE-1 is considered to be dominated by upward flow and discharge, whereas Zone EW-1 is considered to provide a zone of surface recharge associated with predominantly downward flow (Smellie & Laaksoharju, 1992). The predominant flow direction along the Ävrö Zone is taken to be southeastwards and upwards at depth, although some recharge takes place where the Ävrö Zone outcrops to the SE of Äspö. Regional groundwater flow, reflecting the regional topographic gradient, is taken to be approximately WNW to ESE, although more localised deep groundwater flow occurs perpendicular to the line of section.

5.2.4 Groundwater chemistry

For the purposes of the scenario development, the Base Case groundwater chemistry has been described according to the presence of the following five groups of water, classified according to ^{18}O, D and Cl contents (Glynn & Voss, 1996):

- recent Na-HCO_3-rich waters present to a few hundred metres depth;
- old, dilute glacial meltwater group present in isolated shallow sections in the northern part of Äspö;
- highly saline deep water group found at depths greater than about 500 m;
- intermediate 4000 to 6000 mg/l Cl group found at c.200 to 500 m depths;
- group with a seawater or Baltic signature present only in very isolated areas below 300 m.

It has been assumed that the combination of these chemistries resulted solely from the previous glacial cycle. This is unlikely, but for the purposes of this scenario exercise, the groundwater chemistries for the subsequent glacial scenarios are described with regards to the presence or absence of these water groups.

5.3 Periglacial: c.48 000 Years (Scenario 2)

5.3.1 Scenario

During this phase, periglacial conditions are considered to prevail over all of southern Sweden, in front of the growing ice sheet to the north. Permafrost is considered to be present in the Äspö region and extends to a maximum depth of about 250 m, although it is punctuated by taliks. For the purposes

of the Central Scenario, NE-1 has been assumed to form a talik within the permafrost, whereas both EW-1 and the Ävrö Zone are assumed to be sealed by the permafrost to a depth of 250 m. Isostatic uplift is considered to be negligible during this period, although development of a forebulge in front of the advancing ice sheet situated further north may affect at Äspö at this time. The forebulge may reach a maximum height of tens of metres at Äspö when it is a hundred kilometres or so in front of the ice sheet margin (see Section 3.4.2). Sea level is considered to be approximately 50 m below the present-day level at Äspö for this scenario. Lakes may develop on the periglacial surface within topographic depressions, perhaps where the sea once was present in the Base Case. Vegetation will be scarce in these tundra conditions and it is likely that the ground surface will be characterised by bare rock with only local organic accumulations as tundra marshes in isolated poorly-drained topographic lows, which may develop along outcropping fracture zones. Thermal loading effects of the repository are considered to be minimal at this time (see Section 4.3.1).

5.3.2 Rock stresses

During this period of the scenario sequence, there will be no direct glacial (ice) effects on the bedrock at Äspö. However, as the Scandinavian ice sheet grows and advances towards Äspö, development of a flexural forebulge will affect stress patterns within the bedrock. As the ice advances, the site and area will be subjected to a complex series of stress changes (Section 4.2.1). Since the upwarping bedrock is not confined by ice, tensional fracturing or reactivation of fractures may occur. However, there is apparently no evidence for reactivation of fractures during glacial advances and, therefore, fracture reactivation is not considered in this scenario. As permafrost develops, the formation of ice within any fractures in the bedrock and the resulting expansion of the fracture water volume will exert stresses that tend to propagate the fractures although they will remain sealed within the permafrost zone.

5.3.3 Groundwater flow

With the development of permafrost, the groundwater system at Äspö will undergo certain modifications. Infiltration and recharge will be severely restricted by permafrost, particularly where the zones of Base Case flow are sealed by ice (EW-1 and the Ävrö Zone). If lakes or major rivers are present, perhaps in depressions to the west or east of Äspö where the sea was once situated, these may be underlain by taliks of variable horizontal and vertical extent. If these taliks completely penetrate the permafrost, pathways will be available either for recharge or discharge of sub-permafrost water. There is little evidence that existing rivers are diverted from their course during a glacial advance and lakes in low relief terrain are unlikely to be of sufficient surface area and depth to create an open talik in previously frozen ground

(McEwen & de Marsily, 1991). On the other hand, if a lake existed before development of the permafrost, which may be the case here, an open talik could develop. The concentration of recharge in smaller areas and fewer points can lead to increased recharge and discharge rates at these points, such as along fracture NE-1 or beneath a lake. Although permafrost is not considered to form at repository depths, it may well have an indirect effect on the repository by altering the volume of groundwater flow as well as flow directions through the repository. Expansion of bedrock porosity due to forebulge uplift may increase the drawdown of surface waters into the bedrock, although this effect is likely to be counteracted by the restrictive nature of the permafrost. Forebulge uplift and related downwarp may result in a re-orientation of regional flow directions, assumed here to be predominantly a function of topographic gradient (see Figure 4.7), such that regional NW to SE flow may temporally become NW-directed.

5.3.4 Groundwater chemistry

The formation of very saline waters may occur at the base of the permafrost zone owing to the longer residence times of groundwaters trapped beneath the permafrost (McEwen & de Marsily, 1991). If radionuclides are present in the groundwaters, they may become concentrated amongst these saline waters beneath or within the permafrost zone. Alternatively, they may be concentrated at the lower levels of chemically stratified lakes acting as lacustrine taliks. Subsequently, the radionuclides may be released as a concentrated pulse when thawing takes place (see below).

5.4 Glacial Advance: 50 000 - 60 000 Years (Scenarios 3a-c)

5.4.1 Scenario

Full glacial conditions are considered to develop in the Äspö region during this phase. It is apparent that the ice sheet will grow and advance across Sweden, with ice reaching the Äspö area perhaps as early as 52 000 years from now. By comparison with reconstructions of the last European ice sheet (e.g. Böse, 1990; Boulton et al., 1985), ice sheet advance may involve irregular growth of the ice sheet with relatively rapid on-land expansion of the central south-eastern sector of the ice sheet in contrast to calving-inhibited growth along the north-western margin. During the first c.5 000 years of this phase, the sea level at Äspö is predicted to be below present-day sea level such that the ice sheet will be completely land-based as it advances and will initially reach Äspö on dry land (3a). The margin of the ice sheet is considered to have an approximately WSW-ENE orientation as it passes across Äspö (although a lobate ice front could result in a different orientation of the ice margin at Äspö). The ice sheet will advance across permafrosted bedrock,

possibly with permafrost reaching depths up to 200-300 m. The ice sheet will, therefore, be cold-based until temperatures at the base of the ice sheet reach the pressure melting point and the permafrost melts (3c).

5.4.2 Rock stresses

As the ice sheet advances towards Äspö, the flexural forebulge will prograde further ahead of the ice front and away from the Äspö region. As the ice front comes within several tens of kilometers of Äspö, the bedrock will begin to downwarp owing to the loading effect of the ice sheet to the north (3a). Downwarping will continue as the ice sheet itself advances onto the Äspö bedrock (3b & c). As downwarping begins to take place, it is likely that subhorizontal fractures, such as the Ävrö Zone, will begin to close owing to the increasing vertical stresses. Near-vertical fractures, such as EW-1 and NW-1, may close to a lesser degree (owing to a lower increase in horizontal stresses than in vertical stresses) or may undergo shearing which, in combination with increased porewater pressures, may act to enhance the conductivity of the fractures. In bulk, the bedrock will tend to experience overall compression during loading. However, the response of fractures to glacially-induced stress changes is very difficult to predict and requires an understanding of the pre-glacial nature and history of the fracture system.

5.4.3 Groundwater flow

During the initial advance of the ice into the Äspö region, the ice sheet will probably be cold-based and overlie permafrost, so that little or no sub-glacial meltwater will be generated (Hindmarsh et al., 1989; Drewry, 1986; Section 4.3). Groundwater recharge and discharge patterns may be similar to those under periglacial conditions (3a). However, any groundwater present within the bedrock beneath the permafrost zone underlying the ice sheet will be forced outwards and, subsequently, upwards in front of the ice margin owing to the excess hydraulic gradients considered, as a conservative first approximation, to be controlled by the thickness profile of the ice sheet (Sections 4.3.8 and 4.3.9). In addition, groundwater generated from sub-glacial melting further towards the centre of the ice sheet is also expected to make its way to the ice sheet margins (see below). Upward flow would, therefore, be possible along EW-1, NE-1 and the Ävrö Zone, although only NE-1 is considered to allow groundwater discharge at the surface for the purposes of the scenario. This discharge is likely to greatly exceed that of either the Base Case or the Periglacial Case owing to the high pore pressures and hydraulic gradients exerted by the ice sheet. However, the duration of such discharge is likely to be short since the ice sheet is expected to pass across the site within a few hundred years at most, based on average rates of advance (e.g. 50m/a for the Weichselian Ice Sheet; see Section 3.4.5) although the possibility of a stillstand, brief retreat or surge cannot be ruled out. Insulation by the permafrost is likely to induce the build-up of high porewater

pressures and, hence, may cause hydrofracturing in the outer sub-glacial or proglacial permafrost zones. Supraglacial meltwater will provide some surface run-off and potential recharge.

As the ice sheet covers the Äspö area, local groundwater flow will be reduced and both NE-1 and the lake to the west of Äspö are likely to become frozen owing to the cold-based nature of the ice (3b). Hence, recharge and discharge will continue to be severely inhibited. Flow will be directed downwards along faults EW-1 and NE-1, but is likely to remain upwards along the Ävrö Zone, although closure of the zone may start to prevent flow directly along it. High excess hydraulic gradients, which may be considered to be induced by the thickness of the ice sheet margin (see Section 4.3.8) will control any groundwater flow beneath the permafrost during these early stages of glacial advance (3a & b).

As the ice sheet advances and thickens, the base of the ice is expected to reach pressure melting point and, hence, melting will occur of both the permafrost and basal ice (3c). Sub-glacial water pressures will build up as the ice sheet thickens and will lead to sub-glacial water discharge into available transmissive zones in the bedrock (e.g. NE-1 and EW-1) and/or along tunnels at the base of the ice where the bedrock is of low transmissivity (see Section 4.3.3, 4.3.6). Ice pressures and the hydraulic gradient exerted by the ice will tend to force the flow downwards and towards the ice front. Regional flow beneath the ice sheet would be likely to occur in a direction approximately perpendicular to the ice margin (Section 4.3.3, 4.3.4), almost parallel to the line of section. Sub-glacial tunnels may feed other transmissive fractures or will channel sub-glacial flow to the margin of the ice sheet, to be discharged as glaciofluvial outwash. Sub-glacial tunnels may affect local hydraulic pressures by decreasing hydraulic pressures in their vicinity and increasing local hydraulic gradients (see Section 4.3.6), although such local, unpredictable effects are not considered in this scenario. Sub-glacial melting will probably provide the majority of glacial water recharge into the bedrock. Groundwater flows may be many times that of the unglaciated or present-day case owing to the excess head gradient exerted by the ice sheet and potential influx of sub-glacial meltwater. Groundwater discharge is less likely to occur within the Äspö region during this stage since water will be forced out towards the margins of the ice sheet, far to the SE of Äspö.

Hence, as the ice sheet advances towards and across the Äspö area, patterns of recharge and discharge change according to the position of the ice front. The groundwater flow patterns are likely to become increasingly larger in scale due to the overriding control by the thickness of the ice sheet and flow rates may increase as a result of increased hydraulic pressures and hydraulic gradients exerted by the ice sheet.

5.4.4 Groundwater chemistry

For the early advance of the ice sheet (3a & b), groundwater chemistry will be similar to that of the periglacial scenario (2) although glacial runoff may locally infiltrate the uppermost parts of the bedrock. As the ice advances and basal meltwater is produced (3c), any meltwater infiltrating the bedrock will tend to dilute the existing groundwaters, particularly any previous deep brines or saline waters concentrated beneath the recently melted permafrost. Oxidising glacial waters will penetrate to increasing depth as the ice sheet grows and hydraulic pressures increase. Any radionuclides stored beneath the melting permafrost will tend to be flushed out towards the east and will then enter the sub-glacial discharge to either re-enter the groundwater system or be discharged as glacial outwash east of Äspö.

5.5 Glacial Maximum: c.60 000 Years (Scenario 4)

5.5.1 Scenario

At the glacial culmination, the ice sheet is expected to reach a thickness of 2200 m at Äspö. Downwarping owing to ice loading may be c.500 m in the Äspö area at this time. It is likely that Äspö will still lie beneath the melting zone of the ice sheet and, hence, it is assumed that the bedrock will continue to receive sub-glacial discharge (Boulton & Payne, 1992).

5.5.2 Rock stresses

The maximum ice thickness will cause maximum downwarping of the bedrock at this time. Confinement by the large thickness of ice may prevent tectonic stress release during the entire period of glacial loading. Loading stresses are expected to cause maximum closure of the subhorizontal Ävrö Zone. The effect of stresses on the near-vertical fracture zones is not clear due to the play-off between moderately high horizontal stresses acting to reduce fracture apertures and high porewater pressures which may act to open the fractures.

5.5.3 Groundwater flow

It is considered that the Äspö area will still lie beneath the melting zone of the ice sheet at this time, hence, high infiltration rates are expected to continue into localised transmissive zones within the Äspö bedrock, although infiltration could be reduced owing to the formation of tunnels at the base of the ice sheet. Estimates of mean erosion of only a few tens of metres for past glaciations (Okko, 1964) suggest that erosion is unlikely to affect significantly the local sub-glacial topography and, hence, the hydrogeology of the Äspö area, although localised erosive channels may form. Groundwater discharge

will be highly unlikely in the Äspö area owing to the high downward pressures acting on the groundwater system. Hydraulic connections between the surface of the ice sheet and its base are considered to be unlikely because of the sealing of crevasses and fissures by ice flow, such that the entire meltwater supply will arise from basal melting of the ice sheet. The ice sheet will probably remain grounded as it extends over what (if any) remains of the Baltic Sea far to the east of Äspö, although the transgression of the ice sheet over the more deformable substrates (sedimentary formations) of the Baltic area and beyond may result in the thinning of the ice sheet in these areas (see Section 3.2), but probably not at Äspö (Figure 5.2, stage 4). The transmissivity of the Ävrö Zone may be reduced owing to the high vertical stress which further closes the fractures making up the zone. NE-1 and EW-1 are still considered to be transmissive owing to the play-off between increased porewater pressures and increased horizontal stresses.

5.5.4 Groundwater chemistry

The chemistry of the groundwater will reflect the continued high input of dilute, oxygenating, glacial meltwater into the fracture systems. Maximum downward flushing of these dilute, oxic waters is expected at this stage. It is not clear whether such waters will reach repository depths, but scoping calculations do suggest that this is possible (e.g. Arthur, 1996).

5.6 Glacial Retreat: 60 000 - 70 000 Years (Scenarios 5a-d)

5.6.1 Scenario

The ice sheet is predicted to retreat in water across Äspö. Hence, the ice margin is likely to be in the form of an ice cliff of the order of a hundred metres high (Scenarios 5b, c), although it is likely to remain grounded (Thomas, 1977; Section 3.2). As the ice sheet recedes away from Äspö, permafrost will not become re-established since the area will be beneath the sea. When the ice front has retreated back to Stockholm, the sea level is predicted to be 80-100 m above the present-day coastline at Äspö. Rapid retreat may be facilitated by the process of frontal calving at the seaward margin. During this period of retreat, glacial deposition is likely to be more significant than at other times in the glacial cycle, although it is not considered to modify the topography significantly.

5.6.2 Rock stresses

As the ice sheet thins and retreats across Äspö, the bedrock will begin to uplift and undergo extension, releasing the stresses which had built up during

loading by the ice sheet (e.g. Muir-Wood, 1993; Section 4.2.2). Certain major fracture zones may be reactivated, although it is not possible to predict which ones are likely to be affected. For the purposes of the scenario exercise, it is assumed that NE-1 undergoes reactivation with a normal sense of displacement (Scenario 5c). This displacement would be consistent with greater uplift to the SE (owing to rapid retreat of the ice sheet across the Baltic area) and overall extension which is likely to accompany rebound. Normal fault reactivation and accompanying seismicity is likely to induce coseismic compression of the local bedrock (Muir-Wood, 1993). Surface parallel unloading joints may also be initiated within the upper 100 m of the surface, as indicated by banking features in other glaciated terrains of Sweden, or reactivation of low-angled joints may occur. The Ävrö Zone is expected to open up as the loading stresses decrease.

5.6.3 Groundwater flow

If the ice sheet is considered to remain grounded as it retreats, the effect of the ice sheet on the Äspö groundwater will be significant. High basal melting will continue as the ice sheet will remain warm-based (owing to retreat of the sea) and, hence, groundwater flow in the Äspö area will continue to be directed downwards and outwards (Scenarios 5a, b). The hydraulic gradient across the ice front is likely to be very high, causing strong upward flow and discharge of groundwater in front of the margin (Scenario 5c) as the ice cliff passes over Äspö. The duration of such discharge is likely to be short, within decades to a few hundred years at most, since the ice sheet is expected to retreat across the site at even greater rates than its initial advance (e.g. 150-200 m/a, even up to 1000 m/a; see Section 3.4.5). However, this does not account for the possibility of stillstands in retreat or ice surging (such as the Younger Dryas event; see Section 3.4.5). The overall state of extension of the bedrock as it rebounds will tend to increase its porosity and, hence, induce recharge in the areas where glacial discharge is not dominating or has passed out of the area (Scenario 5d). As an extreme scenario, NE-1 is considered to be reactivated during post-glacial uplift, such that its transmissivity is increased and coseismic compression related to normal fault reactivation induces short-term (days to months) discharge of groundwater (Section 4.3.8). A lower-impact scenario would assume no seismic reactivation of the faults (see Section 5.9).

It is possible that surface-base connections will be present within the ice during the retreat of the ice sheet, particularly in relation to the unstable calving of the ice sheet (Section 4.3.7). Such connections may increase the potential supply of meltwater by introducing surface meltwater to the base of the ice sheet such that sub-glacial meltwater discharge could be increased by up to two orders of magnitude (Sugden & John, 1976; Boulton & Payne, 1992). It is unlikely that a surface lake of any permanence would occur in this unstable marginal zone, although small jökulhlaup-type events may occur owing to rapid discharge of a surface or sub-glacial lake.

As the ice sheet retreats further, the sea will pass over the Äspö region (Scenario 5d). Since permafrost will not develop because of the high sea level, the pressurised sub-glacial water input into the groundwater system will be dramatically reduced and eventually stop completely as the ice front retreats more than a few kilometres away. Continued rebound and extension of the bedrock will tend to induce groundwater recharge and the infiltration of seawater.

5.6.4 Groundwater chemistry

As the ice sheet retreats, the marine-fresh water interface is considered to occur in a landward thinning wedge, modified by the transmissive fracture system. However, the rapid nature of the retreat and the flushing of dilute meltwaters upwards in front of the ice sheet is likely to cause the interface to lag behind the ice margin (Scenarios 5c, d), although the rate of migration of the interface is difficult to predict. Once the ice sheet has moved well away from Äspö, dilute seawater may begin to infiltrate the Äspö bedrock, although to insignificant depths. Glacial meltwater will contribute less to the groundwater system as the ice sheet retreats away.

5.7 Damming of the Baltic: c.70 000 - 71 000 Years (Scenarios 6a-b)

5.7.1 Scenario

If it is considered that future glaciations follow a similar sequence of events to the last glaciation to affect northern Europe (e.g. Eronen, 1989), there is a possibility that the Baltic will become dammed during the later stages of deglaciation to 10-30 m above sea level (Scenario 6a). The predicted damming of the Baltic could cause the ice sheet to become ungrounded and form an ice shelf, but this is not considered likely because of the low topographic gradients in SE Sweden. Damming of the Baltic will cause the waters of the Baltic to become increasingly dilute with time as the meltwater input increases. Incursion of the sea owing to breakdown of the ice dam is then possible, causing a jökulhlaup event or several events (Scenario 6b).

5.7.2 Rock stresses

Major fracture zones may continue to be reactivated, although no further fault movements are considered in this scenario sequence. The Ävrö Zone is expected to continue to open up as rebound continues. A jökulhlaup event may cause seismic activity and reactivation of fracture zones, but this is not considered directly in this scenario step.

5.7.3 Groundwater flow

The dammed lake level will exert a constant hydraulic head over the region and, hence, groundwater flow will be low. Incursion of the sea after damming of the Baltic (Scenario 6b) may be facilitated by a jökulhlaup event, or several events, where water escapes rapidly from the dammed lake after breakdown of the ice barrier or depositional topography causing damming. By comparison with the development of the Baltic Ice Lake during the last glaciation (Eronen, 1989), the path of water escape may be to the north of Äspö such that the Äspö area is not directly affected. However, there is no reason to believe that breaching of the ice dam could not occur in the Äspö vicinity. If this were to be the case, then rapid westward flow may be expected to occur to before the sea re-established itself across the Äspö area.

5.7.4 Groundwater chemistry

Damming of the Baltic will cause the Baltic's waters to become increasingly dilute with time as the meltwater input increases. Hence, the low density lake water is not likely to infiltrate to great depths. Re-establishment of the sea across the area may eventually lead to more saline waters gradually infiltrating into the bedrock, encouraged by continued expansion of the bedrock during glacial rebound.

5.8 Interglacial: 71 000 - 75 000 Years (Scenario 1 or 7)

5.8.1 Scenario

By about 75 000 years from now, permafrost may only exist in northern Sweden and the climate at Äspö may be similar to those present in northern Scandinavia. Up to 500 m of post-glacial uplift may occur in the Äspö region. This scenario assumes that hydrogeological, hydrochemical and stress conditions revert fully to those of the present-day (Base Case) before the following glacial period starts.

In fact, the present situation at Äspö is known to reflect various changes (transients) owing to the last glaciation such as groundwater chemistry with glacial signatures (e.g. Glynn & Voss, 1996) and it is highly likely that the next glacial period will imprint the site with yet more glacial relicts. Thus, an alternative scenario may be needed to describe this period (Scenario 7). For example, during this scenario (71 000 - 75 000 years) it is still expected that sea level will be higher than at the present day by 10-20 m, such that conditions at Äspö will not revert fully to those of the present day. The predicted high sea level implies that flushing of groundwater by meteoric

waters and deep saline waters during post-glacial uplift and subaerial exposure will not occur to the extent experienced by the Äspö area prior to the present day. Topographic gradients will be subdued owing to submergence beneath the sea and, hence, groundwater flow will be reduced. Marine waters (and perhaps glacial waters) could, therefore, provide a greater component of the groundwater beneath Äspö at the start of the next glacial cycle in comparison to the present situation. In addition, there are many other transient features, such as isostatic rebound and its effect on rock conductivity, which may not necessarily revert to conditions experienced at Äspö at the present time before the onset of the next glacial period.

5.9 Alternative Glacial Cycle Scenarios

As highlighted at the beginning of the section, the glacial cycle scenarios outlined above do not comprise a unique description of the future glacial evolution at Äspö, but merely aim to provide a reasonable illustration of the most likely and significant FEPs (features, events and processes) likely to influence the safety of a repository. For purposes of Performance Assessment and generation of a Central Scenario, it was necessary to define a single evolutionary sequence making numerous assumptions. However, it is also necessary to identify as many of the potential variables involved in the future glacial evolution of the site, in addition to defining a single scenario sequence. This will allow at least a qualitative understanding of the assumptions and uncertainties involved in defining a single Central Scenario and may allow alternative Central Scenarios to be constructed if necessary.

In addition to the uncertainties identified in defining the climate evolution to affect Äspö (Section 2.7), there are uncertainties in the following areas:

- *The development or not of permafrost*. Discontinuous permafrost is considered to be the most likely and the most significant, but this may not necessarily be the case.

- *The melting regime of the base of the ice sheet*. Cold-based ice is considered most likely to give way to warm-based ice during the advance and growth of the ice sheet, but this may not necessarily be the case.

- *The relative sea level during advance and retreat*. Advance is considered most likely to be on land and retreat to be in water (see Section 2), including the likelihood and spatial extent of damming, but this may not necessarily be the case.

- *The influence of erosion and deposition*. Erosion and deposition are considered to have an insignificant effect on the hydrogeology of the site. Both features appear to have been of small magnitude during past glaciations, but this may not necessarily be the case in the future.

- *The response of fracture zones to loading*. Shallow-dipping zones have been assumed to close during ice loading, but vertical zones are considered to be essentially unchanged owing to the complexities involved, but this may not necessarily be the case.

- *The likelihood and sense of fracture reactivation and seismicity during retreat*. Normal fault reactivation and associated seismicity has been assumed for fracture zone NE-1, since its impact may be significant despite little evidence of reactivation in southern Sweden during past deglaciations, but this may not necessarily be the case.

These uncertainties or variables are in addition to those outlined at the beginning of the section, concerning quantitative features such as ice thickness. There are an infinite number of alternatives to the glacial cycle scenario sequence described. However, some of the main alternatives to the sequence are summarised in Figure 5.4.

The impacts of a few alternative scenarios are described very briefly below:

- *Development of permafrost throughout the glacial cycle, ie. that the permafrost does not melt beneath the ice sheet.* This will result in the inhibition of any glacial meltwater entering the groundwater system beneath the ice sheet. Hence, recharge rates will be severely decreased, possibly to zero.

- *Advance and retreat of ice sheet on land, ie. that sea level is not higher than present during retreat*. This is likely to result in a wedge-shaped margin geometry of the ice sheet throughout the glacial cycle. The local hydraulic gradient in the vicinity of the margin is, therefore, likely to be slightly less severe than in the case of a ice-cliffed margin retreating in water. On the other hand, discharge will occur directly into the biosphere without the diluting effects of the sea/dammed lake.

- *No damming of the Baltic during deglaciation*. This will result in lower predicted sea levels during glacial retreat, but only by a few tens of metres, which will not have a major impact. However, the absence of damming may have a slightly different impact on groundwater chemistry, although this is difficult to quantify.

- *Significant localised deposition and erosion*. This may be possible via the formation of canyons, which may be formed up to a depth of 90 m or more, although few have been recognised in parts of Sweden where deglaciation occurred below sea level (Olvmo, 1992; Section 4.3.4). Such features will channel sub-glacial meltwaters, perhaps reducing local groundwater recharge, and will reduce the local depth of the repository. Deposition may occur, and be preserved, during the final

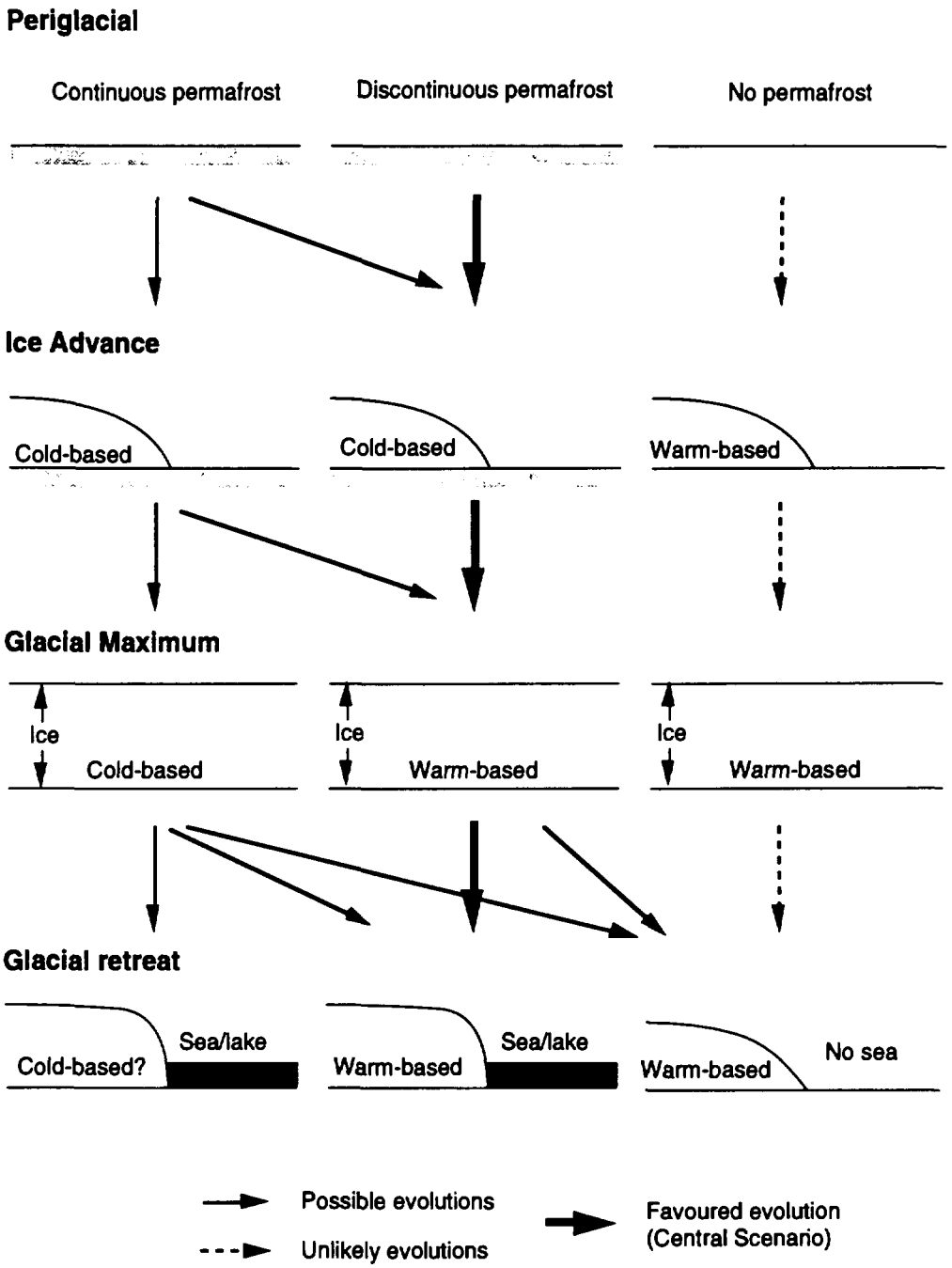

Figure 5.4. Illustration of the possible evolution sequences of the Äspö site during the main steps of a glacial cycle.

stages of glacial retreat. Deposits of a few tens of metres thickness may alter the near-surface hydrogeological regime, but will not tend to alter deeper groundwater patterns, unless they act to seal a conductive fracture zone or if they become very hard and impermeable, thus increasing the potential hydraulic head towards the outer region of the ice sheet.

- *Fracture zones showing unpredictable or varied response to ice loading*. This is very likely and can only be described via detailed modelling of a representative rock volume containing realistic fracture zones, such as work by the KTH Group (pers comm, 1994).

- *No fracture reactivation during deglaciation, or reactivation in a different sense, ie. reverse or strike-slip*. The location of Äspö in southern Sweden, away from the proposed area of maximum glacial loading, may be suggestive that fracture reactivation is unlikely to occur (from analogy with past glaciations). Alternatively, if reactivation were to occur (e.g. owing to extreme loading and/or regional tectonic effects) it may occur along one of the other fracture zones, perhaps with a different sence of displacement. This would have different effects on the local recharge and discharge patterns (see Section 4.3.8).

6 The Central Scenario: 130 ka of Climate Change at Äspö

The following section discusses a full temporal sequence for the glacial cycles predicted to affect the Äspö region in the next 130 000 years, according to the SITE-94 Climate Change Scenario (Section 2.8; Figure 2.16). The scenario sequence outlined in Section 5 has been extended and modified in order to represent the glacial evolution of the Äspö region over the 130 000-year period. As outlined in Section 2, it has been assumed that the Äspö region is covered by an ice sheet during both the 50-70 ka and the 80-120 ka glacials and that permafrost melts beneath the ice sheets by a few ka after ice advance (Scenario (iii) of Section 2.9). Alternatives to this climate evolution are discussed in Section 2 and below.

6.1 Minor Glacial: 0 - 10 000 Years

The climate in Sweden will gradually change to cooler conditions with growth of an ice sheet in the Scandinavian Caledonides. Ice sheet thickness in the central mountains will be approximately 1000 m, with no ice in Stockholm or southwards. Crustal downwarping of c.300 m in the central mountainous part. Sea level will gradually drop to 20 to 40 m below present-day sea level in the Stockholm region as well as in the Äspö region. During the colder parts of this period, permafrost will occur in northern Sweden. The water in the Baltic will gradually become fresher as the connection to the oceans decreases.

This period may, therefore, be represented by the Base Case Scenario (1, Figure 5.3) although more extreme boreal conditions will prevail in the Äspö region than at the present day and may, hence, influence surface conditions (Section 4.5.1).

6.2 Glacial: 10 000 - 30 000 Years

After a minor, somewhat warmer, period, the climate will get colder and fully glacial conditions will prevail around 20 000 years from now. The glacial peak will last perhaps 5000 years. The ice sheet is estimated to reach the Stockholm area, but probably not the Äspö region. Ice thickness in the central part of the ice sheet will be c.1500 m, while the ice sheet thickness in the Stockholm region will be c.800 m. Crustal downwarping of about 500 m in the central part of the ice sheet and c.60 m in the Stockholm latitude will occur. During deglaciation, when the ice front is located at the Stockholm region, the sea level is estimated to be c.25 m below present-day sea level. At Äspö, sea level will drop to c.50 m below present-day sea level (Figure 2.17A). The total effect of the glacial loading at Äspö is difficult to evaluate, but will probably not be large. Permafrost conditions may exist down to southern

Sweden, including the Äspö area. The water in the Baltic will be fresh, but probably in level with the oceans, owing to erosion at its outlets.

This period may, therefore, be represented by the Periglacial Scenario (2; Figure 5.3). Forebulge uplift may affect the Äspö region during the climax of ice advance, but it is likely to be less than for the Periglacial Scenario described above (perhaps in the order of 20-50 m).

6.3 Interstadial: 30 000 - 50 000 Years

Interstadial with a dry and cold climate (like the climate today on Greenland). During this phase, periglacial conditions will prevail over all of Scandinavia, with a dry and cold climate, glaciers in the Swedish mountains and permafrost in northern Sweden. Permafrost may be present throughout the period at Äspö, but may be thin and discontinuous during the middle of the interstadial (0-50 m, Section 2.9). At Äspö, there will not be significant isostatic uplift during this period. The sea level will therefore be c.30-40 m below the present-day level. However, one or more episodes of damming of the Baltic may occur, such that Baltic lake levels may be closer to those of present-day sea levels. This may inhibit the development of permafrost. The Baltic will mainly be fresh but some saline water may enter.

This period may be represented by a combination of the Base Case Scenario (1; Figure 5.3) and the Periglacial Scenario (2; Figure 5.3). The climate is expected to be cooler than that of the Base Case Scenario (1), but if permafrost does develop, it will be thinner and more discontinuous than that predicted in the Periglacial Scenario (2). Hence, groundwater flow may not be as restricted, and groundwater chemistry not as saline, as in the Base Case Scenario.

6.4 Glacial: 50 000 - 70 000 Years

Full glacial conditions. Owing to the previous cold conditions, the ice sheet will respond more rapidly. The glacial culmination will be around 60 000 years. The ice sheet will cover the whole of Sweden down to north Germany.

Full glacial conditions are predicted to occur from c.50 000-70 000 years from now. Owing to the previously cold interstadial conditions, the ice sheet is expected to respond more quickly than for the previous glacial period. At the glacial culmination, the ice sheet is expected to cover the whole of Sweden down to northern Germany, comparable in extent to the maximum of the Weichselian glaciation. The thickness of the ice sheet may reach a maximum of c.3000 m in the central part. In the Stockholm region, the ice thickness may be c.2500 m. The Stockholm region will probably be covered by the ice sheet for at least 10 000 years and possibly longer. Downwarping of c.700 m in the central part of the ice sheet, c.600 m in the Stockholm area and c.500 m at

Äspö is predicted. During deglaciation, when the ice front is located at the Stockholm region, the sea level is estimated to be c.150 m at Stockholm and c.80 m above the present-day coastline at Äspö. There could also be a damming of the Baltic to 10-30 m above ocean level. The Baltic is likely to be mainly fresh but during deglaciation, saline water may enter the Baltic through isostatically depressed areas. Permafrost will be widespread in large areas of Europe. Even with the thermal effect of a repository taken into consideration, permafrost may develop up to a thickness of 300 m (Section 2.9).

This period is represented by the Glacial Scenarios (3a-6b; Figure 5.3) described above. Only one episode of damming has been considered in the main Damming Scenario descriptions (Scenarios 6a, b; Figure 5.3), but more than one episode may occur as has been considered to be the case for the formation of the Baltic Ice Lake and the Ancylus Lake during the period 10 000-9 000 BP.

6.5 Interglacial: c.70 000 - 80 000 Years

By c.75 000 years from now, permafrost may only exist in northern Sweden and the climate at Äspö is expected to be similar to that of the present day in northern Scandinavia. Up to 500 m of post-glacial uplift may occur in the Äspö region, c.700 m in central parts of the previous ice sheet and c.600 m at Stockholm. This will be a relatively 'warm' period with a climate in the Stockholm region similar to the present climate in northern Sweden. Small mountain glaciers and permafrost may be present in the far north. Parts of southern Sweden will be resettled and farming might be possible. Sea level and salinity will be similar to the present day all over and the land uplift will restore the land surface to approximately its present state. Permafrost will only exist in the far north of Scandinavia. At this time, sea level may still be higher than at the present day by 10-20 m. This could mean that conditions at Äspö will not revert back fully to those of the present-day Base Case before the following glacial period starts.

Therefore, this period may not be fully represented by the Base Case Scenario (1; Figure 5.3), but may be more akin to the Sea Incursion Scenario (6b; Figure 5.3) albeit with lower sea level. A separate scenario, the Alternative Interglacial Scenario (7) may be used to describe this period, as described in Section 5.8.

6.6 Glacial: c.80 000 - 120 000 Years

The climate is predicted to become colder during this period, culminating in maximum glacial conditions at c.100 000 years. The ice sheet will be extensive, covering large parts of Fennoscandia. A maximum ice thickness of 1200 m is predicted for the Äspö area; the maximum downwarping is

estimated to be c.400 m for the Äspö area and c.500 m at Stockholm. Permafrost thicknesses up to 250 m, including thermal effects of the repository, may be present at Äspö. The sea level at deglaciation may be c.80 m above present-day sea level, but damming of the Baltic to 10-30 m above sea level is possible. The Baltic is likely to be mainly fresh but during deglaciation, saline water may enter the Baltic through isostatically depressed areas.

This period may be represented by the Glacial Scenarios (3a-6b; Figure 5.3) described above, although ice loading effects will be less than that for these scenarios.

6.7 Interglacial: c.120 000 - 130 000 Years

This will be the next period with a climate similar to the present day at Äspö. Sea level and salinity in the Baltic will be similar to the present.

This period may, therefore, be represented by the Base Case Scenario (1; Figure 5.3), but similar aguements to the 70 000-80 000 interglacial are likely to apply (see above).

7 Graphical Representation and Data Transfer to Assessment Modelling

7.1 Application of the Central Scenario to Modelling

The Central Scenario is intended to provide both qualitative and quantitative input to the Performance Assessment work for the SITE-94 project (SKI, 1997). The qualitative descriptions of glacial cycle scenarios in the previous two chapters are intended to provide a framework for modelling. In addition, key parameter values have been determined for various stages of the Central Scenario, in order to provide more quantitative input to the SITE-94 modelling. Changes in climate, hydrogeological, hydrochemical and stress parameter values for the Äspö site are graphically represented in Figure 7.1 as a function of time and are tabulated in Appendix 2 where appropriate. These are intended only to give an insight into potential temporal changes and not necessarily to represent absolute changes in magnitude. In most cases the vertical scales in Figure 7.1 are only approximate. The errors, simplifications and assumptions involved with determination of these parameters are discussed in the following sections and in Section 5.1. In most cases, the parameter values are assumed to revert back to their Base Case values prior to the beginning of the next glacial cycle although, as discussed in previous sections, this may not be a fully representative assumption.

7.2 Climate, Permafrost and Ice Sheet Data

The climate data comprise sea level, ice thickness, temperature variations at the ground surface and at repository depths. Permafrost thickness estimates are as described in Section 2 for the three scenarios:

(i) Two successive ice sheets formed at c.50-70 ka and c.90-110 ka, with moderately warm-based ice;

(ii) Only one ice sheet formed at c.50-70 ka, with moderately warm-based ice;

(iii) Two successive ice sheets formed at c.50-70 and c.90-110 Ka, but with warmer-based ice.

For the Central Scenario, only Scenario (iii) is considered since it appears to more consistent with modelled ice sheet behaviour. The data are summarised in Figure 7.1a and in Appendix 2a.

Average rates of ice sheet and permafrost development may also be determined for input into hydrogeological modelling. For example, average rates of permafrost growth and decay appear to be in the order of 15-25 m/ka (from Central Scenario calculations; Figure 2.20), and average rates of

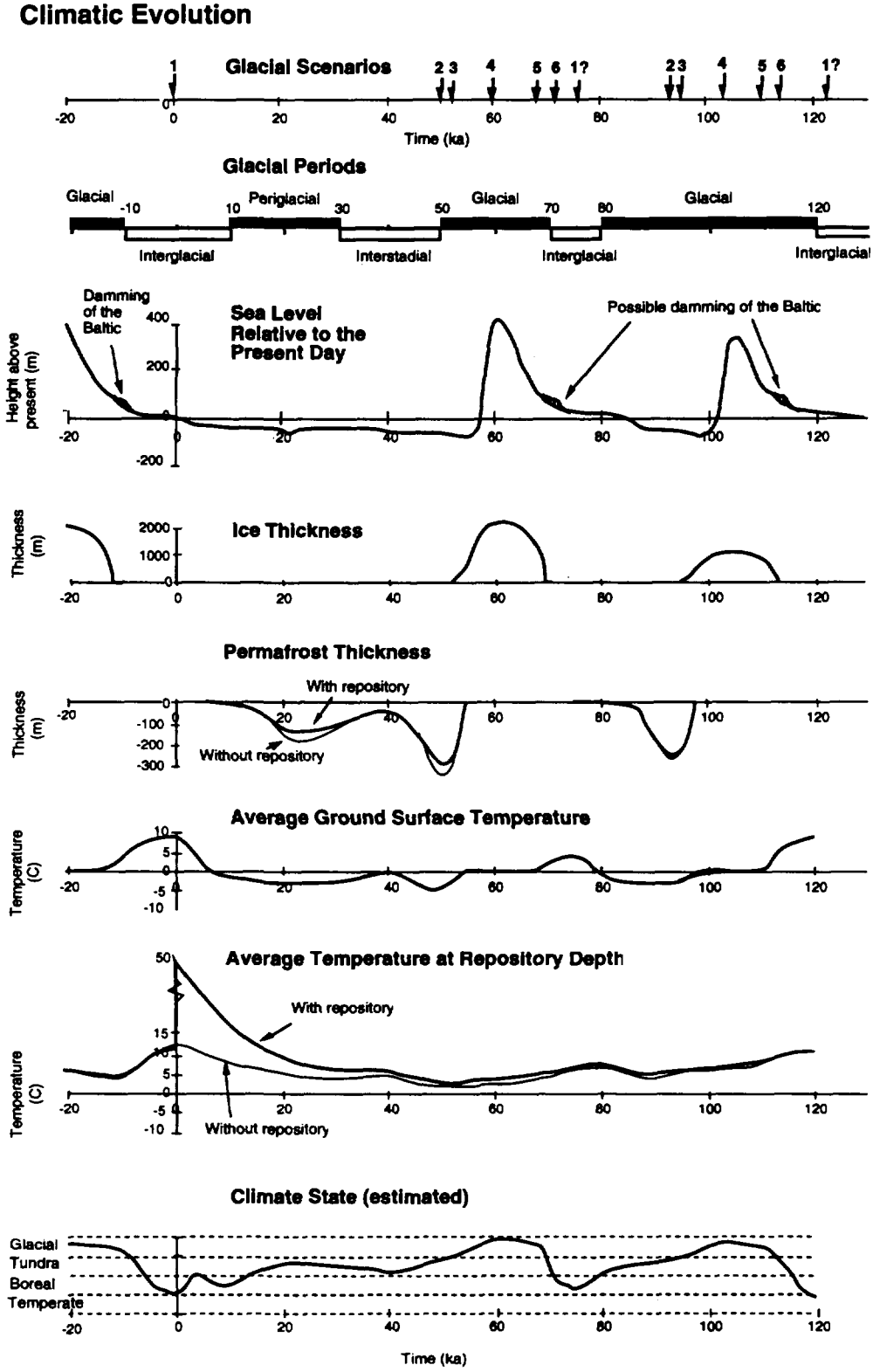

Figure 7.1a. Estimated glacial and climate parameter changes with time over the next 120 000 years (see Section 2).

Stress Evolution

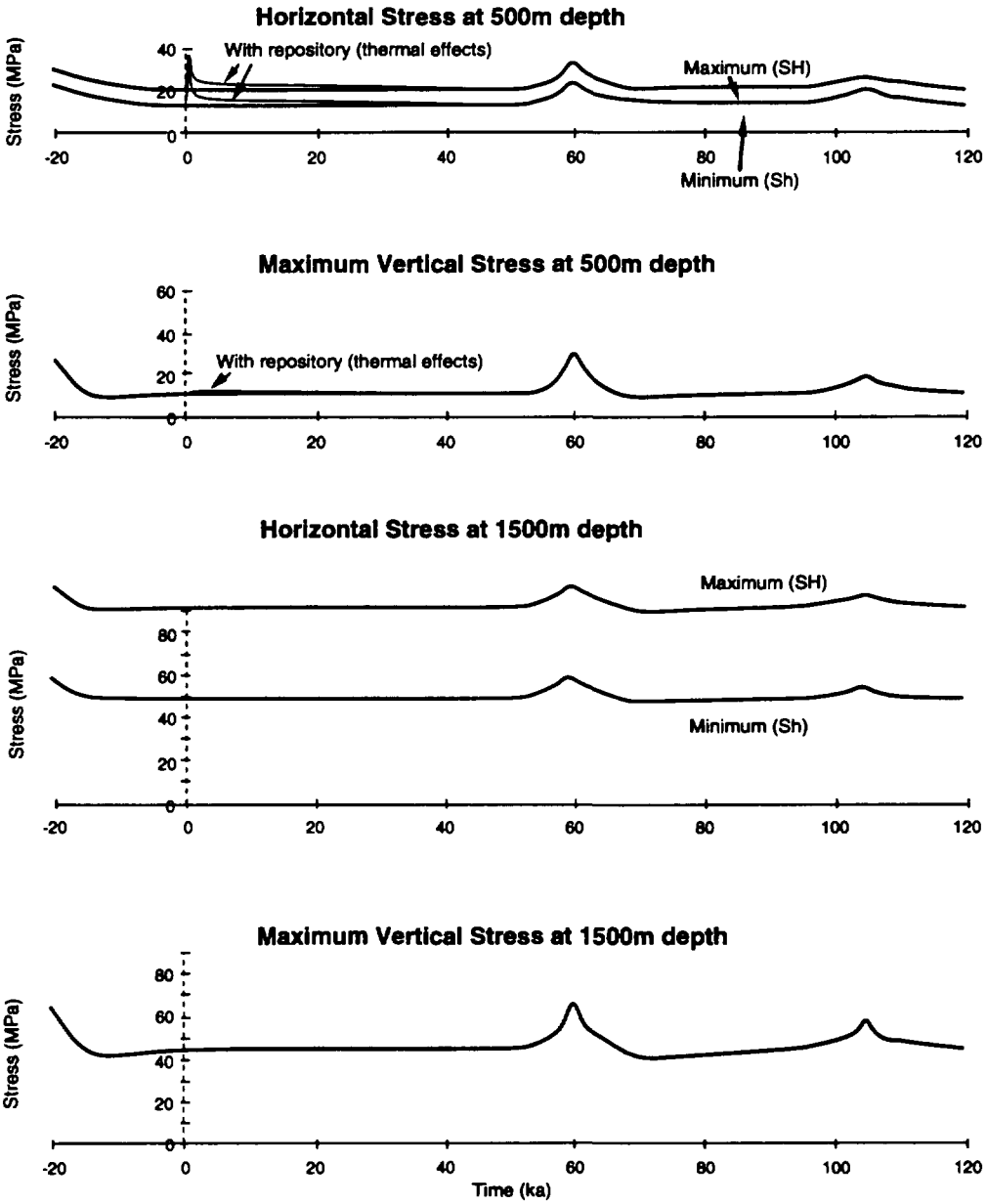

Figure 7.1b. Estimated stress changes over the next 120 000 years based on modelling of a 4 km^3 block with 23 fracture zones by the KTH Group (pers. comm.) and Shen & Stephansson, 1995; see Appendix 2b.

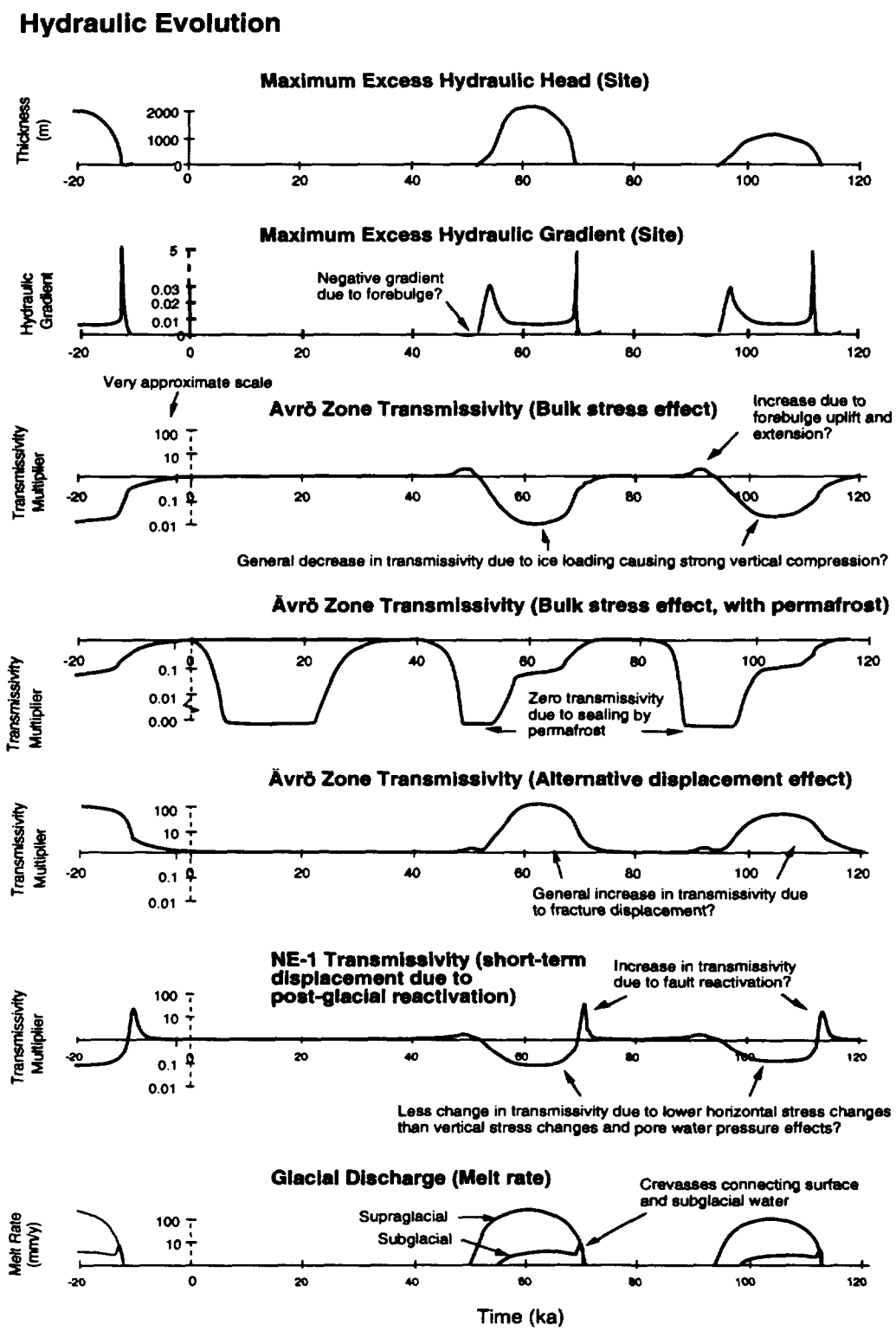

Figure 7.1c. Estimated hydraulic parameter changes over the next 120 000 years. Note that the vertical scales are only approximate (dashed lines).

Hydrochemical Evolution

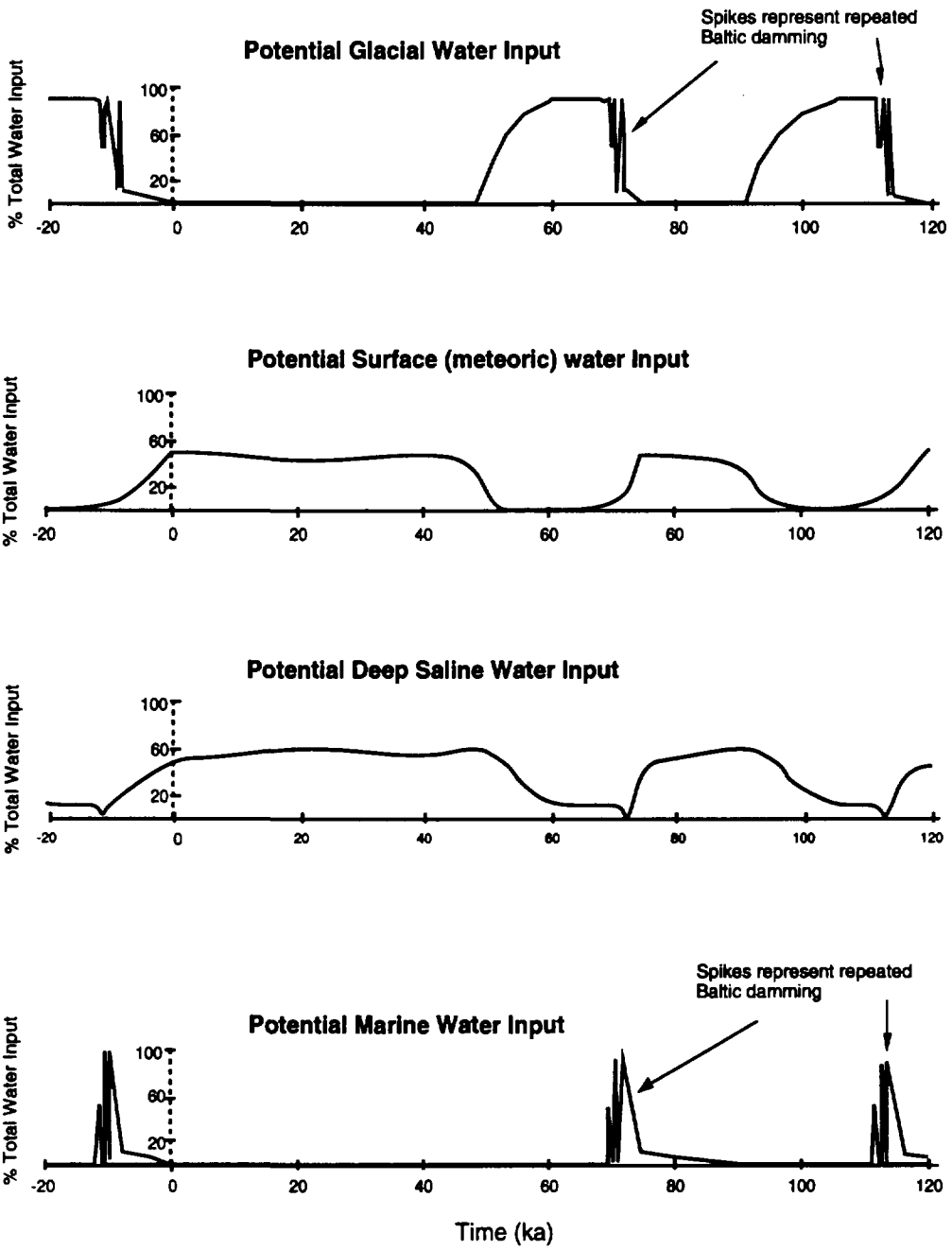

Figure 7.1d. Estimated groundwater chemistry changes over the next 120 000 years. Note that the vertical scales are only approximate (dashed)

ice sheet advance and retreat may be considered to be in the order of 150-200 m/yr, although rates as high as 1000 m/yr may occur during rapid collapse and retreat of a calving ice sheet and rates as low as 50 m/yr have been modelled for the Weichselian glaciation (Section 3.4.5; Boulton & Payne, 1992). On the other hand, average rates of vertical ice build-up may be less than 1 m/yr (approximately 0.2 m/yr, as determined from Figure 7.1a).

Maximum ice sheet thickness values are as specified in the Central Climate Change Scenario (Figure 2.7). Ice sheet profiles and thickness gradients have been determined from examination of data for the Greenland and Antarctic ice sheets and work by Boulton & Payne (1992). It must be noted that the formula derived by Embleton & King (1975) to describe the geometry of an ice sheet ($H=4.76\sqrt{R}$; see Section 3.2) would lead to an apparent overestimate of maximum ice thickness for the Weichselian Scandinavian ice sheet (c.5000 m assuming a maximum radius, R, of 1200 km or so). Hence, this expression has not been used for the Central Scenario, although it may be used to derive maximum thickness estimates for input to sensitivity tests or alternative scenario analysis. Assumption of a single ice dome during future glaciations is also likely to lead to over-estimates of ice sheet thickness (Section 5.1).

7.3 Stress Data

The Central Scenario only provides a qualitative description of the response of stress to future climate changes. However, Figure 7.1c (Appendix 2b) shows a graphical representation of potential changes in horizontal and vertical stresses for a $4 \times 4 \times 4$ km rock volume with 23 fractures, from work by the KTH Group (pers. comm. and Shen & Stephansson, 1995). Their results for a single (50-80 ka) glacial have been extrpolated to fit the rest of the 120 ka period. The influence of forebulge development on stress has not been modelled by the KTH Group. Increases in both vertical and horizontal stresses are apparent during loading by the ice sheets. The thermal loading of the repository has a similar magnitude effect on stress as the ice sheet loading, but loses its impact during the first few thousand years.

7.4 Hydrogeological Data

The following parameter values have been compiled for input into the hydrogeological modelling (Figure 7.1b; Appendix 2c):

- Ice sheet thickness (excess hydraulic head);
- Ice sheet thickness gradient (excess hydraulic gradient);
- Fracture transmissivity (approximate);
- Bulk rock transmissivity (approximate);
- Supraglacial and sub-glacial discharge (approximate);
- Flow directions (approximate).

The excess hydraulic head at the ground surface is considered to be equivalent to the total thickness of the ice sheet, with the approximation that the density of ice is similar to that of water. This is a major assumption (Section 4.3.6), but is considered to provide at least an upper limit to the likely head values of groundwater beneath the ice sheet.

Hydrogeological parameters; excess hydraulic head, excess hydraulic gradient and transmissivity values are tabulated in Appendix 2c.

Fracture transmissivity values are considered to be very approximate, owing to the complexity of the response of fractured bedrock to differential loading stresses and porewater pressures (Section 4.3.8). The values have been given as multipliers of the Base Case values (unspecified). These values are included only in order to highlight potential changes in the transmissivity of the far-field as a result of climate changes. For example, near-horizontal fracture zones such as the Ävrö Zone are considered to undergo closure and, hence, decrease in transmissivity during glacial loading, and permafrost is considered to reduce fracture and bulk rock transmissivity to zero over the depths at which it is developed (Figure 7.1c). Alternatively, fractures may undergo displacement (shearing or opening) which may increase their transmissivity (Figure 7.1c). It is not intended that these changes should, or can, be incorporated directly into hydrogeological modelling, but such potential alternative changes must be at least identified within any Performance Assessment and may be included within sensitivity studies.

Glacial melt rates have been represented, as determined from calculations by Boulton & Payne (1992), such that the potential sub-glacial discharge into the bedrock may be considered. However, these estimates assume that there is no sub-glacial tunnel discharge and, hence, represent the maximum extent of possible discharge into the bedrock (Section 4.3.6).

7.5 Hydrochemical Data

A semi-quantitative representation of changes in groundwater chemistry has been attempted (Figure 7.1d; Appendix 2d) in terms of the combination of different potential end-member water chemistries for the site area (Section 5.2.4; P. Glynn pers. comm.):

- Glacial meltwater;
- Surface (meteoric) water;
- Deep, very saline water;
- Marine water.

In addition, more generalised proportions have been determined for the region area for input into hydrogeological modelling or as a more basic guide to the changes in water chemistry considered to take place through a glacial cycle

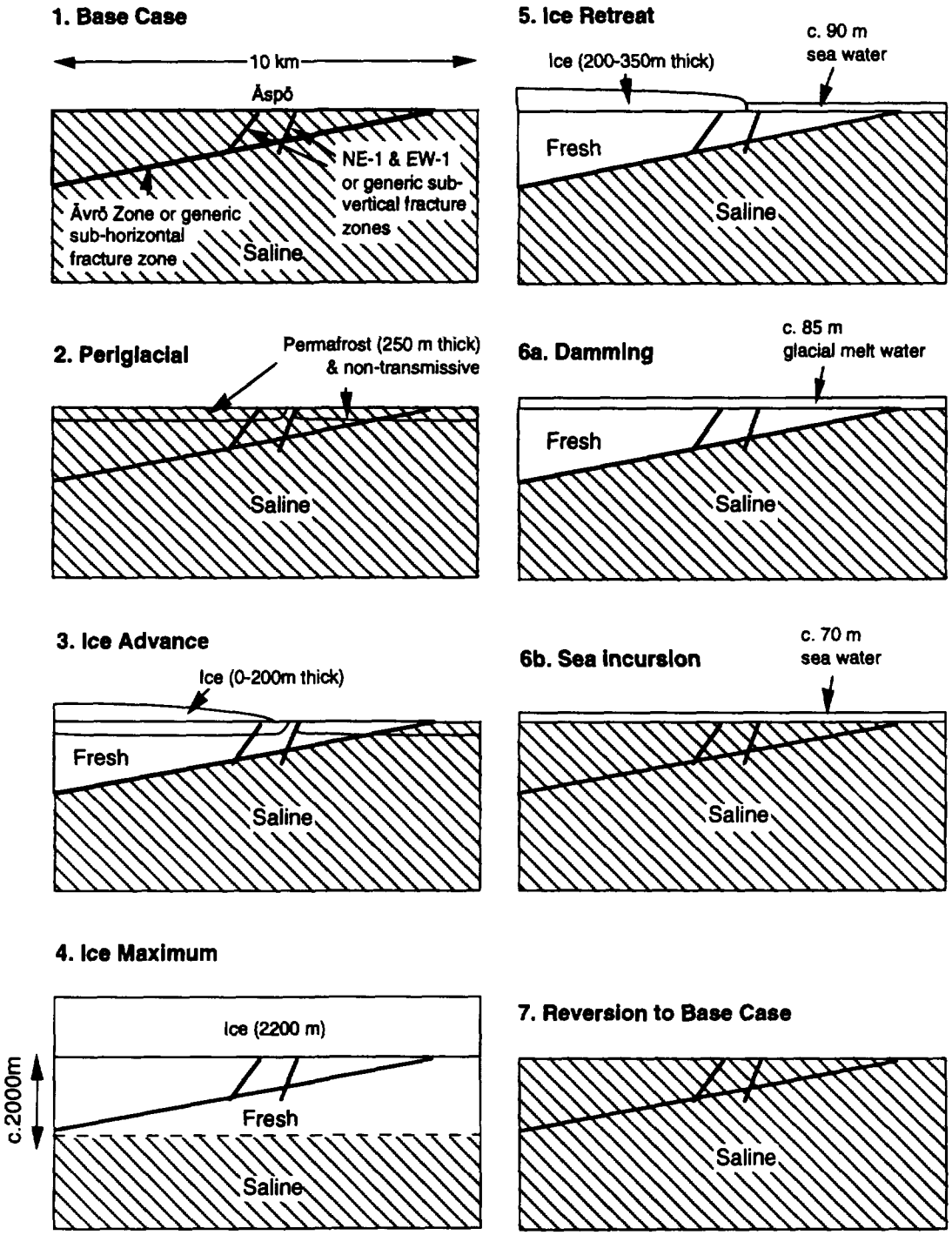

Figure 7.2. Series of more stylised scenario figures, including simplified water chemistry (saline and fresh).

(Figure 7.2; Appendix 2d) in terms of :

- Saline/dense water (incorporating both deep saline and marine components);
- Fresh/dilute water (incorporating both meteoric and glacial water).

The values in Appendix 2d are approximate and serve simply to provide an indication of the types of water which may affect the groundwater composition (down to a depth of 2000 m). No attempt has been made to determine the degrees of mixing and resultant groundwater compositions. The simplified scenario sequence depicted in Figure 7.2 has taken the Ävrö Zone to act as an arbritary divide between the two main water types. If the Ävrö Zone is not considered in the modelling, a similar position for the divide may still be used.

However, this method of imposing artificial density fields on to a structural model may require refinement by the modellers. The imposition of artificial density fields may give rise to large, spurious groundwater flows (A. Provost, pers. comm, 1994) and the incorporation of simple, physically motivated mechanisms into the model may be appropriate. It may be more appropriate to impose an intial (Base Case) density field which is then allowed to evolve with the flow field, such as has been undertaken by Provost et. al. (1997). The initial Base Case field may, therefore, be slightly more complex than depicted, for example, showing increase in density with depth.

7.6 Surface Data

The approximate evolution of surface conditions through the next 120 000 years has also been estimated (Appendix 2e). The distribution of organic accumulations (such as within peat bogs and tundra marshes), in particular, may have an influence on the hydrochemistry of the Äspö site (P. Glynn pers. comm.).

8 Conclusions

8.1 Summary of the Central Scenario

A Central Scenario, involving prediction of the climate and consequent surface and subsurface environments at the site for the next c.130 000 years, lies at the heart of the scenario definition work for the SITE-94 project (SKI, 1997). The Central Scenario required the following main components:

- a deterministic description of the most probable climate state for Sweden, with special reference to the Äspö area;
- a description of the likely nature of the surface environment in the site area at each stage of the climate sequence selected;
- quantitative information on how these changes might affect the disposal system.

The Climate Change Central Scenario has been based on the climate models ACLIN (Astronomical climate index), Imbrie & Imbrie (1980) and the PCM model by Berger et al. (1990). The timing and extent of coming glaciations and sea level variations in Fennoscandia were based on parallels with the last glaciation, guided by the output of the climate models used. These models suggest glacial maxima at c.5000, 20 000, 60 000 and 100 000 years from now. The Äspö region is predicted to be significantly affected by the latter three glacial episodes, with the ice sheet reaching and covering the area during the latter two episodes (by up to c.2200 m and 1200 m thickness of ice, respectively). Only periglacial conditions are predicted to affect the area during the glacial episode at c.20 000 years from now and no glacial effects are predicted at c.5000 years. Calculations of permafrost thickness and duration indicate that permafrost could reach a thicknesses of 50 to 300 m over much of the 120 000 year period. Permafrost could be present at Äspö during the periods 10 000-60 000 years and 80 000-95 000 years from now.

8.2 Summary of Future Climate (Glacial) Effects

It has been the intention that the Central Scenario illustrates potentially significant aspects of climate change for analysis of the future safety of a hypothetical repository for spent fuel. Thus, the objective of scenario development has been to provide an indicator of the physical, chemical and hydrogeological conditions at the front of and beneath the advancing and retreating ice sheets, with the aim of identifying critical aspects for Performance Assessment modelling. The effect of various factors, such as ice loading, the development of permafrost, temperature changes and sea level changes, are considered in terms of their impact on hydrogeology, groundwater chemistry, rock stress and surface environments.

The significance of the features, events and processes (FEPs) that may occur during a glacial cycle are summarised below.

8.2.1 Rock stress and rock mechanics

During loading by the ice sheet, the bedrock is expected to undergo bulk compression, whereas subsequent glacial unloading causes expansion of the rock volume which may, in turn, affect the hydraulic properties of the rock. A significant period in terms of rock mechanics at Äspö appears to occur during the final retreat of the ice sheet as the rock mass begins to unload and undergo uplift. During this period, fault reactivation and associated seismic activity may occur. Stresses in the bedrock, on the other hand, will be at a maximum when the maximum ice sheet thickness overlies the potenial repository site. At this point, the bedrock will be under maximum compression and fracture apertures will be reduced, particularly those with horizontal or subhorizontal orientations. However, the complexity of the fracture system will result in a differential stress distribution in the rock mass and sub-glacial porewater pressures will further complicate the reaction of the bedrock to glacial loading, tending to open fractures rather than to close them. The relationship between glacial loading, rock mechanics and hydraulic properties of the rock is complex and requires more work in the future.

8.2.2 Groundwater flow

The groundwater flow beneath Äspö is likely to be modified significantly at all stages of a glacial cycle. Local groundwater flow patterns will be re-organised on a continental scale, a probable function of the ice sheet thickness distribution. Groundwater flow is restricted during the periglacial and early ice advance stages and then undergoes large-scale enhancement and modification during the main duration of the ice sheet. A net downward and outward flow vector beneath the ice sheet and a strong upward flow beyond it is expected owing to basal meltwater overpressuring and ice loading effects. The main periods of groundwater discharge, which are of considerable significance to the Performance Assessment of a potential repository, are considered to occur during the early advance (e.g. c.52 000 years AD) and late retreat (e.g. c.70 000 years AD) phases of a glacial cycle. The latter discharge phase is considered to be more significant than the former phase which is inhibited by the development of permafrost in the proglacial zone. During ice sheet retreat, permafrost is unlikely to exist in the proglacial zone and, hence, groundwater discharge ahead of the ice sheet will be uninhibited and high. However, both phases are likely to be of moderately short duration (tens to thousands of years), depending on the advance/retreat rates of the ice sheet. During initial ice advance, Äspö will lie under the outer cold-based zone of the ice sheet which is underlain by permafrost, such that sub-glacial discharge is inhibited. In the proglacial

region, permafrost may seal off potential sub-glacial aquifers or fault zones which would otherwise allow groundwater discharge. Excess pore pressures are likely to exist which may tend to cause hydrofracturing in the permafrost and pressure release. The Äspö area is not predicted to underly the central, cold-based zone of the ice sheet at any stage of a glacial cycle, where the groundwater will be essentially stagnant. Rather, Äspö is considered to be situated beneath the zone of melting for the majority of the time of ice coverage (except during intial ice advance), where groundwater flow will occur, with head gradients increasing towards the ice sheet margins. Sub-glacial meltwater tunnels are expected to form under these conditions, particularly where bedrock transmissivity is low and is, therefore, unable to accommodate all the glacial meltwater as groundwater flow. The presence of tunnels may complicate the local groundwater flow patterns.

8.2.3 Groundwater chemistry

The chemistry of the groundwater beneath Äspö appears to be influenced markedly throughout a glacial cycle. It tends to become more saline as it is trapped beneath the permafrost in the periglacial and early glacial advance phases. Radionuclides may also concentrate during these phases if they have been released from the potential repository. As the base of the ice sheet and the permafrost melt, the groundwaters become increasingly dilute as glacial meltwater is forced downwards into the bedrock. Oxygenated waters may be forced deeper, particularly via more transmissive fracture zones, by a combination of head increases and permafrost sealing. Maximum depths of penetration may be reached during the glacial maximum and it is possible that oxidising conditions may reach repository depths, a scenario of great significance for the stability and release from the near-field of the repository. Flushing by dilute meltwaters continues until the ice sheet retreats away from the Äspö region and marine water begins to infiltrate the bedrock. Subsequent damming of the Baltic may temporarily induce minor infiltration of dilute or brackish waters until the sea is re-established. As the land surface continues to rebound and the sea level returns to present-day levels, continued extension of the bedrock will cause near-surface, meteoric waters to be flushed down to greater depths.

8.3 Alternative Scenarios, Uncertainties and Simplifications

The numerous estimates and assumptions made during the development of the Äspö scenarios have been outlined (Sections 2.7 and 5.9). A major point to be stressed is the uncertainty inherent in the prediction of future climate change. The Central Scenario description formulated here only covers a single representation of the possible outcomes which could affect the Äspö area. Alternatives to the Central Scenario and glacial cycle scenarios have been described and discussed in Sections 2.7 and 5.9. However, it has been the intention that the chosen Central Scenario should represent the most probable

and significant climate change impacts on a potential repository for spent fuel.

It must also be noted also that the features described in the scenarios may occur in an irregular, periodic manner, rather than as continuous processes. For example, processes such as ice surging, calving, jökulhlaups and unloading will introduce episodic events into the evolution of an ice sheet. This irregularity may also result in the repetition of advance and retreat phases over the Äspö area during a single glacial cycle. However, for the purposes of the Central Scenario, such irregularities were not considered, except for the possible occurrence of repeated damming of the Baltic, although this may itself be uncertain to be repeated in future glaciations. The thresholds between the Baltic basin and the sea are shallow and very sensitive to erosion, deposition and ice movement, so that future damming of the Baltic may occur in a different way, if at all.

Examples of the features, events and processes (FEPs) likely to be related to the future climate evolution at Äspö, but which are inherently uncertain are listed below:

- The effects of Greenhouse warming;
- The timing and extent of the predicted climatic changes, such as permafrost, ice sheet development and relative sea level (including damming effects which may differ significantly to the past, since the thresholds between the Baltic basin and the sea are shallow and very sensitive to erosion and deposition);
- Ice sheet parameters such as thickness and geometry;
- Depositional and erosional features which may have a significant effect on the sub-glacial hydrogeology;
- The significance and likelihood of hydrofracturing and fault reactivation during ice sheet loading and permafrost development;
- Response times of groundwater chemistry and flow to sea level changes and ice sheet migration and resulting transience of these parameters;
- Hydro-mechanical coupling under glacial loading conditions, particularly for complex, poorly understood fracture systems.

Wherever possible, direct observations and measurements of features have been sought to provide information. However, it has been found that there appears to be a general lack of observational data on the direct effects of an ice sheet on the hydrogeology, hydrogeochemistry and rock mechanics of the underlying bedrock. Although this is understandable on practical grounds, it

means that there is a dependence on the modelling of the processes which may occur below an ice sheet. In particular, the response of fractured crystalline bedrock to glacial conditions may be significantly different to that of interbedded aquifers and aquitards.

However, it is apparent that palaeohydrogeological data may hold the key to answering many of the uncertainties regarding the impact of past glaciations on groundwater flow, chemistry and rock mechanical behaviour. For example, analysis of fracture infilling minerals, such as calcite, may provide valuable evidence on the depth to which glacial meltwaters have penetrated in the past and the mechanical history of the fractures.

8.4 What Next?

Compilation of the Central Scenario has necessitated the development of a highly simplified temporal scenario evolution. However, from the proceding discussions, it is clear that there is no singular response to the predicted climate change and probably no exclusive pattern of climate change. Hence, it may be necessary, in future evaluations of the future behaviour of a deep repository for spent fuel, to consider alternative or peripheral scenarios to that of the Central Scenario.

The following uncertainties, adjustments or alternatives to the Central Scenario are perhaps the most significant features which may have to be considered:

- The effects of human-induced global warming;
- Examination of the impacts of alternative sub-glacial temperature distributions on the development of permafrost and hydrogeology (e.g. Scenario (i) of Section 2);
- Modification of the timing and extent of the predicted climatic changes as predictions of future climate become refined;
- Consideration of alternative syn/post-glacial damming effects or the effects of no damming at all;
- Modification of ice sheet parameters such as thickness and geometry to allow for features such as multiple ice domes, ice streams and ice lobes which may influence the direction and timing of ice sheet advance and retreat;
- Inclusion of localised depositional and erosional features which may have a significant effect on the sub-glacial hydrogeology;
- The significance and likelihood of hydrofracturing and fault

reactivation during ice sheet loading and permafrost development;

- Development of a better understanding of the response of groundwater chemistry to climatic changes, particularly with regard to response times to sea level changes and ice sheet migration and resulting transience.

- More detailed consideration of the impact of climate changes on the biosphere.

In order to address many of these uncertainties, it is clear that the following are necessary:

- Improved models of climate (including anthropogenic effects) and of the thermo-chemical-hydrological-mechanical coupled behaviour of the rock-water-ice system;

- More focussed data collection and interpretation in several areas, such as:
  - present-day sub-glacial hydrogeological environments,
  - palæo-chemical indicators (chemical and isotopic studies of fracture coatings and their hydrochemical zonation) and
  - palæo-seismic indicators.

- Time dependent modelling of groundwater flow and radionuclide transport (as investigated in Provost et al., 1997 and King-Clayton & Smith, 1996)

It is apparent that palaeohydrogeological data may hold the key to answering many of the uncertainies regarding the impact of past glaciations on groundwater flow, chemistry and rock mechanical behaviour at specific sites. For example, fracture infilling minerals, such as calcite, may provide valuable evidence on features such as the depth to which glacial meltwaters have penetrated in the past and the mechanical history of the fractures.

8.5 Acknowledgements

The authors wish to thank all those who have been involved in the various reviews of this report (Ove Stephansson, Matti Eronen, Jan Lundqvist, Svante Björk, Cliff Voss, Alden Provost; we apologise for anyone missed from this list) and those who aided the final drafting (Paul Weston, Lee Ewert). The principal author would like to acknowledge Nils-Olof Svensson's leading contribution to the climate sections 2.1-2.8 and the permafrost modelling work by Ghislain de Marsily and Emmanuel Ledoux in section 2.9.

9 References

Ahlbom, K., Äikäs, T. and Ericsson, L.O., 1991. SKB/TVO Ice Age Scenario. SKB Technical Report, 91-32.

Ahlbom, K. and Olsson, O., 1992. Temperature conditions in the SKB study sites. Conterra report for the Swedish Nuclear Fuel and Waste Management Co.

Anderson, A.J., 1984. Geophysical interpretation of the features of the marine geoid in Fennoscandia. Marine Geophysical Research 7, pp. 191-203.

Andersen, B.G., 1981. *In:* The last great ice sheets, Denton, G.H. and Hughes, T.J. John Wiley & Sons.

Andersen, B.G. and Mangerud J., 1989. The last interglacial-glacial cycle in Fennoscandia. Quaternary International, vol 3/4 pp. 21-29.

Andersson, J. (editor), 1989. The joint SKI/SKB scenario development project. Swedish Nuclear Power Inspectorate Report No. TR-89:14, Stockholm, 168pps.

Anundsen, K., 1990. Evidence of ice movement over southwest Norway indicating an ice dome over the coastal district of west Norway. Quaternary Science Reviews 9, pp 99-116.

Anundsen, K., 1993. Crustal Movements and the Late Weichselian ice sheet in Norway. SKI Technical Report KAN 3 (93) 12.

Aronsson, M., Hedenäs, L., Lagerbäck, R., Lemdahl, G. and Robertsson, A.M., 1993. Flora och fauna i Norrbotten för 100 000 år sedan. Svensk Botanisk tidskrift. 87, pp. 241-253.

Arthur, R., 1996. Estimated rates of redox-front migration in granitic rocks (SITE-94), SKI Report, 96:35, Swedish Nuclear Power Inspectorate, Stockholm.

Bäckblom, G. and Stanfors, R. (eds.), 1989. Interdisciplinary study of post-glacial faulting in the Lansjärv area, Northern Sweden, 1986-1988. SKB Technical Report, 89-31.

Bein, A. and Arad, A., 1992. Formation of saline groundwater in the Baltic region through freezing of seawater during glacial periods. J. Hydrology, 40, 75-87.

Berger, A.L., 1978. Long-term variations of caloric insolation resulting from the earth's orbital elements. Quaternary Research 9, pp. 139-167.

Berger, A.L., 1984. Accuracy and frequency stability of the earth's orbital elements during the Quaternary. *In:* Milankovitch and climate, A.L. Berger, J. Imbrie, J. Hays, G. Kukla and B. Salzman (eds.), pp. 3-39. D Reidel Publishing Company.

Berger, A., Gallée, H., Fichefet, T. and Tricot, C., 1990. Testing the astronomical theory with a coupled climate-ice sheet model. *In:* Global and Planetary Change, Labeyrie, L. (ed.).

Berger, A., 1995. Modelling the Astronomical Theory of Palaeoclimates. Journal of Coastal Research Special Issue No 17: Holocene Cycles: Climate, Sea Levels, and Sedimentation. pp. 355-362.

Berger, A., Loutre, M.F, and Gallée, H., 1996. Sensitivity of the LLN 2-D climate model to the astronomical and CO_2 forcings (from 200 kyr BP to 130 ky AP). Universite Catholique de Louvain, Faculté des Sciences, Department de Physique, Unité ASTR, Scientific Report 1996/1.

Berglund, B.E. and Lagerlund, E., 1981. Eemian and Weichselian stratigraphy in south Sweden. Boreas 10, 323-362.

Berner, W., Stauffer, B. and Oeschger, H., 1977. Dynamic glacier flow model and the production of internal meltwater. Zeit. Gletscherk. Glazialgeol., 13 (1/2), 209-17.

Bjerhammar A. 1977. The gravity field of Fennoscandia and postglacial crustal movements. KTH, Stockholm.

Björck, S. and Digerfeldt, G., 1991. Allerød-Younger Dryas sea level changes in southwestern Sweden and their relation to the Baltic Ice Lake development. Boreas 20, pp. 115-113.

Björck, S. and Svensson, N-O., 1992. Climatic change and uplift patterns—past, present and future. SKB Technical Report, 92-38.

Björnsson, H., 1974. Explanation of jökulhlaups from Grimsvotn, Vatnajökull, Iceland. Jökull, 24, 1-26.

Bloom and Yonekura, 1985. Coastal Terraces generated by sea-level change and tectonic uplift. In: Woldenberg (ed.) Models in geomorphology. Binghampton symposia in geomorphology, international series 14. 139-154.

Bond G.C., 1995. Climate and the conveyor. Nature 377, 383-384.

Böse, M., 1990. Reconstruction of ice flow directions south of the Baltic Sea during the Weichselian glaciations. Boreas, 19, 217-226.

Boulton, G.S., 1991. Proposed approach to time-dependent or 'event-

scenario' modelling of future glaciation in Sweden. SKB Arbetstrapport, 91-27.

Boulton, G.S. and Broadgate, M., 1992. A glacial model for TIME-4 applicable to the Sellafield and Dounreay areas. HMIP Technical Report, TR-D&M-24.

Boulton, G.S. and Clark, C.D., 1990. The Laurentide ice sheet through the last glacial cycle: the topology of drift lineations as a key to the dynamic behaviour of former ice sheets. Trans. Roy. Soc. Edinburgh, 81, 327-348.

Boulton, G.S. and Jones, A.S., 1979. Stability of temperate ice sheets resting on beds of deformable sediment. Journal of Glaciology, 24, 29-43.

Boulton, G.S. and Payne, A., 1992. Reconstructing past and predicting future regional components of global change: The case of glaciation in Europe. Waste Disposal and Geology: Scientific perspectives. The committee of the workshop WC-1 of the 29th IGC, Tokyo.

Boulton, G.S. and Payne, A., 1993. Simulation of the European ice sheet through the last glacial cycle and prediction of future glaciation. SKB Technical Report, 93-14.

Boulton, G.S., Slot, T., Blessing, K., Glasbergen, P., Leijnse, T. and van Gijssel, K., 1993. Deep circulation of groundwater in overpressured sub-glacial aquifers and its geological consequences. Quat. Sci. Rev. 12, 739-745.

Boulton, G.S., Smith, G.D., Jones, A.S. and Newsome, J., 1985. Glacial geology and glaciology of the last mid-latitude ice sheets. Journal of the Geological Society of London, 142, 447-474.

Boulton, G.S., Smith, G.D., and Morland, L.W., 1984. The reconstruction of former ice sheets and their mass balance characteristics using a non-linearly viscous flow model. Journal of Glaciology, 30, 140-52.

Boulton, G.S. and Spring, U., 1986. Isotopic fractionation at the base of polar and subpolar glaciers. Journal of Glaciology, 32, 475-485.

Broecker, W.S., Bond, G., McManus, J., Klas, M. and Clark, E., 1992. Origin of the North Atlantic's Heinrich Events. Climate Dynamics, 6, 265-273.

Broecker, W.S., 1994. Massive iceberg discharges as triggers for global climate change. Nature 372, p 421-424.

Brownlee, D.E., 1995. A driver of Glaciation cycles?. Nature 378, p 558.

Chapman, N.A., Andersson, J., Robinson, P., Skagius, K., Wene, C-O., Wiborgh, M. and Wingefors, S., (1995). Systems Analysis, scenario

construction and consequence analysis definition for SITE-94, SKI Report 95:26, Swedish Nuclear Power Inspectorate, Stockholm.

Chappell, J. and Shackleton, N.J., 1986. Oxygen isotopes and sea level. Nature 324, pp. 137-140.

Chen, R., 1991. On the horizontal crustal deformation in Finland. Report of the Finnish Geodetic Institute 91.1. 98pp.

Clark, J.A., Farrel, W.E. and Peltier, W.R., 1978. Global Changes in Postglacial Sea Level: A Numerical Calculation. Quaternary Research 9, pp. 265-287.

Clark, P.U. and Walder, J.S., 1994. Sub-glacial drainage, eskers, and deforming beds beneath the Laurentide and Eurasian ice sheets. Geological Society of America Bulletin, 106, 304-314.

Collins, D.N., 1979. Quantitative determination of the sub-glacial hydrology of two Alpine glaciers. Journal of Glaciology, 23, 347-363.

Coughtrey, P.J., 1992. Radioactive Waste Disposal Assessment: Overview of Biosphere Processes and Models. UK DoE Report DoE/MHIP/RR/92/065.

Dames and Moore, 1992. Modelling of rock mass response to glaciation in the Dounreay area, Scotland. HMIP Technical Report, TR-D&M-21.

Dansgaard, W., White, J.W.C, Johnsen, S.J., 1989. The abrupt termination of the Younger Dryas climate event. Nature, 339, 532-534.

Dansgaard, W., Johnsen, S.J., Clausen, H.B., Dahl-Jensen, D., Gundestrup, N.S., Hammer, C.U., Hvidberg, C.S., Steffensen, J.P., Scveinbjörnsdottir, ZA.E., Jouzel, J. and Bond, G., 1993. Evidence for generally instability of past climate froim a 250-kyr ice-core record. Nature 364, pp. 218-220.

Davenport, C.A., Ringrose, P.S., Becker, A., Hancock, P. and Fenton, C., 1989. Geological investigations of late and post glacial earthquake activity in Scotland. *In:* Earthquakes at North-Atlantic passive Margins: Neotectonics and postglacial rebound, Gregerson, S. and Basham, P.W. (eds.). Kluwe Academic Publishers, 175-192.

Davidson, G.P. and Nye, J.F., 1985. A photoelastic study of ice pressure in rock cracks. Cold Reg. Res. Tech., 11, 141-53.

de Marsily, G., 1988. Quelques considérations pratiques sur la modélisation des flux thermiques et hydrauliques dans les milieux naturels. *In:* La thermomécanique des roches, P. Berest and P. Weber (eds.). Manuel et Méthodes, 16, BRGM Orléans, p. 131-149.

Denton, G.H. and Hughes, T.J. (eds.), 1981. The Last Great Ice Sheets. 484 pp. John Wiley & Sons.

Denton, G.H. and Hughes, T.J., 1983. Milankovitch theory of ice sheet linkage between regional insolation and global climate. Quaternary Research 20, pp. 125-144.

Donner, J., 1989. Transport distances of Finnish crystalline erratics during the Weichselian glaciation. Geological Survey of Finland, Special Paper 7, 7-13.

Drewry, D., 1981. Radio echo sounding of ice masses: principles and applications. *In:* Remote sensing in meteorology, oceanography and hydrology, Cracknell, A.P. (ed.). Ellis Horwood, Chichester, 270-84.

Drewry, D., 1986. Glacial Geologic Processes. Edward Arnold. 276 pp.
Duff, D, 1993. Holmes' Principles of Physical Geology. Fourth Edition. Chapman & Hall.

Duff, D. 1993. Holmes' Principles of Physical Geology. Fourth Edition. Chapman & Hall, London. 791 pp.

Ekman, M., 1977. Postglacial land uplift in Fennoscandia and movement of the geoid (in Swedish with an English Summary). National Land Survey of Sweden, Professional Papers 1977/5.

Ekman, M., 1989. Impacts of geodynamic phenomena on systems for height and gravity. Bull. Geod. 63, pp. 281-296.

Embleton, C. and King, C.A.M., 1975. Glacial Geomorphology, Arnold Publishers Ltd.

Eriksson, K.G., Ahlbom, K., Landdström, O., Larson, S., Lind, G. and Malmqvist, D., 1978-79. Investigation for geothermal energy in Sweden. Pageoph, 117, 196-204.

Eriksson, K.G. and Malmqvist, D., 1979. A review of the past and the present investigations of heat flow in Sweden. *In:* Terrestrial Heat Flow in Europe, Cermak, V. and Rybach, L. (eds.). Springer-Verlag, Berlin, 267-277.

Eronen, M., 1989. Eemian sea levels and crustal deformation in eastern Fennoscandia. Geologiska Föreningens i Stockholm Förhandlingar 111, pp. 295-296.

Eronen, M. and Olander, H., 1990. On the World's Ice Ages and changing environments. YJT Report, YJT-90-13.

Fairbanks, R.G., 1989. A 17 000-year glacio-eustatic sea level record:

influence of glacial melting rates on the Younger Dryas event and deep-ocean circulation. Nature 342, pp. 637-642.

Farley, K.A. and Patterson, D.B., 1995. A 100-kyr periodicity in the flux of extraterrestrial ^{3}He to the sea flor. Nature 378, pp. 600-603.

Fjeldskaar, W. and Kanestrøm, R., 1980. Younger Dryas Geoid-deformation Caused by Deglaciation in Fennoscandia. *In:* Earth Rheology, Isostacy and Eustacy, Mörner, N-A. (ed.). John Wiley & Sons pp. 569-574.

Fjeldskaar, W. and Cathles, L., 1991. Rheology of mantle and lithosphere inferred from postglacial uplift in Fennoscandia. *In:* Glacial isostasy, sea level and mantle rheology, Sabadini, R., Lambeck, K. and Boschi, E. (eds.). Nato ASI Series C. vol 334. pp 1-19.

Fjeldskaar, W., 1994. Modelling of the post-glacial uplift in Fennoscandia with a thin ice model. *In:* Abstracts 21:a Nordiska Geologiska vintermötet, Perdahl, J-A (ed.). Tekniska Högskolan i Luleå.

Forsström, L., Aalto, M., Eronen, M. and Grönlund, T., 1988. Stratigraphic evidence for Eemian crustal movements and relative sea level changes in eastern Fennoscandia. Palaeogeography, Palaeoclimatology, Palaeoecology 68, pp. 317-335.

Freeze, R.A. and Cherry, J.A., 1979. Groundwater. Prentice-Hall, New Jersey.

Gallée, H. 1989. Conséquences pour la prochaine glaciation de la disparition eventuelle de la calotte glaciaire recouvrant la Groenland. Scientific Report 1989/7, Institut d'Astronomie et de Géophysique G. Lemaitre, Université Catholique de Louvain-la-Neuve, Belgium.

Gallée, H., van Ypersele, J.P., Fichefet, T., Tricot, C. and Berger, A., 1991. Simulation of the last Glacial cycle by a coupled sectorially avaraged climate-ice sheet model 1. The climate model. Journal of Geophysical research, 96, pp 13.139-13.161.

Glynn, P. and Voss, C., 1996. Geochemical characterization of Simpevarp groundwaters near the Äspö Hard-Rock Laboratory (SITE-94), SKI Report 96:29, Swedish Nuclear Power Inspecorate, Stockholm.

Gow, A.J., Ueda, H.T. and Garfield, D.E., 1968. Antarctica Ice Sheet: preliminary results of the first core hole to bedrock. Science, 161, 1011-13.

Gow, J.G and Meese, D.A. (1996). Nature of Basal Debris in the GISP2 and Bryd ice cores and its relevance to bed processes. Annals of Glaciology, 22, 134-140.

Hallet, B., 1976. Deposits formed by sub-glacial precipitation of $CaCO_3$.

Geol. Soc. Am. Bull., 87 (7), 1003-15.

Hays, J.D., Imbrie, J. and Shackleton N.J., 1976. Variations in the earth's orbit; Pacemaker of the ice ages. Science 194, pp. 1121-1132.

Heinrich, H., 1988. Origin and consequences of cyclic ice rafting in the Northeast Atlantic Ocean during the past 130 000years. Quaternary Research, 29, 143-152.

Hindmarsh, R.C.A., Boulton, G.S. and Hutter, K., 1989. Modes of operation of thermomechanically coupled ice sheets. Annals of Glaciology, 12, 57-69.

Hobbs, B.E., Means, W.D. and Williams, P.F., 1976. An Outline of Structural Geology. John Wiley & Sons. 474 pp.

Hodge, S.M., 1976. Direct measurement of basal water pressures: a pilot study. J. Glaciology, 16 (74), 205-18.

Holmlund, P. (1993). Den senaste istiden i Skandinavien. En modellering av Weichselisen. SKI Teknisk Rapport 93:44, SKI, Stockholm.

Holmlund, P. and Fastook, J., 1993. Numerical modelling provides evidence of a Baltic Ice Stream during the Younger Dryas. Boreas, 22, 77-86.

Hooke, R. le B., 1970. Morphology of the ice sheet margin near Thule, Greenland. Journal of Glaciology, 9, 303-24.

Hooke, R. le B., 1973. Flow near the margin of the Barnes ice cap and the development of ice-cored moraines. Bulletin of the Geological Society of America, 84, 3929-48.

Hooke, R. le B., 1977. Basal Temperatures in Polar Ice Sheets: A Qualitative Review. Quaternary Research, 7, 1-13.

Hubbert, M.K. and Rubey, W.W., 1959. Role of fluid pressure in mechanics of overthrust faulting. Geol. Soc. Amer. Bull., 70, 115-206.

Huybrechts, P. and Oerlemans, H., 1988. Evolution of the East Antarctic ice sheet: a numerical study of therm-mechanical response patters with changing climate. Annals of Glaciology, 11, 52-59.

Imbrie, J., and Imbrie, J.Z., 1980. Modelling the climate response to orbital variations. Science, 207, 943-953.

Imbrie, J., Hays, J.D., Martinson, D.G., McIntyre, A., Mix, A.C., Morley, J.J., Pisias, N.G., Prell, W.L. and Shackleton, N.J., 1984. The orbital theory of Pleistocene climate: support from a revised chronology of the marine ^{18}O record. *In:* Milankovitch and climate, Berger, A.L., Imbrie, J., Hays, J., Kukla,

G. and Salzman, B. (eds). , pp. 269-305. D. Reidel Publishing Company.

Imbrie, J., Boyle, A.E.A., Clemens, S.C., Duffy, A., Howard, W.R., Kukla, G., Kutzbach, J., Martinson, D.G., Mclntyre, A., Mix, A.C., Molfino, B., Morley, J.J., Peterson, L.C., Pisias, N.G., Prell, W.L., Raymo, M.E., Shackleton, N.J. and Toggweiler, J.R., (1992). On the structure and origin of major glaciation cycles, 1, Linear responses to Milankovitch forcing, Paleoceanography, 7. 701-738.

Imbrie, J., Berger, A., Boyle, E.A., Clemens, S.C., Duffy, A., Howard, W.R., Kukla, G., Kutzbach, J., Martinson, D.G., Mclntyre, A., Mix, A.C., Molfino, B., Morley, J.J., Peterson, L.C., Pisias, N.G., Prell, W.L., Raymo, M.E., Shackleton, N.J. and Toggweiler, J.R., 1993. On the structure and origin of major glaciation cycles, 2, The 100 000-year cycle, Paleoceanography, 8. 699-735.

Johnsen, S.J., Clausen, H.B., Dansgaard, W., Gundestrup, N.S., Hammer, C.U. and Tauber, H., 1995. The Eem stable isotope record along the GRIP ice core and its interpretation. Quaternary Research 43, 117-124.

Johnston, A., 1987. Supression of earthquakes by large continental ice sheets. Nature, 330, 467-69.

Johnston, A., 1989. The effect of large ice sheets on earthquake genesis. *In:* Earthquakes at North-Atlantic passive Margins: Neotectonics and postglacial rebound, Gregerson, S. and Basham, P.W. (eds.). Kluwe Academic Publishers, 581-599.

Kakkuri, J., 1987. Character of the Fennoscandian land uplift in the 20th century. *In:* Fennoscandian land Uplift, Perttunen, M. (ed.), pp. 15-20. Gelogical Survey of Finland, special paper 2.

King-Clayton, L.M & Smith, P.A., 1996. Transport Sensitivity Studies for SITE-94: Time-Dependent Site-Scale Modelling of Future Glacial Impact. SKI Report 96:12. Swedish Nuclear Power Inspectorate, Stockholm

King-Clayton, L.M., Chapman, N.A, Kautsky, F, and Ericsson, L.O. (eds.). 1997. Proceedings of a Workshop on the Impacts of Climate Change and Glaciation on Rock Stresses, Groundwater Flow and Hydrochemistry, 17th-19th April, 1996, Stockholm.

Kukla, G., Berger, A., Lotti, R. and Brown, J., 1981. Orbital signature of interglacials. Nature 290, pp. 295-300.

Laaksoharju and Skårmen, (in press). Groundwater sampling and chemical characterisation of the Äspö HRL-tunnel in Sweden. SKB Technical Report. Swedish Nuclear Fuel and Waste Management Company (SKB).

Lagerbäck, R., 1988. Post-glacial faulting and paleaoseismicity in the Lansjärv area, northern Sweden. SKB Technical Report, 88-25.

Lagerbäck, R. and Robertsson, A-M., 1988. Kettle holes-stratigraphical archives for Weichselian geology and palaeoenvironment in northernmost Sweden. Boreas 17, pp. 439-468.

Lagerlund, E., 1987. An alternative Weichselian glaciation model with special reference to the glacial history of Skåne, South Sweden. Boreas 16, pp. 433-459.

Larkin, J.P.A., Ringrose, P.S., Ashton, J. and Nancarrow, D., 1992. Climatic and Environmental Change. *In:* Dry Run 3, Volume 1: The Factual Database Summerling, T.J., Martin, A. and Charles, D. (eds.). UK DoE Report, DoE/HMIP/RR/92.041.

Lehman, S.J., Jones, G.A., Keigwin, L.D., Anderson, E.S., Butenko, G. and Ostmo, S-R., 1991. Initiation of the Fennoscandian ice sheet retreat during the last deglaciation. Nature, 349, 513-516.

Lingle, C.S. and Brown, T.J., 1987. A sub-glacial aquifer bed model and water pressure dependent basal sliding relationship for a west Antarctic ice stream. *In:* Dynamics of the West Antarctic Ice Sheet, van der Veen, C.J. and Oelermans, J. (eds.), 249-285.

Liu, H-S., 1992. Frequency variations of thw Earth's obliquity and the 100-kyr ice-age cycles. Nature 258, 397-399.

Lundqvist, J., 1986. Stratigraphy of the central area of the Scandinavian glaciation. Quaternary Science Reviews 5, pp. 251-268.

Lundqvist, J., 1992. Glacial stratigraphy in Sweden. *In:* Glacial stratigraphy, engineering geology and earth construction, Kauranne, K. (ed.). Geological survey of Finland, Special paper 15, pp. 43-59.

Lundqvist, J. and Laerbäck, R., 1976. The Pärve Fault: A late-glacial fault in the Precambrian of Swedish Lapland. Geologiske Föreningens i Stockholm Förhandingav, 86, 181-205.

Manabe, S., Stouffer, R.J., 1995. Simulation of abrupt climate change induced by freshwater input to the North Atlantic Ocean. Nature 378, 165-167.

McEwen, T.J. and de Marsily, G., 1991. The Potential Significance of Permafrost to the Behaviour of a Deep Radiocative Waste Repository. SKI Technical Report, 91:8.

Meier, M., 1972. Hydraulics and hydrology of glaciers. Int. Ass. Sci. Hydrol. Publ., 107, 353-70.

Michel, F.A. and Wilson, H.C., 1988. Groundwater flow in permafrost regons of Canada. Int. Groundwater Symp. on Hydrogeology of Cold and Temperate Climates and Hydrogeology of Mineralised Zones, Int. Assoc. Hydrogeologists, 149-155.

Milankovitch, M.M., 1941. Kanon der Erdbestrahlung und seine Anwendung auf das Eiszeitproblem. Acad. Roy. Serbe, Éd. spec. 133, 633 pp.

Miller, U. 1977. Pleistocene deposits of the Alnarp Valley, southern Sweden - Microfossils and their stratigraphic application. LUNDQUA Thesis 4.

Mörner, N-A., 1969. Late Quaternary history of the Kattegatt Sea and the Swedish West Coast. Sveriges Geologiska Undersökning serie C nr. 640, 487 pp.

Mörner, N-A., 1971 Eustatic changes during the last 20 000years and a method of separating the isostatic and eustatic factors in an uplifted area. Palaeogeography, Palaeoclimatology and Palaeoecology 9, 153-181.

Mörner, N-A., 1979. The Fennoscandian uplift and Late Cenozoic geodynamics: geological evidence. GeoJournal 3.3, pp. 287-318.

Mörner, N-A., 1989. The Fennoscandian uplift and Late Cenozoic geodynamics: geological eveidence. Geojournal, 3.3, 287-318.

Muir-Wood, R., 1989. Extraordinary deglaciation reverse faulting in Northern Fennoscandinavia. *In:* Earthquakes at North-Atlantic passive Margins: Neotectonics and postglacial rebound, Gregerson, S. and Basham, P.W. (eds.). Kluwer Academic Publishers, 141-173.

Muir-Wood, R., 1992. Earthquakes, water and underground waste disposal. *In:* Waste Disposal and Geology; Scientific Perspectives. Proceedings of Workshop WC-1 of the 29th International Geological Congress, Tokyo, 169-192.

Muir-Wood, R., 1993. A review of the seismotectonics of Sweden. SKB Technical Report, 93-13.

Muller. R.A. and MacDonald, G.J., 1995. Glacial cycles and orbital inclination. Nature 377, pp. 107-108.

Nesje, A. and Dahl, S.O., 1990. Autochtonous block fields in southern Norway: implications for the geometry, thickness, and isostatic loading of the Late Weichselian Scandinavian ice sheet. Journal of Quaternary Science 5, pp. 225-234.

Nesje, A., Dahl S. O., 1992. Geometry, thickness and isostatic loading of the

Late Weichselian Scandinavian ice sheet. Norsk Geologisk Tidskrift. Vol. 72, 271-273.

Nurmi, P., 1985. Mahdolliset ympäristöolosuhteiden pitaaikais-muutokset Suomessa ja niiden vaikutukset syvällä oleviin kalliopohjavesiin. Voimayhtioiden ydinjätetoimikunta. Raportti JYT-85-21.

Nye, J.F., 1976. Water flow in glaciers: jökulhlaups, tunnels and veins. Journal of Glaciology, 17 (76), 181-207.

Oerlemans, J. and Van der Veen, C.J., 1984. Ice sheets and climate. Reidel, Dordrecht.

Okko, V., 1964. Maaperä. *In:* Suomen geologia, Rankama, K. (ed.). Kirjayhtymä, Helsinki. 239-232.

Olvmo, M., 1989. Meltwater Canyons in Sweden: A study of the canyons of the kursu-, skura- and grav-type. GUNI Rapport 27. University of Göteborg. 134 pp.

Peltier, W.R., 1987. Glacial isostasy, mantle viscosity, and Pleistocene climatic change. *In:* North America and adjacent oceans during the last deglaciation, Ruddiman, W.F. and Wright Jr., H.E. (eds.). The Geological Society of America, The Geology of North America, Vol. K-3, pp. 155-182.

Persson, T., 1974. Eskers, plateaux, terraces and other glaciofluvial forms in the southern and central parts of the South-Swedish Highlands. Geologiska Föreningens i Stockholm Förhandlingar, 96, 411-419.

Petersen, K.S., 1984. Stratigraphical position of Weichselian tills in Denmark. *In:* Ten years of Nordic till research, Königsson, L-K. (ed.). Striae, col 20, 75-78.

Pitty, A.F., 1988. Geomorphological Processes in Britain in a Periglacial Age. Nirex Safety Studies Report NSS/R134. UK Nirex Ltd, Didcot, Oxfordshire.

Provost, A., Voss, C. and Neuzil., C., (in press). Glaciation and regional groundwater flow in the Fennoscandian shield (SITE-94), SKI Report 96:11, Swedish Nuclear Power Inspectorate, Stockholm.

Rahmstorf, S., 1995. Bifurcations of the Atlantic thermohaline circulation in response to changes in the hydrological cycle. Nature 378, 145-149.

Raymond, C.F. and Harrison, W.D., 1975. Some observations on the behaviour of liquid and gas phases in temperate glacier ice. Journal of Glaciology., 14 (71), 213-33.

Rosengren, L. and Stephansson, O., 1990. Distinct element modelling of the

rock mass response to glaciation at Finnsjön, central Sweden. SKB Technical Report, 90-40.

Röthlisberger, H., 1972. Water pressure in intra- and sub-glacial channels. Journal of Glaciology, 11 (62), 177-203.

Roulet, N.T. and Woo, M., 1986. Hydrology of wetland in the continuous permafrost region. Journal of Hydology, 89: 1-2, 73-91.

Roulet, N.T. and Woo, M., 1988. Runoff generation in a low Arctic drainage basin. Journal of Hydrology, 101: 1-4, 213-226.

Ruddiman W.F. and Wright Jr, H.E., 1987. Introduction. *In:* North America and adjacent oceans during the last deglaciation, Ruddiman, W.F. and Wright Jr., H.E. (eds.). The Geological Society of America, The Geology of North America Vol. K-3, pp. 1-12.

Saltzman, B. and Verbitsky, M.Y., 1992. Astenospheric ice-load effects in a global dynamical-system model of the Pleistocener climate. Climate Dynamics 8 pp. 1-11.

Selby, M.J., 1971. The Surface of the Earth. Volume 2. Climate, Soils and Vegetation. Cassell, London. 437 pp.

Shackleton, N.J., 1987. Oxygen isotopes, ice volume and sea level. Quaternary Science Review 6, pp. 183-190.

Shackleton, N.J. and Opdyke, N.D., 1973. Oxygen isotope and paleomagnetic stratigraphy of equatorial Pacific core V28-238; oxygen isotope temperatures and ice volumes on a 105 and 106 year scale. Quaternary Research 3, pp. 39-55.

Shen, B. and Stephansson, O., 1990. 3DEC Mechanical and Thermo-Mechanical Analysis of Glaciation and Thermal Loading of a Waste Repository. SKI Technical Report 90:3. Swedish Nuclear Power Inspectorate, Stockholm.

Shen, B. and Stephansson, O., 1995. Near-field rock mechanics modelling for nuclear waste disposal (SITE-94). SKI Technical Report 95:17. Swedish Nuclear Power Inspectorate, Stockholm.

Sigurdsson, F., 1990. Groundwater from glacial areas in Iceland. Jokull, 40, 119-146.

SKI, 1996. SKI SITE-94, Deep Repository PerformanceAssessment Project. Volumes I and II. SKI Report, 96:36. Swedish Nuclear Power Inspectorate, Stockholm.

Skinner, B.J. and Porter, S.C., 1987. Physical geology. 750 pp. John Wiley & Sons.

Sloan, C.E. and van Everdingen, R.O., 1988. Region 28, Permafrost region. *In:* The Geology of North America, O-2, Hydrogeology, Black, W., Rosenshein, J.S. and Seaber, P.R. (eds.). Geol. Soc. Amer., 263.

Smellie, J. and Laaksoharju, M., 1992. The Äspö Hard Rock Laboratory: Final evaluation of the hydrogeochemical pre-investigations in relation to existing geologic and hydraulic conditions. SKB Technical Report, 92-31.

Sollid, J.L. and Sørbel, L., 1994. Innlandsisen i sen-Weichel sammenlignet med utbredelsen av blockmark i sør-Norge. In J-A Perdahl (editor), Abstracts, 21:a Nordiska Geologiska Vintermötet, Luleå 1994, p. 196.

Stocker, T. and Wright, D., 1991. Rapid transitions of the ocean's deep circulation induced by changes in surface water fluxes. Nature, 351, 729-732.

Sugden, D., 1982. Arctic and Antarctic. Blackwell, Oxford. p.98.

Sugden, D. and John, B.S., 1976. Glaciers and Landscape. A Geomorphological Approach. 376 pp. Edward Arnold.

Sundberg, J., 1991. Thermal properties of the rocks on Äspö island. Thermal conductivity, heat capacity, geothermal gradient and heat flow. SKB Äspö Hard Rock Laboratory Progress Report 25-91-09, SKB, Stockholm.

Svensson, N-O., 1991. Late Weichselian and early Holocene shore displacement in the central Baltic sea. Quaternary International 9, pp. 7-26.

Svensson, N-O., 1989. Late Weichselian and early Holocene shore displacement in the central Baltic, based on stratigraphical and morphological records from eastern Småland and Gotland, Sweden. Lundqua Thesis 25, 195 pp.

Svensson, N-O., 1996. The Nordic shoreline database. *In:* Climatological processes of importance for the long therm stability of a final repository for radioactive waste. Kautsky, F. (ed.). Nordisk Seminar och arbejdsrapporter. In press.

Sörensen-Aaris, K., Petersen, K. and Tauber, H., 1990. Danish finds of Mammoth (Mammuthus primigenius (Blumenbach)) Stratigraphical position, dating and evidence of Late Pleistocene environment. Danmarks Geologiske Undersögelse serie B nr. 14.

Tarendi, T., 1983. Calculated temperature field in and around a repository for spent nuclear fuel. SKBF/KBS Teknisk Rapport 83-22, SKB, Stockholm.

Thomas, R.H., 1977. Calving-bay dynamics and ice sheet retreat up the Saint Lawrence Valley. Geog. Phys. Quat., 31, 347-356.

Thorne, M.C., 1992. NSARP Reference Document: The Biosphere. Nirex Safety Series, NSS/G119 & Report No 314.

Todd, D.K., 1980. Groundwater Hydrology. John Wiley & sons. 535 pp.

Tranter, M. and Mills, R., 1989. Chemical Weathering reactions in Alpine glacial meltwaters. *In:* Water-Rock Interaction. Miles (ed.). Balkema, Rotterdam.

van Everdingen, R.O., 1976. Geocryological terminology. Canadian Journal of Earth Sciences, 13:6, 862-867.

van Everdingen, R.O., 1981. Morphology, hydrology and hydrochemistry of karst in permafrost terrain near Great Bear Lake, N.W.T; Nat. Hydrology Res. Inst., Inland Water Dir., NHRI Paper 11.

Vuorela, P., Äikäs, T. and Blomqvist, R. 1996. Characterisation of Long-Term Geological Changes for Final Disposal of Spent Fuel in Finland. Characterisation of Long-term Geological Changes for Disposal Sites. Proceedings of an NEA Workshop, Paris, France, 19-21 September, 1994.

Walcott, R.I., 1970. Isostatic response to loading of the crust in Canada. Canadian Journal of Earth Sciences, 7, 716-726.

Walder, J.S. and Hallet, B., 1979. Geometry of former sub-glacial water channels and cavities. J. Glaciology, 23 (89), 335- -46.

Wallin, B., 1995. Palaeohydrological implications in the Baltic area and its relation to the groundwater at Äspö, south-eastern Sweden—A literature study. SKB Technical Report, TR 95-06, Swedish Nuclear Fuel and Waste Management Company, Stockholm.

Walroth, T. and Gustafson, G., 1993. Sub-surface conditions produced by future climate changes, including glaciation. Data support for modelling. SKB Arbetstrapport 92-77.

Washburn, A.L. (1980) Permafrost features as evidence of climatic change. Earth Sci. Rev., 15, 327-402.

Watkins, B.M., Little, R.H., and Cooper, N.S., 1994. Provision of Information of Climate Change on the Biosphere Transport of Repository Derived Radionuclides. Intera Report to MAFF Food Science Division. Intera, Henley-upon Thames, UK.

Weertman, J., 1966. Effect of a basal water layer on the dimensions of ice

sheets. J. Glaciology, 6 (44), 191-207.

Weertman, J., 1972. General theory of water flow at the base of a glacier or ice sheet. Rev. Geophys. Space Phys., 10 (1), 287-333.

Zagwijn, W.H., 1989. The Netherlands during the Tertiary and the Quaternary: A case history of Coastal Lowland evolution. Geologie en Mijnbouw 68, pp. 107-120.

Appendix 1: Permafrost Modelling

A1.1 Permafrost Model Parameter Input

The characteristics of the permafrost model were described in Section 4.6. The parameters used in the model, with the origin of the data, are given below.

Surface temperature:

The three selected histories (i)-(iii) described in Section 2.9 were derived using the calculated temperature history at the ground surface from Boulton and Payne (1993, for a standard sea level temperature of -10°C), selected at the distance 1 000km on their cross-section going from the Norwegian shelf to Poland. This location is assumed to be representative of the Äspö conditions, as Äspö does not exactly fall on this cross-section. These data were further adjusted to fit the succession of glacial-interglacial events, as chosen by SKI. For the scenario with two ice sheets, since the Boulton & Payne model does not predict a second ice sheet around 100 000 years at location 1 000 km, the effect of the second ice sheet on the ground surface temperature was assumed to follow approximately the same pattern as the first one, which forms around 60 000 years. A warm-based ice sheet is represented by bringing the surface temperature to zero soon after the arrival of the ice sheet. Past temperatures are also given in Holmlund (1993).

Rock properties, heat flux and geothermal gradient :

- Thermal conductivity: 3 W/m.K from Sundberg (1991);
- Rock heat capacity: 2.16 J/m^3.K derived from Sundberg (1991);
- Rock porosity: 1 % (no reference);
- Heat flux at 8 km depth: 0.042 W/m^2 from Boulton & Payne (1993), which is consistent with the range 0.03 to 0.05 given by Sundberg (1991). With the selected thermal conductivity, this heat flux is consistent with a steady state geothermal gradient of 14°C per km, in the range 11.5-15.5 given by Sundberg (1991);
- Freezing latent heat of water: 3.35 10^6 J/kg from Boulton & Payne (1993).

All these properties are assumed constant in time and space. They are all consistent with data from Ahlbom & Olson (1992), Eriksson et al. (1978/79), Eriksson & Malmqvist (1979).

Waste properties, from Tarendi (1983):

- Density of waste: 1 canister per 150 m^2 (canister spacing 6 m, tunnel spacing 25 m);
- Depth of emplacement: 500 m;
- Deposition at 40 years, initial heat load per canister for 1.41 tons of waste: 850 W;
- Heat decay curve 331 W at 100 years after deposition: 68 W at 1000 years, 20 W at 4000 years. Exponential decay curves are fitted to these decaying values and the integral of the heat flux during each time step is prescribed as a source term for the model; the consistency of this modelling with that of Tarendi's has been checked with a preliminary calculation using his assumptions and his rock properties.

Time step and discretisation:

After several preliminary tests, a time step of 100 years and a vertical discretisation of 2.5 m were used. The need for a fine discretisation arises from the instability that can result when the freezing latent heat of water is taken into account. Preliminary tests have shown, however, that with a 1 % porosity, this effect can be neglected without significantly modifying the results. It was kept in the calculations for completeness.

A1.2 Permafrost Model Supplementary Figures

The following figures are those generated during permafrost and subsurface temperature calculations and which provided the basis of the summary figures in Section 2.9.

The calculations were carried out for the following three scenarios (as outlined in Section 2.9):

(i) Two successive ice sheets formed at c.50-70 ka and c.90-110 ka, with moderately warm-based ice;

(ii) Only one ice sheet formed at 50-70 ka, with moderately warm-based ice;

(iii) Two successive ice sheets formed at c.50-70 and 90-110 ka, but with warmer-based ice.

(i)

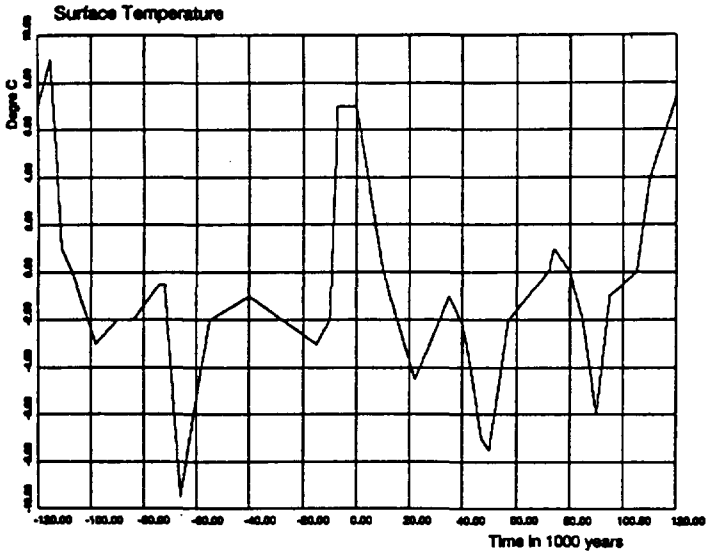

(ii)

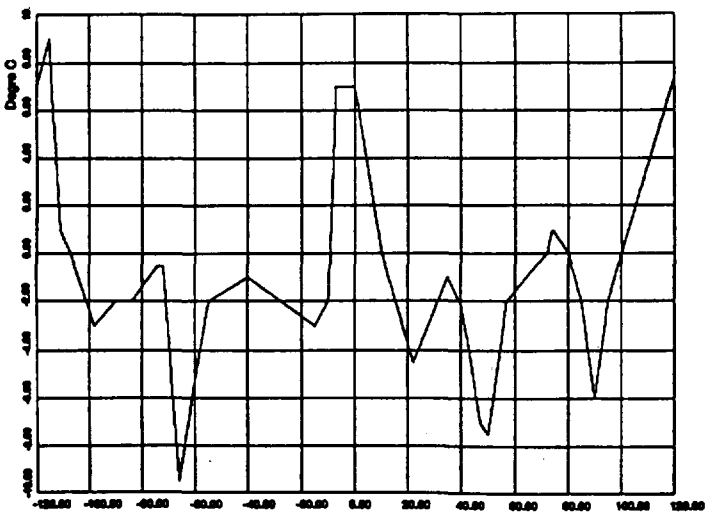

(iii)

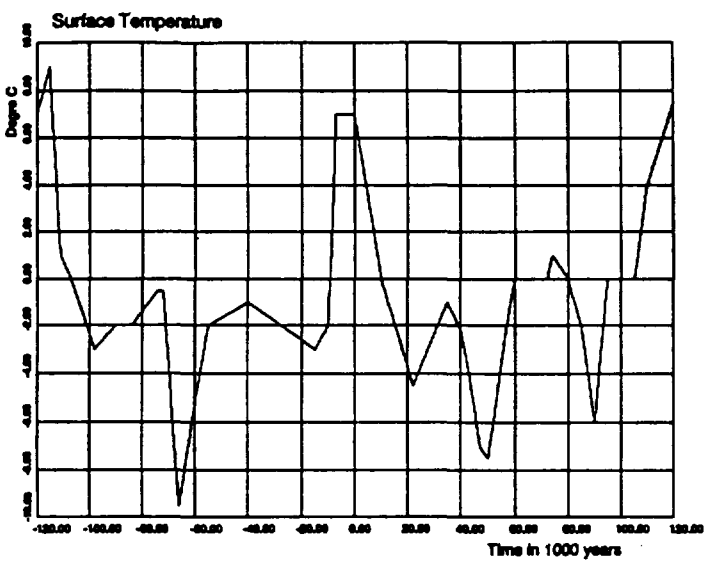

Figure A1.1. Prescribed temperature at the rock surface as a function of time, from 120 ka BP to +120 ka. Adjusted from Boulton and Payne (1993), to fit the SKI climate change model, for three different scenarios: (i) to (iii) as outlined above.

(i)

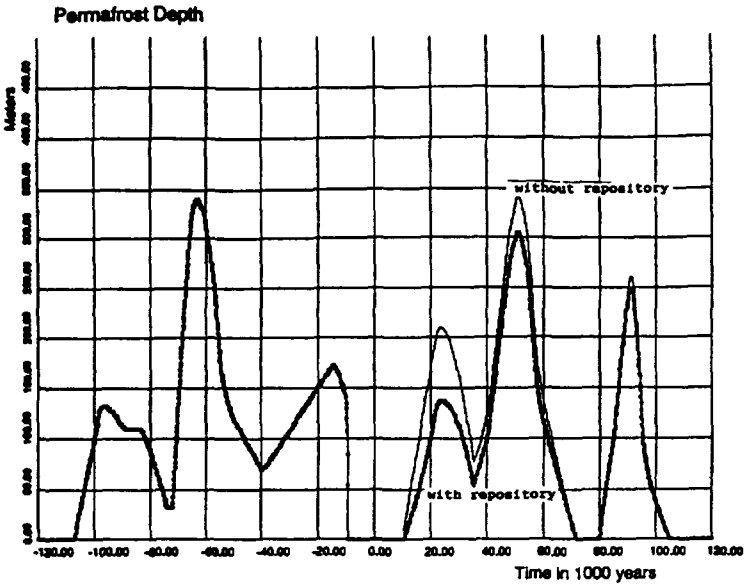

(ii)

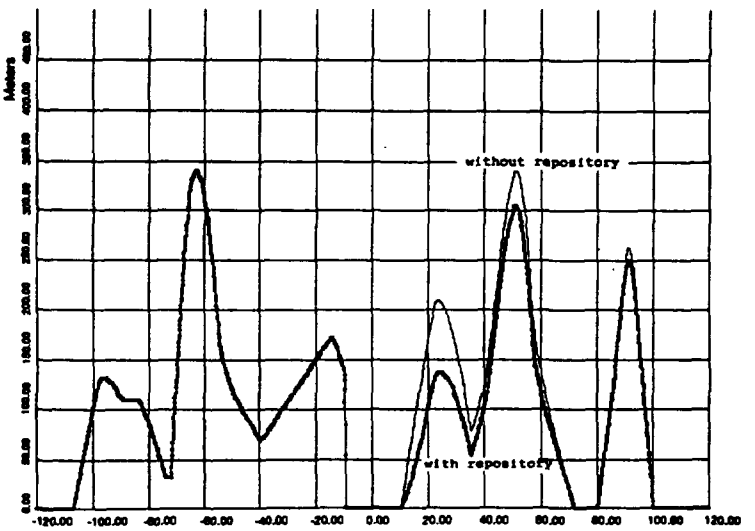

(iii)

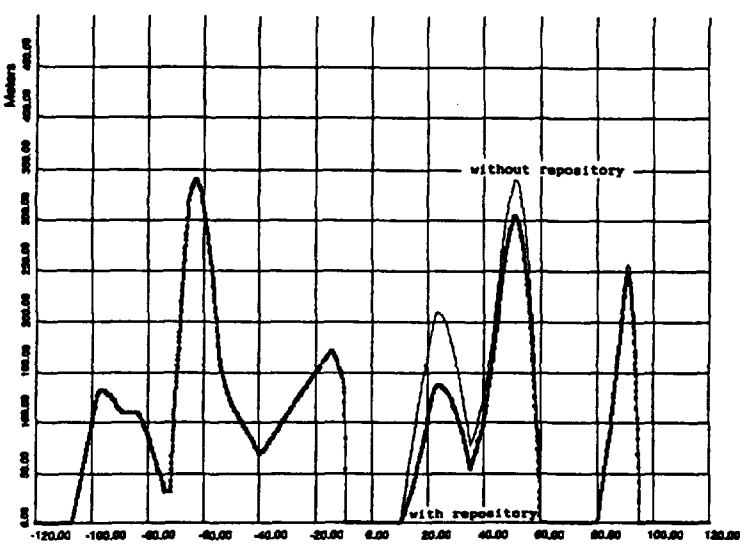

Figure A1.2. Prescribed permafrost depths as a function of time, from 120 ka BP to +120 ka for the three different scenarios: (i), (ii) and (iii) as outlined above.

(i)

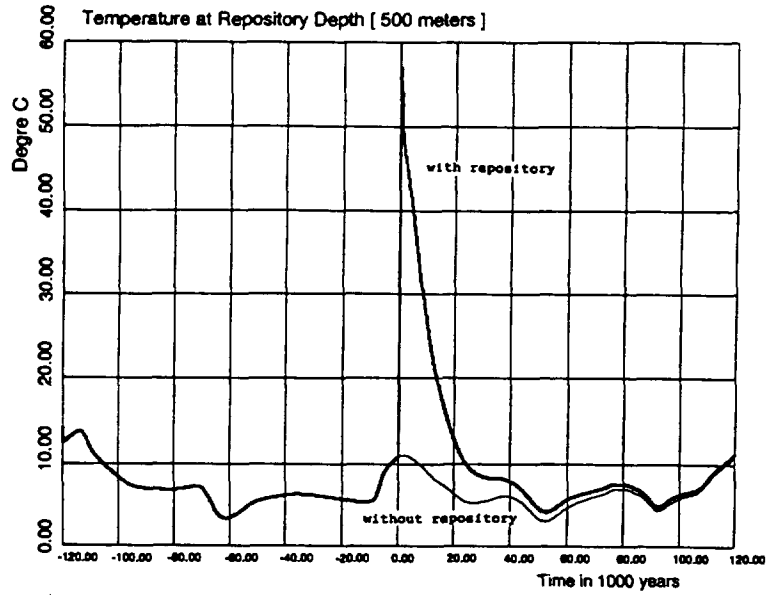

(ii)

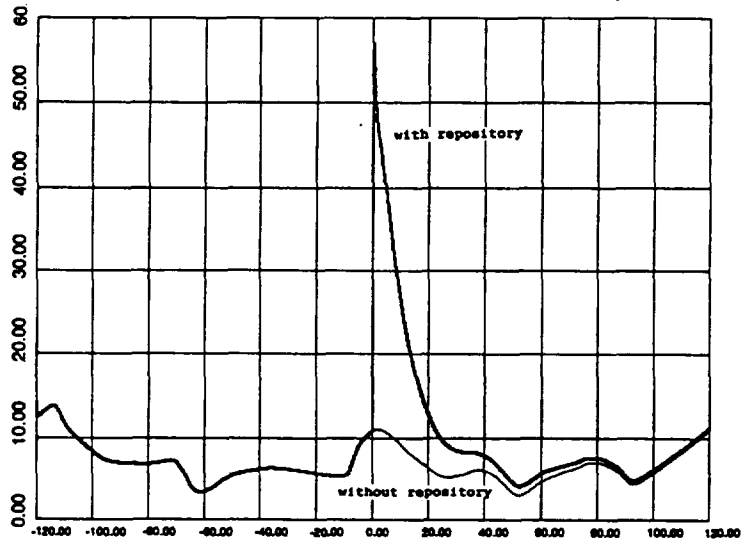

(iii)

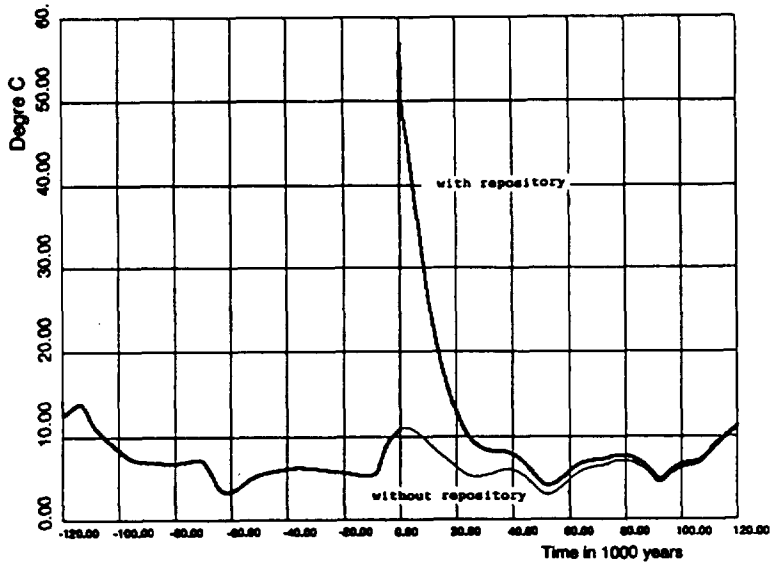

Figure A1.3. Temperature at repository depth, from 120 ka BP to +120 ka for the three scenarios, and for the case with and without the repository. The two curves after time zero (present) correspond to the cases with and without a repository at a depth of 500 m.

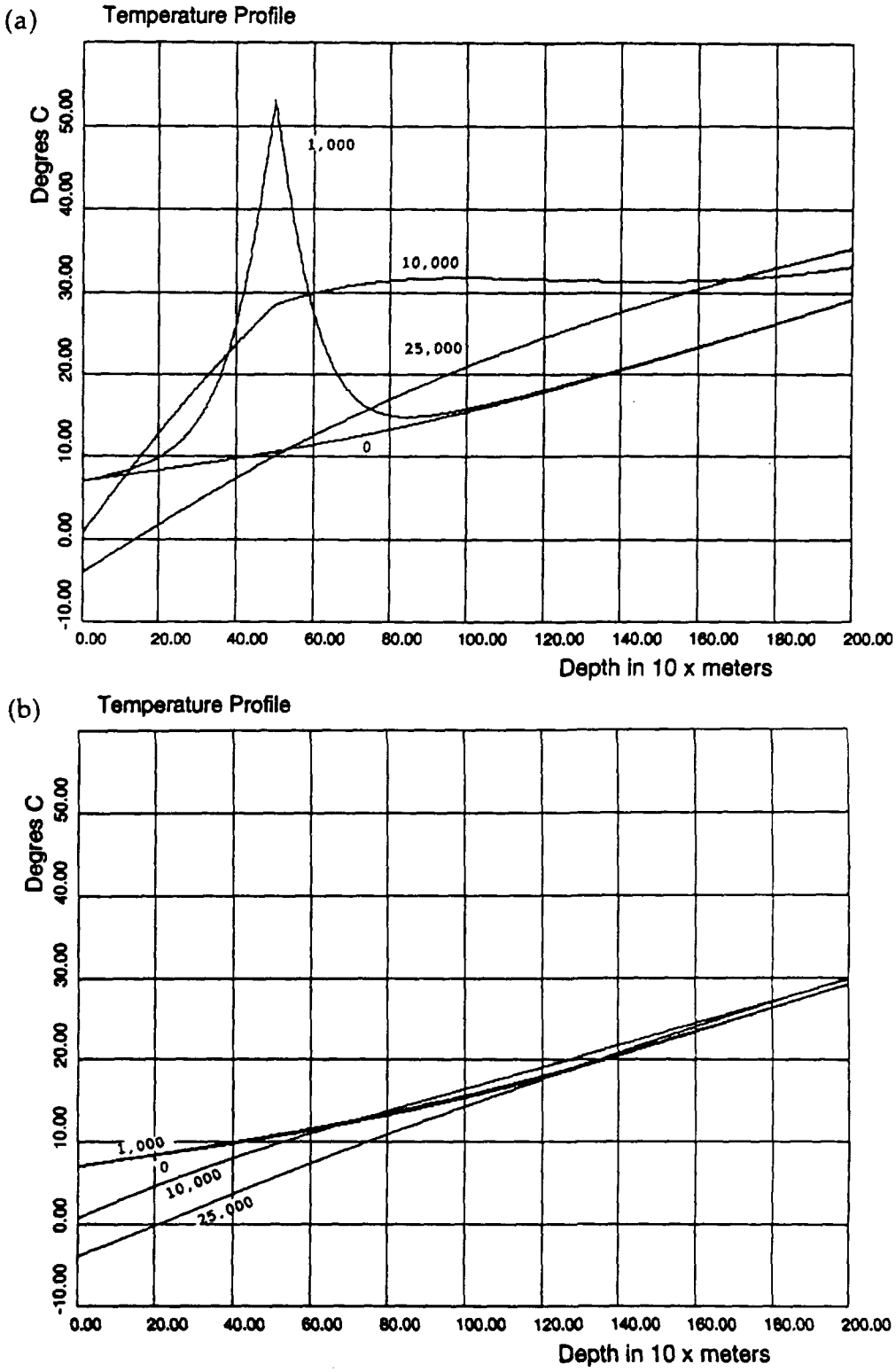

Figure A1.4. Temperature profiles within the bedrock at selected times 0, 1,000, 10 000, and 25 000 years, for (a) the case with the repository and (b) without the repository for scenarios (i)-(iii) (all the same).

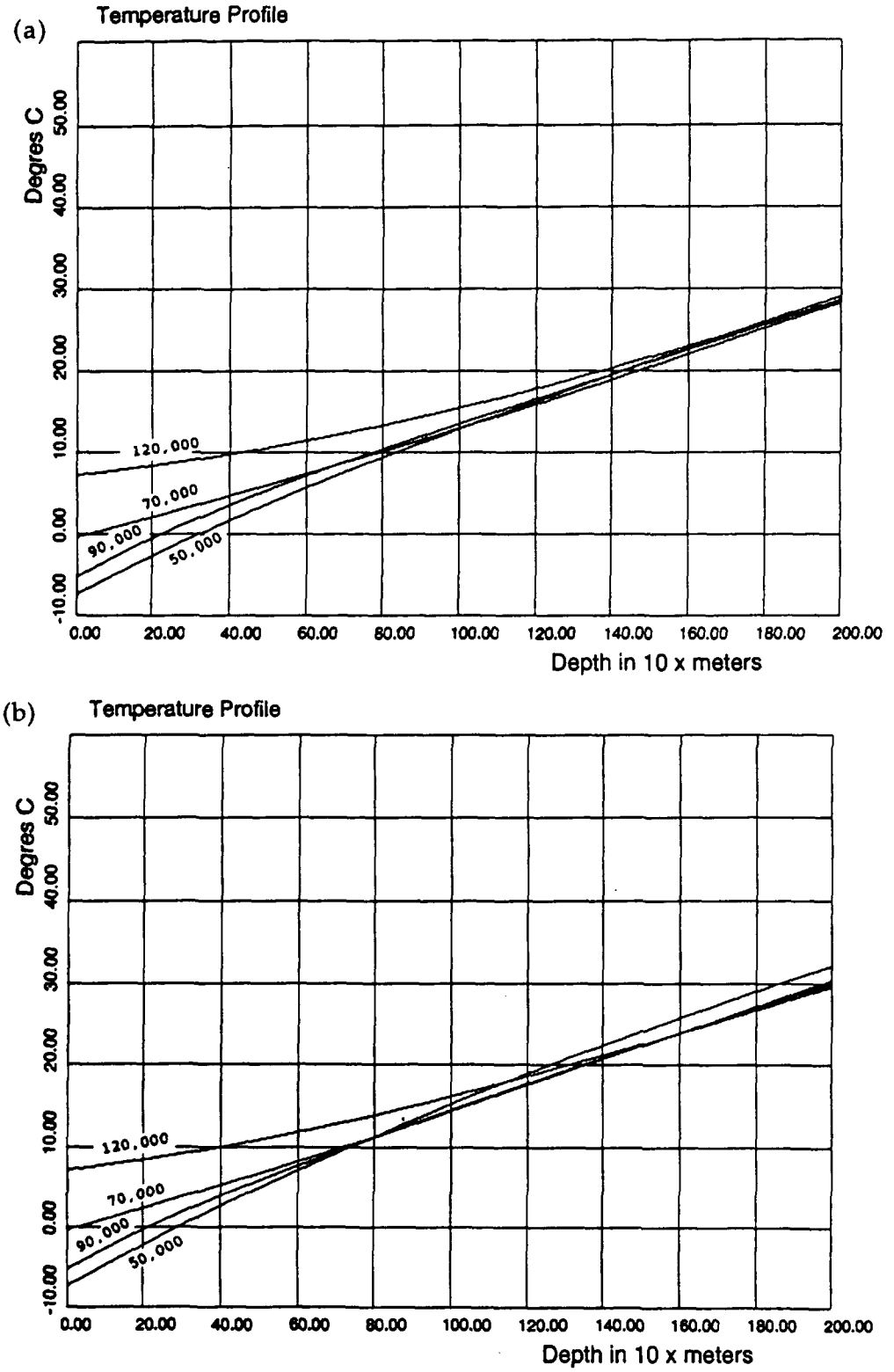

Figure A1.5. Temperature profiles within the bedrock at selected times 50 000, 70 000, 90 000, and 120 000 years, for (a) the case with the repository and (b) without the repository for Scenario (i).

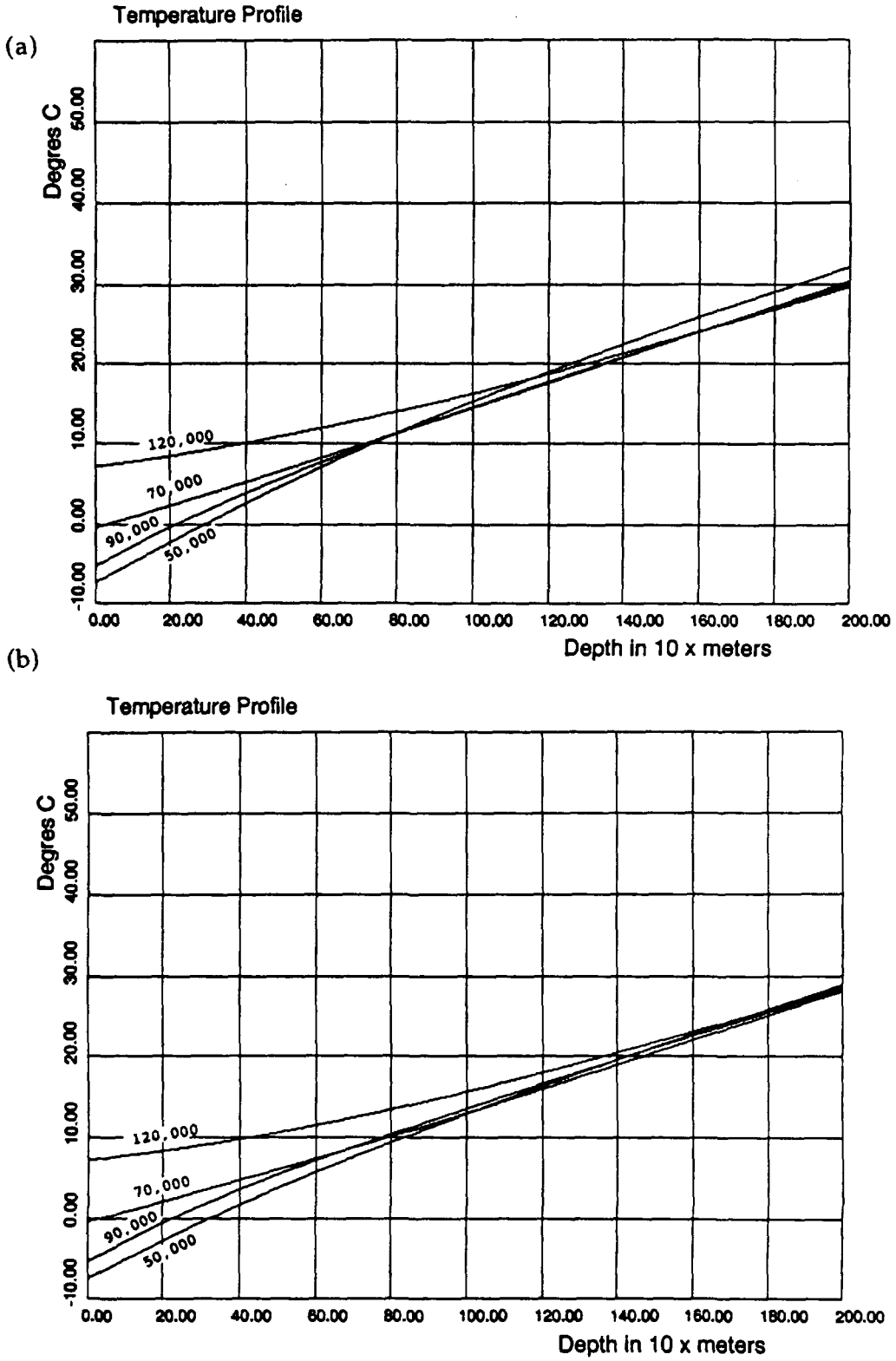

Figure A1.6. Temperature profiles within the bedrock at selected times 50 000, 70 000, 90 000, and 120 000 years, for (a) the case with the repository and (b) without the repository for Scenario (ii).

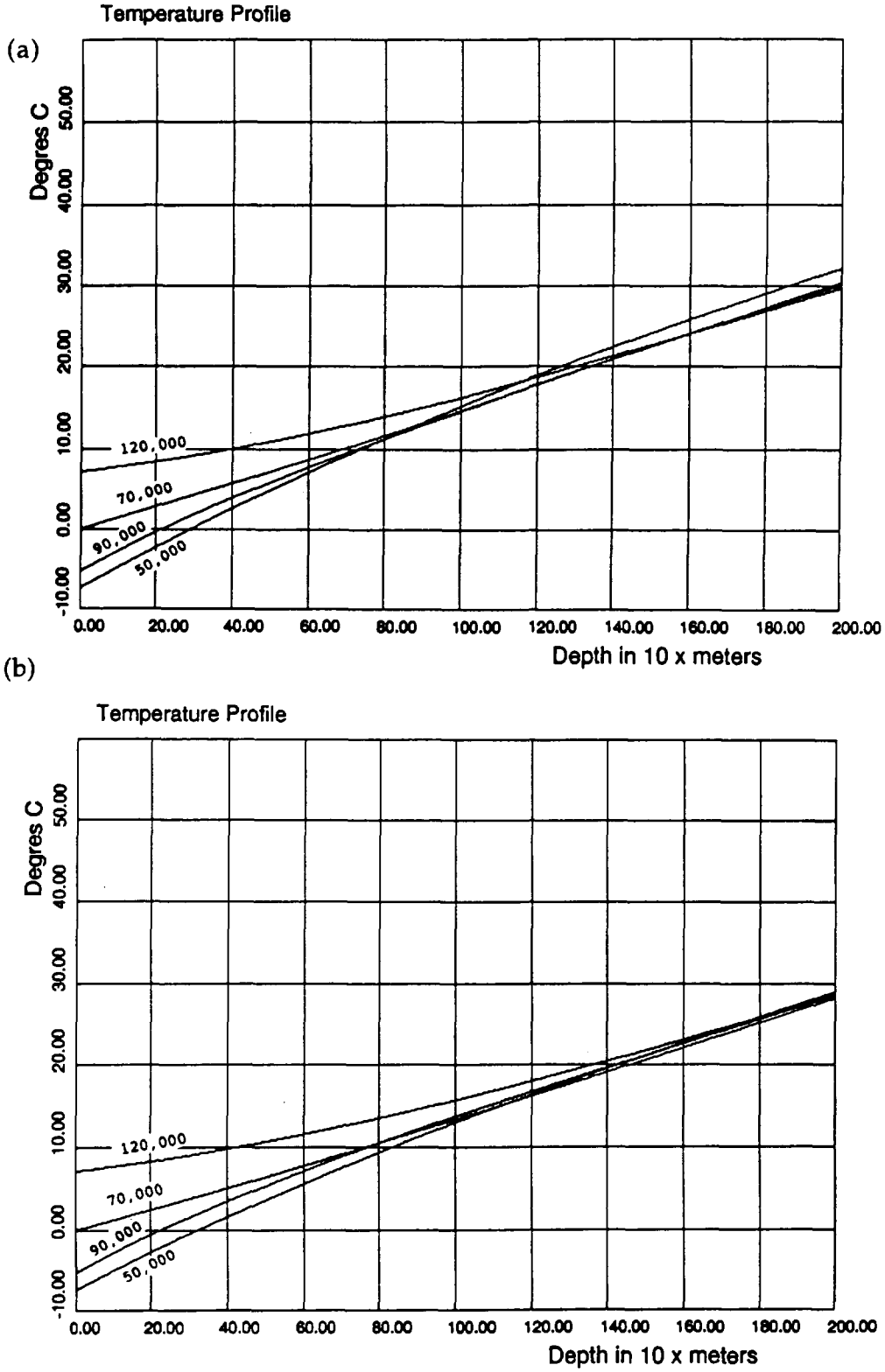

Figure A1.7. Temperature profiles within the bedrock at selected times 50 000, 70 000, 90 000, and 120 000 years, for (a) the case with the repository and (b) without the repository for Scenario (iii).

Appendix 2:

Data Tables for the Central Scenario

The following data tables accompany the graphical representation of the Central Scenario as outlined in Section 7:

Table 2a: Climate data

Table 2b: Stress data

Table 2c: Hydrogeological data

Table 2d: Hydrochemical data

Table 2e: Surface data

KEY to the Tables:

Areas highlighted in bold type represent the single glacial cycle scenario sequence described qualitatively in Section 6.

All other keys are included to the base of the tables.

Table 2a: Climate Data

Time		Description	Sea level	P'F thick.		Ice thick.	Temperature (C)		
ka	Scenario Stage		(m)	with rep. (m)	no rep. (m)	(m)	Ground surface	500m with *rep.*	depth no *rep.*
-20	4	Glacial maximum	300+	0	0	2000	-1	6	6
-13	5a	Glacial retreat	100	0	0	1000	-1	5.5	5.5
-12.2	5b	Glacial retreat	95	0	0	200-350	0	5.5	5.5
-12.1	5c	Glacial retreat	90	0	0	200-300	1	5.5	5.5
-12	5d	Final retreat	85	0	0	0	-2.2	5.5	5.5
-10.5	6	Damming of Baltic	85	0	0	0	-2	5.5	5.5
0	1	Interglacial	0	0	0	0	7	57	57
6	1	Interglacial (end)	-30	0	0	0	2	35	10
22	2	Periglacial	-70	0-135	0-210	0	-4.2	12	5
40	1	Interglacial	-50	0-55	0-80	0	-1	8	6
48	2	Periglacial (forebulge)	-55	0-305	0-345	0	-7	7	5.5
52	3a	Start glacial advance	-70	0-305	0-345	0-200	-6	5	4
53	3b	Glacial advance	-72	50-250	50-250	0-250	-3	5.5	4.5
55	3c	Glacial advance	-75	0	0	1000-1075	-2	5.5	4.5
60	4	Glacial maximum	400	0	0	2200	0	6	5
69	5a	Glacial retreat	100	0	0	1000-1075	0	7	6
69.8	5b	Glacial retreat	95	0	0	200-350	0	7	6
69.9	5c	Glacial retreat	90	0	0	200-300	0	7	6
70	5d	Final retreat	85	0	0	0	1	8	7
70.5	6a	Damming of Baltic	85	0	0	0	1	8	7
	6b	Sea incursion	70	0	0	0	1	8	7
75	7	Interglacial	20	0	0	0	1	8	7
80	2	Start Periglacial	10	0	0	0	0	8	7
91	2	Periglacial (forebulge)	-60	0-250	0-260	0	-6	5	4.5
95	3a	Start glacial advance	-65	0-200	0-200	0-200	-2	5.5	5
96	3b	Glacial advance	-70	0-50	0-50	0-250	-1	6	5.5
98	3c	Glacial advance	-75	0	0	1000-1075	0	6	5.5
105	4	Glacial *maximum*	320	0	0	1200	0	7.5	6
111	5a	Glacial retreat	100	0	0	750	4	8	8
111.8	5b	Glacial retreat	90	0	0	200-350	4	8	8
111.9	5c	Glacial retreat	85	0	0	200-300	5	8.5	8.5
112	5d	Final retreat	80	0	0	0	5	8.5	8.5
112.5	6a	Damming of Baltic	80	0	0	0	5	8.5	8.5
120	6b	Interglacial	10	0	0	0	8	12	12

KEY:

with rep. with repository present

no rep. without repository

P'F thick. permafrost thickness

Table 2b: Stress Data (KTH Group)

Time		Description	Horizontal Stress (MPa)			Vertical Stress (MPa)		
ka	Scenario stages		Minimum 500m depth	1500m	Maximum 500m	1500m	Maximum 500m	1500m
-20	4	Glacial maximum	*19.9*	*58.6*	*26.1*	*101.9*	*32.8*	*66.3*
-13	5a	Glacial retreat	*16.2*	*52*	*22.2*	*95.6*	*22*	*50.7*
-12.2	5b	Glacial retreat	*14.1*	*49.1*	*19.6*	*93.7*	*15.2*	*43.6*
-12.1	5c	Glacial retreat	*14.1*	*49.6*	*19.6*	*93*	*15*	*44.7*
-12	5d	Final retreat						
-10.5	6	Damming of Baltic						
		Start interglacial	*13.9*	*49.3*	*19.5*	*92.7*	*14.8*	*44.3*
0	1	**Interglacial**						
6	1	Interglacial (end)						
22	2	Periglacial						
40	1	Interglacial	*7.8*	*49*	*16.3*	*92.6*	*17.3*	*44.5*
48	2	**Periglacial (forebulge)**						
52	3a	**Start glacial advance**						
53	3b	**Glacial advance**						
55	3c	**Glacial advance**	17	54.1	22.3	97.5	21.9	56.1
60	4	**Glacial maximum**	19.9	58.6	26.1	101.9	32.8	66.3
69	5a	**Glacial retreat**	16.2	52	22.2	95.6	22	50.7
69.6	5b	**Glacial retreat**	14.1	49.1	19.6	93.7	15.2	43.6
69.9	5c	**Glacial retreat**	14.1	49.6	19.6	93	15	44.7
70	5d	**Final retreat**						
70.5	6a	**Damming of Baltic**						
	6b	**Sea incursion**						
75	7	**Interglacial**	13.9	49.3	19.5	92.7	14.8	44.3
80	2	Start Periglacial						
91	2	Periglacial (forebulge)						
95	3a	Start glacial advance						
96	3b	Glacial advance						
98	3c	Glacial advance						
105	4	Glacial maximum	*17*	*54.1*	*22.3*	*97.5*	*21.9*	*56.1*
111	5a	Glacial retreat						
111.8	5b	Glacial retreat	*14.1*	*49.1*	*19.6*	*93.7*	*15.2*	*43.6*
111.9	5c	Glacial retreat	*14.1*	*49.6*	*19.6*	*93*	*15*	*44.7*
112	5d	Final retreat						
112.5	6a	Damming of Baltic						
120	6b	Interglacial	13.9	49.3	19.5	92.7	14.8	44.3

KEY:

7.8	Data provided from modelling of a 4 x 4 x 4 km rock volume with 23 fractures by the KTH Group. Thermal effects are not included.
7.7	Estimated values for the other glacial cycles (assuming that stresses revert back to their original values before the next glacial cycle)

Table 2c: Hydrogeological Data

Time ka	Scenario stages	Description	Excess Hydraulic Head (Maximum) (m)	Excess Hydraulic Gradient	Transmissivity Multiplier (Approximate)	
			Region	Region	Avro (>250m)	Avro (<250m)
-20	4	Glacial maximum	2000	0.005	*0.01*	*0.01*
-13	5a	Glacial retreat	1000-1075	0.005	*0.02*	*0.02*
-12.2	5b	Glacial retreat	200-350	0.02	*0.1*	*0.1*
-12.1	5c	Glacial retreat	200-300	0.02 (5)	*0.2*	*0.2*
-12	5d	Final retreat	*85*	0	*0.2*	*0.2*
-10.5	6	Damming of Baltic	*85*	0	*0.2*	*0.2*
0	**1**	**Interglacial**	**0**	**0**	*1*	*1*
6	1	Interglacial	0	0	*1*	*1*
22	2	Periglacial	0	0	*1*	*0*
40	1	Interglacial	0	0	*1*	*0*
48	**2**	**Periglacial (forebulge)**	**0**	**0**	*5*	*0*
52	**3a**	**Start glacial advance**	**0-200**	**0.04**	*1*	*0*
53	**3b**	**Glacial advance**	**0-250**	**0.03**	*0.2*	*0*
55	**3c**	**Glacial advance**	**1000-1075**	**0.01**	*0.1*	*0.1*
60	**4**	**Glacial maximum**	**2200**	**0.005**	*0.01*	*0.01*
69	**5a**	**Glacial retreat**	**1000-1075**	**0.005**	*0.02*	*0.02*
69.8	**5b**	**Glacial retreat**	**200-350**	**0.02**	*0.1*	*0.1*
69.9	**5c**	**Glacial retreat**	**200-300**	**0.02 (5)**	*0.2*	*0.2*
70	**5d**	**Final retreat**	*85*	**0**	*0.2*	*0.2*
70.5	**6**	**Damming of Baltic**	*85*	**0**	*1*	*1*
75	**7**	**Interglacial**	*20*	**0**	*1*	*1*
80	2	Start Periglacial	0	0	*1*	*1*
91	2	Periglacial (forebulge)	0	0	*5*	*0*
95	3a	Start glacial advance	0-200	0.04	*1*	*0*
96	3b	Glacial advance	0-250	0.03	*0.2*	*0*
98	3c	Glacial advance	1000-1075	0.01	*0.1*	*0.1*
105	4	Glacial maximum	1200	0.005	*0.02*	*0.02*
111	5a	Glacial retreat	750	0.005	*0.013*	*0.013*
111.8	5b	Glacial retreat	200-350	0.02	*0.1*	*0.1*
111.9	5c	Glacial retreat	200-300	0.02 (5)	*0.2*	*0.2*
112	5d	Final retreat	*80*	0	*0.2*	*0.2*
112.5	6	Damming of Baltic	*80*	0	*0.2*	*0.2*
120	1	Interglacial	*10*	0	*1*	*1*

KEY:

85 Italics under hydraulic head represent water head and not ice head

0.01 Italics under transmissivity multiplier indicate the very approximate nature of the numbers

Table 2d: Hydrochemical Data: Site and Region

Time		Description	Potential Hydrochemical input							
							Site		Region	
ka	Scenario stages		c.500m depth	G %	S	D	M		Dilute	Saline
-20	4	Glacial maximum	Glacial	90		10			100	
-13	5a	Glacial retreat	Glacial	90		10				
-12.2	5b	Glacial retreat	Glacial	90		10				
-12.1	5c	Glacial retreat	Glacial	90		10			50	50
-12	5d	Final retreat	Glacial, marine	50			50			
-10.5	6	Damming of Baltic	Glacial	90		10			50	50
0	1	Interglacial	Surface, Deep		50	50				100
6	1	Interglacial (end)	Surface, Deep		50	50				100
22	2	Periglacial	Surface, Deep		40	60				100
40	1	Interglacial	Surface, Deep		50	50				
48	2	Periglacial (forebulge)	Surface, Deep		40	60				100
52	3a	Start glacial advance	Glacial	50		50			50	50
53	3b	Glacial advance	Glacial	60		40			50	50
55	3c	Glacial advance	Glacial	70		30				
60	4	Glacial maximum	Glacial	90		10			100	
69	5a	Glacial retreat	Glacial	90		10				
69.8	5b	Glacial retreat	Glacial	90		10				
69.9	5c	Glacial retreat	Glacial	90		10			50	50
70	5d	Final retreat	Glacial, marine	50			50			
70.5	6a	Damming of Baltic	Glacial	90		10			50	50
	6b	Sea incursion	Marine	10			90			100
75	7	Interglacial	Surface, Deep, marine		45	45	10			100
80	2	Start Periglacial	Surface, Deep		45	50	5			
91	2	Periglacial (forebulge)	Surface, Deep		40	60				100
95	3a	Start glacial advance	Glacial	50		50			50	50
96	3b	Glacial advance	Glacial	60		40			50	50
98	3c	Glacial advance	Glacial	70		30				
105	4	Glacial maximum	Glacial	90		10			100	
111	5a	Glacial retreat	Glacial	90		10				
111.8	5b	Glacial retreat	Glacial	90		10				
111.9	5c	Glacial retreat	Glacial	90		10			50	50
112	5d	Final retreat	Glacial, marine	50			50			
112.5	6a	Damming of Baltic	Glacial	90		10			50	50
	6a	Sea incursion	Marine	10			90			100
120	7	Interglacial	Surface, Deep		50	50				100

KEY:

G	Glacial meltwater	**Dilute**	Dilute water (meteoric &/or glacial melt)
S	Surface water	**Saline**	Saline water (deep saline &/or marine)
D	(Deep) saline water		
M	Marine water		

Table 2e: Site Surface Data

Time		Description	Climate state	Surface conditions
ka	Scenario stages			
-20	4	Glacial maximum	Glacial	Under ice
-13	5a	Glacial retreat	Glacial	Under ice
-12.2	5b	Glacial retreat	Glacial	Under ice
-12.1	5c	Glacial retreat	Tundra	Marine
-12	5d	Final retreat	Boreal	Marine
-10.5	6	Damming of Baltic	Boreal	Ice lake
0	1	Interglacial	Boreal/temperate	Bare rock/peat bog
6	1	Interglacial (end)	Boreal	Forest/Bare rock/peat bog
22	2	Periglacial	Tundra	Tundra marsh/bare rock
40	1	Interglacial	Boreal/tundra	Tundra marsh/bare rock
48	2	Periglacial (forebulge)	Tundra	Tundra marsh/bare rock
52	3a	Start glacial advance	Glacial	Under ice
53	3b	Glacial advance	Glacial	Under ice
55	3c	Glacial advance	Glacial	Under ice
60	4	Glacial maximum	Glacial	Under ice
69	5a	Glacial retreat	Glacial	Under ice
69.8	5b	Glacial retreat	Glacial	Under ice
69.9	5c	Glacial retreat	Glacial	Marine
70	5d	Final retreat	Tundra	Marine
70.5	6a	Damming of Baltic	Tundra	Glacial Lake
	6b	Sea incursion	Tundra	Marine
75	7	Interglacial	Boreal	Marine
80	2	Start Periglacial	Tundra	Marine
91	2	Periglacial (forebulge)	Tundra	Tundra marsh/bare rock
95	3a	Start glacial advance	Glacial	Under ice
96	3b	Glacial advance	Glacial	Under ice
98	3c	Glacial advance	Glacial	Under ice
105	4	Glacial maximum	Glacial	Under ice
111	5a	Glacial retreat	Glacial	Under ice
111.8	5b	Glacial retreat	Glacial	Under ice
111.9	5c	Glacial retreat	Glacial	Marine
112	5d	Final retreat	Tundra	Marine
112.5	6a	Damming of Baltic	Tundra	Glacial Lake
120	6b	Interglacial	Boreal/temperate	Forest/bare rock/peat bog

Postadress/Postal address	Telefon/Telephone	Telefax	Telex
SKI S-106 58 STOCKHOLM	Nat 08-698 84 00 Int +46 8 698 84 00	Nat 08-661 90 86 Int +46 8 661 90 86	11961 SWEATOM S